# Conversion of Plastic Waste into Poly-Crude

A Thesis Presented for the

Master of Science

Degree

The University of Tennessee, Knoxville

Rakesh Patter

December 2024

## ACKNOWLEDGEMENTS

First, I would like to express my deepest gratitude to my advisor, Prof. Brian Long, for his invaluable guidance, support, and encouragement throughout my research. His insights and expertise have been instrumental in shaping the direction of this work, and I am truly fortunate to have had the opportunity to gain experience under his mentorship. I am also grateful to my committee members, Prof. Michael Kilbey and Prof. Johnathan Brantley, for their thoughtful feedback and constructive criticism, which have helped improve my thesis's quality.

Special thanks go to Maggie Powell, Christy Witcher, Godwin Ochola, Mason Jones, Nathan Kunzler, and Karina Guerrero whose camaraderie and collaboration have made the challenges of research more manageable. I would also like to acknowledge the National Science Foundation (NSF) for providing the financial support necessary to carry out this research and the Institute for Advanced Materials and Manufacturing (IAMM) for access to laboratory facilities and equipment.

Finally, I deeply appreciate my family and friends, particularly my father, brother, son, and wife, for their unwavering love, patience, and encouragement. Their constant support has been a source of strength throughout this journey. I miss you, Maa.

To all who contributed in ways both big and small, thank you. This thesis would not have been possible without you.

## ABSTRACT

Plastic waste, particularly from polyolefins like polyethylene (PE) and polypropylene (PP), presents significant environmental and recycling challenges due to their chemical stability and resistance to degradation. Current recycling methods often fail to deliver high-value outputs, with chemical recycling hindered by inefficiencies in catalyst performance and a limited understanding of polymer-catalyst interactions. This thesis addresses these challenges by proposing a hypothesis that by tailoring catalyst surface properties and optimizing solvent interactions, it is possible to design a system that selectively adsorbs larger polymer molecules for catalytic breakdown while facilitating the desorption of smaller, processed molecules. To test this hypothesis, end-functionalized polyethylene models of controlled molecular weights were synthesized using ring-opening metathesis polymerization (ROMP) with Grubbs 2$^{nd}$ generation catalyst. Chain transfer agents (CTAs) were employed to introduce distinct terminal functionalities, creating a library of polyethylene models for systematic analysis. These models were evaluated for their adsorption behavior and catalytic degradation efficiency over catalyst surfaces under controlled conditions. High-temperature size exclusion chromatography (HT-SEC) was used to analyze the molecular weights of depolymerized products, while catalytic performance metrics correlated with the polymers' molecular weight and molecular weight distribution. By addressing the knowledge gaps in polymer-catalyst interactions, this research will contribute to developing more efficient and sustainable recycling technologies for polyolefins, advancing the transition to a circular economy for plastic waste.

## TABLE OF CONTENTS

## LIST OF TABLES

## LIST OF FIGURES

# CHAPTER ONE

# MOTIVATION AND BACKGROUND

## Motivation and Goals

Plastics, often mistakenly referred to as "the hallmark of modernity," are deeply embedded in everyday life, dramatically reshaping the modern world.[1] However, their ubiquitousness in everyday life has also led to drastic impacts that have negatively affected modern society. In 1907 Belgian chemist Leo Hendrik Baekeland invented the first synthetic plastic "Bakelite". He was also the first researcher to use "plastic" to describe the products created from macromolecules. Plastics, being an inexpensive, lightweight, and durable material, can be molded into a variety of products that have a wide range of applications such as cheap synthetic clothing, hospital syringes/gloves, food wrappings, etc. Most things we use or encounter in daily life are made from plastic in some way. Production and usage levels have risen so much that these have been mistakenly viewed as crucial assets in global markets, often being used as a "bargaining chip" by many nations.[2]

Due to high collection costs and insufficient infrastructure, more than 60% of plastic becomes waste after just a single use.[3] Reports indicate that global plastic production has surged from 2 million tons in 1950 to 360 million tons in 2018 and is estimated to surpass the 12 billion mark by 2050.[4] The massive amount of plastic waste generated by the rapid increase in production and consumption is a major concern because plastics generally do not break down on their own and can remain in the environment for decades.[5] Plastic waste is occupying significant landfill space, which is increasingly scarce and costly. Of all the plastic produced, only 14% is recycled. The

remaining 86% is incinerated, dumped in landfills, or ends up in the environment.[1] Of the 14 % plastic that is recycled, only 2% remains in the circulation, the remaining 12 % is either “downcycled” (8%), resulting in the materials of lower quality, or it is lost in the recycling process (4%).[6] Plastic debris can physically injure wildlife, and many plastics may also pose chemical risks in certain situations either due to their inherent toxicity or because they can absorb other harmful pollutants.[7, 8] Polyolefins are the most widely used polymers due to their low monomer cost and the availability of abundant feedstock. They account for over 60% of global polymer production. In North America alone, the demand for polyethylene and polypropylene has seen a significant rise, growing from over fifty billion pounds in 2013 to more than seventy billion pounds in 2022. Efforts to recycle plastic waste have employed various approaches, with mechanical and chemical recycling being the primary methods utilized.

**Mechanical Recycling**

Mechanical recycling is the most widely adopted method for processing plastic waste into reusable materials through physical reprocessing without altering the chemical structure of the plastics. The process typically begins with separation and sorting, where the plastic waste is segregated based on physical properties such as shape, size, density, color, and chemical composition. Advanced technologies, like magnetic separation, are used to remove metals, while optical sorting systems equipped with FT-NIR (Fourier Transform Near Infrared) technology help distinguish and separate specific types of plastics, including polyethylene terephthalate **(**PET), high-density polyethylene (HDPE), and polypropylene (PP). Additionally, size sorting is employed to remove large items like

plastic bags and smaller items like caps, optimizing the sorting process for better efficiency.

Following sorting, the plastic waste undergoes washing to remove contaminants such as dirt, labels, adhesives, and residues that may affect the quality of the final recycled material. This step is critical because contamination can lead to lower-grade recycled products, limiting their reuse in high-value applications. After washing, the plastic is subjected to grinding and size reduction, where the material is mechanically shredded or ground into smaller flakes or pellets. These smaller particles are easier to handle, store, and further process, making them suitable for regranulation or molding into new products. In cases where additional separation is needed, density-based separation techniques are employed. These methods, such as flotation, exploit the differences in buoyancy between polymers. Lighter plastics like PE and PP float on water, while denser polymers like PET and PVC sink, allowing for more refined separation. However, achieving pure polymer streams can be challenging in complex waste streams, where overlapping density ranges make it difficult to fully separate different polymers, which results in mixed batches that reduce the quality of the recycled output.

Despite its widespread use, mechanical recycling faces several significant challenges. One major issue is the limitation of sorting technologies, such as FT-NIR, which struggles to accurately sort multilayer materials, dark-colored plastics, and products with labels. These limitations can lead to false readings or incomplete sorting, often requiring manual sorting to correct and fine-tune the process, adding labor and cost. Another key challenge is contamination, as even with thorough washing, certain contaminants like adhesives, food residues, or chemical residues may remain, reducing

the overall quality and usability of the recycled plastic. Overlapping density ranges in density-based separation also pose a challenge, particularly in mixed polymer waste streams, where the density differences between plastics may not be sufficient to achieve full separation. This can lead to cross-contamination of polymers, producing lower-grade recycled material. Finally, the mechanical recycling process itself can cause degradation of the material. Repeated heating and mechanical shearing during melting can damage the polymer chains, reducing the molecular weight and weakening the mechanical properties of the recycled plastic. This degradation limits the recyclability of plastics over multiple cycles and can affect the quality of the final product. While mechanical recycling is a crucial component of plastic waste management, its efficiency is limited by challenges such as sorting inaccuracies, contamination, polymer mixing, and material degradation. For polyolefins, which are the most widely used plastic materials, aforementioned challenges are commonly encountered in the recycling process. Continued advancements in sorting technologies, contamination control, and processing methods are essential to overcome these obstacles and enhance the overall effectiveness and sustainability of mechanical recycling processes.

**Chemical Recycling**

Due to the inefficiency of the mechanical recycling process, scientists have shifted their research interest towards chemical recycling. Chemical recycling to monomers involves breaking down plastic waste into its original monomeric building blocks, allowing for the creation of high-quality recycled polymers equivalent to their virgin counterparts. This method is particularly effective for certain plastics, such as polyethylene terephthalate (PET) and polystyrene, which can be depolymerized back to

monomers like terephthalic acid and styrene, respectively. These recovered monomers are then repurposed in new polymer synthesis, maintaining the structural integrity and properties of the resulting material. Unlike mechanical recycling, which can degrade polymer quality over time, chemical recycling preserves material performance by reverting plastics to their molecular precursors.[9] Depolymerization techniques vary depending on the polymer type, with glycolysis, hydrolysis, and methanolysis commonly used for PET, where specific conditions and catalysts allow the breakdown into monomers that are purified for reuse.[10] Catalyst advancements in recent years have increased the efficiency and selectivity of these processes, making chemical recycling a more viable industrial option. Chemical recycling of polyolefins, such as polyethylene (PE) and polypropylene (PP), back to monomeric forms is challenging due to their chemical stability and lack of functional groups that facilitate depolymerization. Unlike polyesters (e.g., PET), which contain easily cleavable ester bonds, polyolefins consist of strong carbon-carbon (C–C) single bonds that are highly resistant to breakdown under typical recycling conditions.[10] This stability requires high temperatures and advanced catalytic systems to cleave the C–C bonds effectively, often resulting in significant energy input and low selectivity, where multiple by-products are produced instead of pure monomers.[9] The kinetic pathway to get back to monomeric form is not readily accessible.

**Hydrogenolysis**

Chemical recycling presents an opportunity to transform plastic waste streams into higher-value chemicals that could serve as drop-in fuel additives, be integrated into chemical refineries, or act as building blocks for the production of next-generation,

recyclable-by-design polymers.[9, 11-13] Current methods like pyrolysis and thermal cracking facilitate the conversion of polyolefin waste into fuel-range chemicals, but these processes demand high operating temperatures (400−900 °C), have low product selectivity and kinetically slow. Drawing on expertise from petroleum refining, the coal chemical industry, and biomass conversion, catalytic hydrogenolysis of polyolefin waste can provide a more efficient alternative, yielding high-value chemicals or liquid fuels. In light of pressing environmental and energy concerns, catalytic hydrogenolysis offers a promising strategy for promoting a circular plastics economy. It is more energy-efficient and reduces the formation of low-value gaseous alkanes compared to conventional thermal cracking.[14-16] Recent advancements in chemical recycling have discovered methods for breaking the strong C−C bonds in polyethylene (PE) at lower temperatures (200−300 °C) using both thermochemical and electrochemical approaches.[12, 17-19] Platinum-based catalysts have demonstrated effectiveness in PE depolymerization via hydrogenolysis and hydrocracking,shown in F**igure 1.1** as well as through a tandem dehydrogenation/metathesis process using a $SnPt/\gamma\text{-}Al_2O_3$ and $Re_2O_7/\gamma\text{-}Al_2O_3$ catalyst system. [20] In a study by Rorrer et. al ruthenium nanoparticles supported on carbon showed effective heterogeneous catalysis for the depolymerization of polypropylene plastic via hydrogenolysis under relatively low temperatures (225-250 °C) and hydrogen (20-25 bar). Hydrogenolysis of polyolefins presents several significant challenges in both the technical and economic realms. However, one of the primary challenges is achieving efficient C−C bond cleavage in polyolefins, as these bonds are relatively strong and still require high pressures and temperatures to break and often noble metal catalysts.

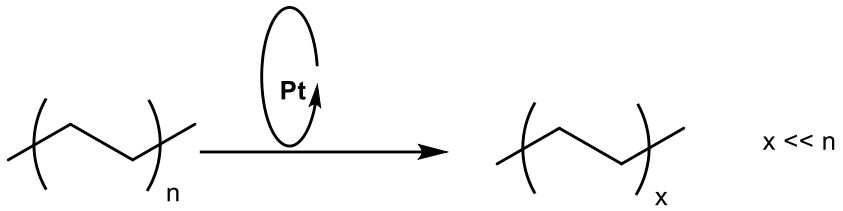


**Figure 1.1** Schematic of hydrogenolysis of polyethylene over Pt metal

Noble metal catalysts can perform hydrogenolysis under relatively low temperatures (225-250 °C) and hydrogen pressures, wherein Ru/C and Rh-based systems have been developed to lower the reaction severity (e.g., reducing the required temperature and pressure), but catalyst optimization remains crucial to increase efficiency and selectivity for desired products such as alkanes. Another significant hurdle is the heterogeneity of feedstocks. Waste streams containing mixed polyolefins, such as polypropylene and polyethylene, complicate the process due to differences in their melting points and degradation behaviors. These differences affect the reaction rates and product distribution, requiring more precise control over reaction conditions and catalyst design to manage the diverse input streams .[21, 22] Additionally, post-consumer polyolefin waste can contain various contaminants such as dyes, additives, or non-polyolefin materials (e.g., PVC), which can poison catalysts or interfere with the reaction, necessitating additional pretreatment steps.

Catalyst stability and recyclability also pose challenges. Catalyst deactivation can occur due to the sintering of metal nanoparticles or char formation, as seen in studies using Ru/C catalysts. These issues can reduce the efficiency of hydrogenolysis over time, necessitating periodic regeneration or catalyst replacement, which increases operational costs.[21] Moreover, the scalability of the process is another concern. Although laboratory-

scale experiments have shown promise, scaling up hydrogenolysis to handle industrial levels of polyolefin waste requires overcoming mass and heat transfer limitations, ensuring efficient hydrogen diffusion through molten polymers, and managing high energy demands.[21, 22] In summary, while hydrogenolysis offers a promising route for upcycling polyolefins into valuable chemicals, challenges related to product selectivity, catalyst performance, and process scalability must be addressed to realize its full industrial potential.

**Catalytic cracking**

Catalytic cracking is a critical process in the petrochemical industry, primarily used for breaking down hydrocarbon molecules into smaller, more valuable compounds such as gasoline, diesel, and olefins. The catalysts employed in this process are predominantly solid acids, such as zeolites **(Figure 1.2),** alumina, and amorphous silica-alumina. However, basic solids like BaO and $K_2O$, as well as metal-loaded activated carbons, have also been explored for depolymerization of polystyrene[23] and the degradation of polyethylene,[24] respectively.

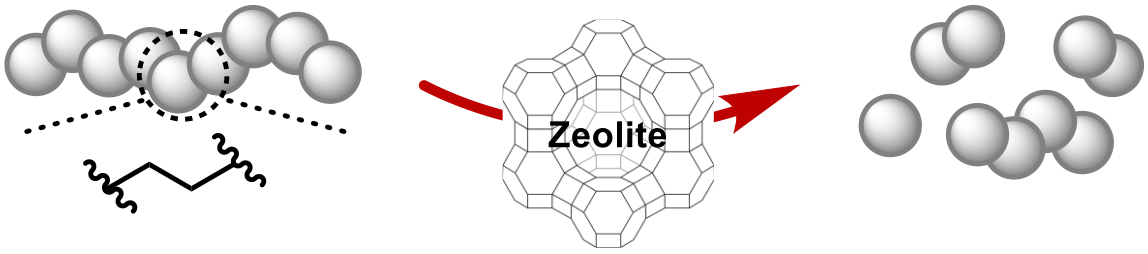


Figure 1.2 Depiction of the mechanism of zeolite catalyst

Among zeolitic catalysts, HZSM-5 has been shown to effectively promote the cracking of polyethylene, resulting in high yields of both gaseous and lower hydrocarbons.[25, 26] In contrast, REY zeolite produces a mixture of hydrocarbons with boiling points comparable to commercial gasoline during the catalytic conversion of heavy oil feedstock, which is derived from the prior thermal cracking of polyethylene.[27] Zeolite-based catalysts are extensively utilized for cracking waste polymers due to their acidity, large surface area, excellent thermal stability, adjustable pore structure, reproducibility, and ability to selectively produce desired products. Among the various types of zeolites, ZSM-5, Beta, USY, and ZSM-11 stand out as promising catalysts. These zeolites have been synthesized or modified in numerous ways to improve both their stability and activity. Research has also delved into advanced forms of zeolites, such as nanozeolites, embryonic zeolites, hierarchical zeolites, composites, and metal-modified zeolites, to enhance their performance in the cracking of polyolefins.[28-30] The catalytic mechanism proceeds through carbenium ion intermediates, contrasting with the free radical mechanism in thermal pyrolysis. The presence of bronsted acid sites on zeolites allows for the formation of these carbenium ions, which undergo multiple rearrangements and β-scissions, leading to a higher yield of desired products, such as n-alkanes, iso-alkanes, and light olefins. This offers more control over the product distribution compared to thermal pyrolysis, where the products tend to be more random due to free radical generation. The conversion of polyolefins is influenced by several factors, including temperature, pressure, reaction mixing rate, reactor design, the choice of solvents, the type of plastics used, and mass transfer efficiency.[31-33] Catalytic cracking faces challenges, including catalyst deactivation due to char formation and the need for

effective heat and mass transfer within the reactor. Char deposits can block the active sites on catalysts, reducing their effectiveness over time.

**Poly-crude**

However, changing our perspective and viewing plastic waste as a readily available and cost-efficient source of carbon and energy could open numerous opportunities for future production. For example, plastics are vital in the wax industry, where specific polymers are combined to improve attributes like durability, gloss, and melting point, making them ideal for coatings, polishes, and sealants. In the lubricant industry, plastic additives are crucial for enhancing viscosity, minimizing wear and tear, and boosting the performance of mechanical systems. Although specialized markets, like those for waxes and lubricants, offer opportunities to increase the value of low-cost materials, they are insufficient in scale to address the enormous volume of plastic waste produced. For a genuine circular economy to develop, solutions must target industries that can cope with plastic waste generation, such as the petrochemical market, which consumed 60.3 million barrels of petroleum in the United States in 2021 alone.[34] Additionally, current refining industries demonstrate an efficiency exceeding 90%. Refineries are presently operated with a primary focus on maximizing profit margins. However, considering the potential reductions in $CO_2$ emission from refining processes and changes in demand and quality standards, refineries may also need to prioritize operational efficiency.[35] The petrochemical and polymer industries have already committed trillions of dollars to developing infrastructure, including refineries and processing facilities. By utilizing these existing facilities, along with the established large-scale operations and energy-efficient methods employed in current petroleum

refining, we can achieve substantial financial and energy savings over the alternative of establishing entirely new industries for repurposing plastic waste. This gap in transformative capabilities presents a strategic opportunity for future industrial initiatives, offering a compelling direction for advancing sustainable practices within the sector.

Polyolefins **(**POs), including polyethylene (PE) and polypropylene (PP), are the most extensively produced polymers globally, and they make up over 70% of all plastic waste.[6] This is attributed to their versatility, low cost, and durability. Polyolefins are preferred because of their high elongation at break, toughness, low glass transition temperature ($T_g$), and high melting temperature ($T_m$).[36] These characteristics prevent the materials from becoming brittle under normal usage conditions and ensure they do not easily melt or deform. However, polyolefins are susceptible to degradation during mechanical reprocessing, with the molecular weight of PE increasing and that of PP decreasing, resulting in greater dispersity for both. Although current methods are not effective for converting PO waste back into its monomeric form, transforming it into new materials or reintegrating it into existing markets offers a feasible solution for managing plastic waste. Transforming polyolefins into new materials or reintegrating them into the existing market could offer a viable solution for industrial feedstock. However, incorporating polyolefin waste into chemical and plastic production is challenging for several reasons. Existing refinery inputs are suitable only for viscous liquids or low-melting solids. Consequently, polyolefins cannot be directly mixed into refineries or steam crackers. Additional obstacles include the widespread distribution of polyolefins globally and the low energy density of raw waste plastic, which adds to transportation challenges. A potential solution to using polyolefins as an industrial feedstock, is to

create a manufacturing process that can selectively and efficiently convert polyolefins into more manageable, long-chain hydrocarbons, a process termed "poly-crude." Poly-crude is an energy-dense liquid or low-melting solid. A distributed poly-crude manufacturing process that reduces energy and molecular inputs, such as hydrogen, could significantly enhance the economics of incorporating polyolefins (POs) into the polymer production supply chain. Additionally, poly-crude could serve as a foundational chemical for various other markets, including precursors for surfactants,[37] fiber-reinforced plastics,[38] graphene nanosheets,[39, 40] fluorescent carbon dots,[41] and electrolyte membranes.[42] Other valuable applications are also likely to arise in the future. The key to realizing these possibilities lies in creating a poly-crude production process that can selectively and efficiently break down POs into more manageable long-chain hydrocarbons.

Our main goal for this project is to develop strategies and methodologies to selectively crack high molecular weight polyolefins into lower molecular weight oils or waxes that can be easily transported and integrated into existing crude oil refining processes. To do this we hypothesize that by tailoring catalyst surface properties and optimizing solvent interactions, it is possible to design a system that selectively adsorbs larger polymer molecules for catalytic breakdown while facilitating the desorption of smaller, processed molecules. To test this hypothesis, we synthesized polyethylene models to study the interactions between polymer, solvent, and support surfaces. To study polymer-solvent-support interactions effectively, we aim to track polymer species adsorption onto the catalyst surface, particularly when different molecular weights are involved (Chapter 2). To differentiate these interactions, we will use two polyethylene

(PE) models, each labeled to identify their adsorption and subsequent degradation behaviors. These models are modified with hexene and acetoxy groups, allowing us to examine adsorption-desorption dynamics within a single polymer species.

For a more complex analysis, we will study the competitive adsorption between high and low molecular weight PE species. The simultaneous presence of both polymers could influence adsorption and desorption patterns, potentially altering surface interactions. By labeling each polymer species distinctly using UV tags and deuterium labels, we can monitor adsorption events and detect degradation products. Analytical techniques, such as neutron scattering length density (NSLD) and UV-Vis spectroscopy, will enable us to determine product distribution. We will also characterize the low molecular weight products that result from the catalytic cracking process. Chapter 3 discusses the limitation of the high-temperature size exclusion chromatography in characterizing the molar masses and molar mass distributions of the products formed (usually a complex mixture of components) from the catalytic cracking processes. The accuracy and limitations of the commonly used triple detection high-temperature size exclusion chromatography (HT-SEC) to analyze the chemical recycling products will be discussed using short polyethylene and alkane models.

# CHAPTER TWO

# SYNTHESIS OF PE MODELS

**Abstract**

This research effort explores the synthesis of end-functionalized polyethylene models through ring-opening metathesis polymerization (ROMP) using the Grubbs 2nd generation **(G2)** catalyst. ROMP, a chain-growth polymerization technique, allows for the conversion of cyclic olefins into macromolecular structures, preserving unsaturation within the polymer backbone. Utilizing the **G2** catalyst, renowned for its stability and functional group tolerance, we achieved control over polymer structure, synthesizing various polyethylene models with specific end-functionalized groups. Through the strategic use of chain transfer agents (CTAs) such as trans-3-hexene, cis-1,4-diphenyloxybut-2-ene, and cis-1,4-dinaphthyloxybut-2-ene, we produced polymers ranging from 1 kg/mol to 10 kg/mol which were characterized via $^{1}H$ NMR and size exclusion chromatography (SEC) confirm the structure, molecular weight, and dispersity of these polymers.

The synthesized end-functionalized polyethylene models, bearing acetoxy, phenoxy, and naphthoxy groups, will be optimized for adsorption studies on catalytic surfaces. These models provide insights into selective adsorption and cracking mechanisms, which are critical for applications in catalysis and materials science. This study underscores the utility of ROMP, especially with the **G2** catalyst, in producing functionalized polymers with tailored properties.

## Introduction

### Ring-opening metathesis polymerization

Ring-opening metathesis polymerization (ROMP) has become a highly effective and versatile method for synthesizing macromolecular materials.[43] The development of well-defined metathesis catalysts that display high catalytic efficiency, functional group tolerance, air and moisture stability has enabled the synthesis of a wide variety of polymers with complex structures and valuable properties.[44, 45] It is a chain-growth polymerization process in which cyclic olefins are transformed into a polymeric material **(Fig. 2.1)**. The polymerization mechanism is based on olefin metathesis, a distinct metal-catalyzed process that involves the exchange of carbon-carbon double bonds. Notably, the unsaturation present in the monomer is retained in the polymer product, setting ROMP apart from conventional olefin addition polymerizations, such as the polymerization of ethylene into polyethylene.[44]

A general mechanism for ROMP is illustrated in **Fig. 2.2**. The process begins with the initiation step, where a transition metal alkylidene complex coordinates to a cyclic olefin. This is followed by a [2+2]-cycloaddition, resulting in the formation of a four-membered metallacyclobutane intermediate, which marks the start of the growing polymer chain. The intermediate then undergoes a cycloreversion, producing a new metal alkylidene complex. Although this complex is larger due to the incorporated monomer, it retains similar reactivity to the initial catalyst, allowing the propagation stage to continue as more cyclic olefins are added. The polymerization proceeds until it stops due to monomer

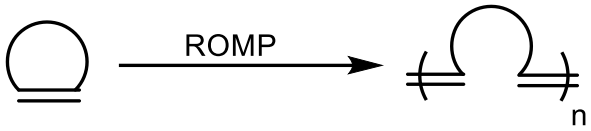


Figure 2.1 Schematic of ring-opening metathesis polymerization

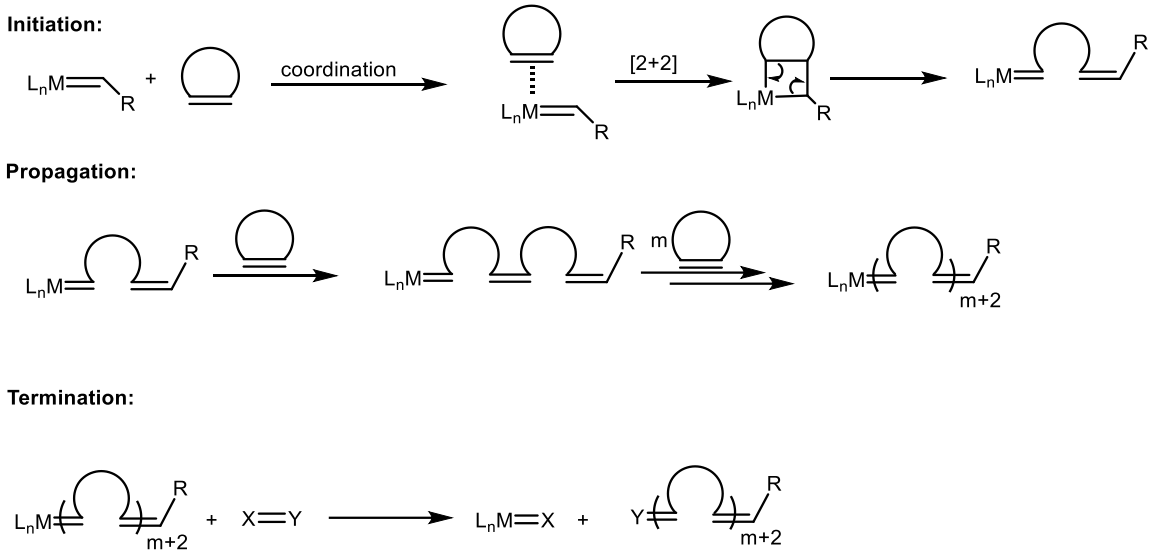


Figure 2.2 Mechanism of ring-opening metathesis polymerization

depletion, equilibrium, or termination. In ROMP, polymerization is often intentionally quenched by adding a specific reagent such as ethylvinyl ether. This reagent serves two purposes: (1) it selectively removes and deactivates the transition metal at the polymer chain's end, and (2) it introduces a known moiety in place of the metal.

When examining the metal-mediated and equilibrium characteristics of most ROMP reactions, it becomes clear that specialized metathesis catalysts are essential to meet specific requirements. These catalysts should: (1) efficiently and rapidly initiate into growing polymer chains, demonstrating fast kinetics; (2) facilitate polymerization with minimal chain transfer (either intramolecular or intermolecular) or premature termination; (3) interact with readily available terminating agents to enable selective end-functionalization; (4) exhibit good solubility in common organic solvents (or ideally, in aqueous media); and (5) possess high stability against moisture, air, and various common organic functional groups for practical applications. The early metathesis catalysts were poorly defined mixtures containing various metals, additives, and required specialized conditions. However, advances in catalysis have led to the development of a series of well-defined catalysts based on metals such as titanium, tantalum, tungsten, molybdenum, and ruthenium. Through further optimization, living ROMP catalysts incorporating most of these metals have been synthesized.

These catalysts are now widely used in many applications, particularly in the creation of macromolecular materials with unique physical and mechanical properties. It is also important to note that there is no "universal" catalyst, each having its own strengths and limitations. Given the wide array of catalysts available, one can typically identify a catalyst suited to a particular application or requirement.  For the synthesis of

polyethylene models for the adsorption studies related to our project Grubbs second generation **(G2)** catalyst was used. The **G2** catalyst is widely recognized as one of the most effective catalysts for ring-opening metathesis polymerization (ROMP) due to its stability, functional group tolerance, and enhanced reactivity. The incorporation of an N-heterocyclic carbene (NHC) ligand in **G2** significantly improves its stability and resistance to decomposition compared to the Grubbs 1st generation catalyst. This added stability allows **G2** to operate effectively in the presence of various polar functional groups, making it versatile for synthesizing complex polymers with functionalized side chains. Such tolerance enables the use of a wide array of monomers, broadening its applicability across fields like drug delivery and material science that makes **G2** ideal for ROMP is its ability to promote "living" polymerization, which ensures a high degree of control over molecular weight and polymer dispersity. The electron-rich NHC ligand increases the catalyst's initiation rate, allowing it to polymerize monomers more quickly and efficiently than the 1st generation catalyst.[46] This rapid initiation relative to the propagation rate is crucial for synthesizing well-defined polymers with narrow molecular weight distributions, making it optimal for applications that require precision, such as advanced material design and biomedical applications.[44, 47, 48]

**Chain Transfer Agents**

The use of chain-transfer agents (CTAs) to regulate polymer molecular weight and introduce functional groups at the polymer chain ends was widely practiced in other polymerization methods before being used in metathesis polymerization. Metathesis polymerization involves adding an acyclic olefin, which participates in cross-metathesis with the active chain-end **(Fig. 2.3)**. During this process, the polymer chain is detached

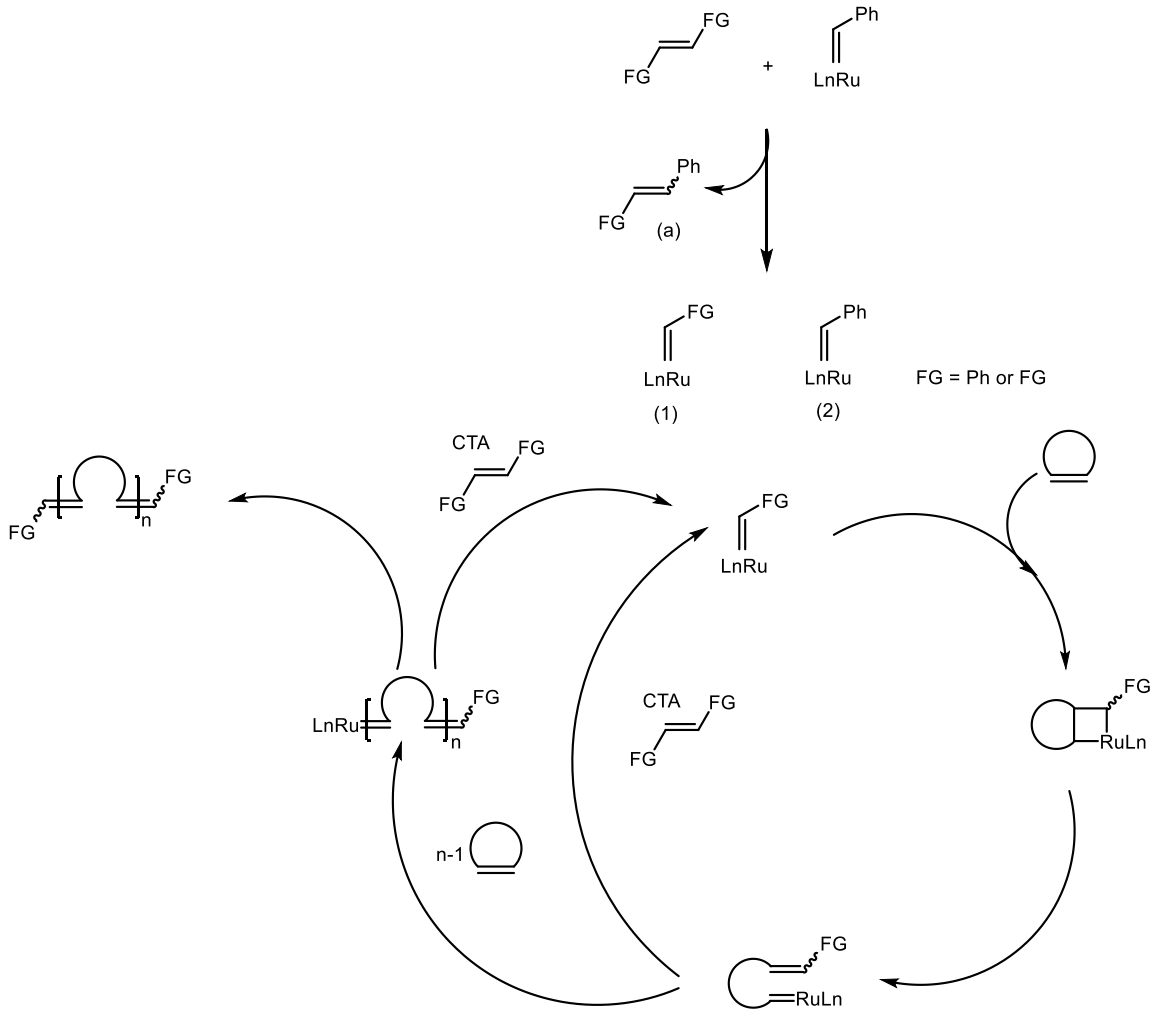


**Figure 2.3** Mechanism for the formation of telechelic polymers by application of chain-transfer agents (CTAs).

from the metal center, and a new polymer chain begins formed through the newly generated metal-carbene species.[49]

The use of chain-transfer agents (CTAs) in polymerization, especially in metathesis polymerization, has evolved significantly. Initially, CTAs were utilized in the synthesis of telechelic polymers with molybdenum and tungsten catalysts, with Schrock pioneering a method using olefin-substituted cyclopentene derivatives. Despite the initial inefficiency, later studies showed that activated improved cross-metathesis activity, leading to better incorporation in polymers like norbornene.[50] Ruthenium-catalyzed ROMP has become the most common method for adding reactive termini to polymer chain ends due to the high functional-group tolerance of ruthenium carbenes. Functional groups such as alcohol,[51] amines,[52] halides,[53] methacrylate, and epoxides[54] have been introduced into polymer chains, providing starting points for further functionalization or reactivity.[55]

Newer ruthenium catalysts with pyridyl ligands have been applied in pulsed-addition ROMP, significantly enhancing reactivity and selectivity.[56] However, molecular weight control in these methods is largely influenced by the reaction kinetics, with sterically demanding monomers leading to broad molecular weight distributions. Different chain transfer agents according to the need were synthesized and discussed later in the document.

**Synthesis of cis-1,4-dipheyloxybut-2-ene and cis-1,4-dinaphthyloxybut-2-ene**

Chain transfer agents were synthesized by modifying the protocols detailed in literature[57] as shown in **Scheme 2.1**. Phenol (1 g, 32 mmol) and potassium hydroxide (1.8 g, 32 mmol) were added to a 250 mL round bottom flask equipped with a magnetic stir

bar and dissolved in tetrahydrofuran (16 mL) and stirred under reflux at 65 °C for 30 minutes. The reaction mixture was cooled down to room temperature and cis-1,4-dichlorobut-2-ene (0.84 mL, 8 mmol) was added slowly. The resulting solution was stirred at 65 °C for 24 hours. Afterward, the precipitate was filtered off, and to the filtrate diethyl ether (50 mL) and water (50 mL) were added. After the transfer to a separatory funnel and shaking of the mixture, the layers were separated, and the aqueous layer was extracted with diethyl ether (3 x 50 mL). The combined organic layer was dried over magnesium sulfate, and filtered, and the solvent was removed under reduced pressure, The product was purified by column chromatography (hexane/ethyl acetate, 95:5, $R_f$ = 0.6) and obtained as a yellow liquid in 83% yield (1.595 g). The NMR spectrum matched prior literature reports.[57] $^1$H NMR (500 MHz, $CDCl_3$): $\delta$ = 4.69 (m, 4H), 5.95 (m, 2H), 6.90-6.99 (m, 6H), 7.27-7.32 (m, 4H). Cis-1,4-dinaphthyloxybut-2-ene was also synthesized following the same procedure.

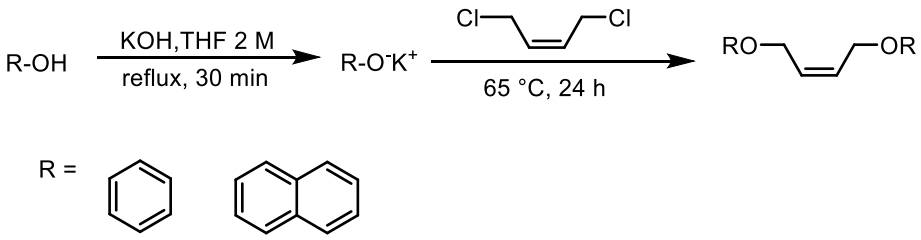


Scheme 2.1 Schematic of synthesis of chain transfer agents

**Synthesis of polyethylene, acetoxy, phenyl, and naphthyl end-functionalized polyethylene models**

After the successful synthesis and characterization of chain transfer agents, polyethylene models of different molecular weights and end-functionalization were

synthesized via ROMP **(Scheme 2.2)**. In a typical polymerization procedure, cyclooctene (1.5 g, 13.6 mmol) was added to a vial equipped with a magnetic stir bar in a glovebox. Solutions of **G2** (0.032 g, 0.0068 mmol) in 2.0 mL of chlorobenzene and trans-3-hexene (0.1 g, 0.68 mmol) in 1 mL of chlorobenzene were prepared in a separate vial, then added to the monomer. The reaction mixture was stirred at 30 °C for 24 h and quenched with ethylvinyl ether before precipitating the reaction mixture into excess methanol. The precipitate was filtered and dried under vacuum at room temperature overnight to yield 1.466 g of the polymeric product (97 %). $^{1}$H NMR ($CDCl_3$): 5.38 (m, 2 H), 1.96 (m, 4 H), 1.28 (m, 8 H), 0.96 (m, 6 H). Polyethylene models having acetoxy, phenoxy, and naphthoxy end groups were also synthesized by the same procedure using their respective CTAs.

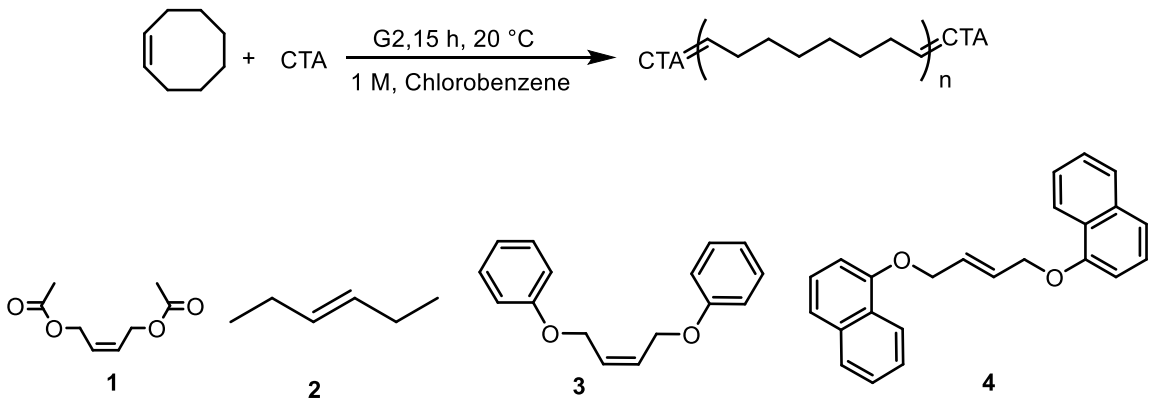


**Scheme 2.2** Schematic of polymerization with various chain transfer agents

## Results and Discussion

### Synthesis of cis-1,4-diphenyloxybut-2-ene and cis-1,4-dinaphthyloxybut-2-ene

As discussed earlier in the document, cis-1,4-diphenyloxybut-2-ene and cis-1,4-dinaphthyloxybut-2-ene were synthesized using a literature protocol.[57] I synthesized cis-

1,4-diphenyloxybut-2-ene and cis-1,4-dinaphthyloxybut-2-ene, which was confirmed with the help of $^{1}$H NMR spectroscopy. Synthesis confirmed from integrated peak areas corresponding to olefinic protons (at 5.9-6.0 ppm; labeled “b” in **Figures 2.4** and **2.5**), protons at the position alpha to oxygen (at 4.68-4.70 ppm and 4.91-4.93 ppm labeled “a” in **Figures 2.4** and **2.5** respectively) and aromatic protons (at 6.90-7.31 labeled “c and d" in **Figure 2.4** and 7.19-7.85 ppm labeled “c,d,e,f, and g” in **Figure 2.5** for cis-1,4-diphenyloxybut-2-ene and cis-1,4-dinaphthyloxybut-2-ene respectively.

**Synthesis of polyethylene and various end-functionalized polyethylene models**

Following the synthesis of chain transfer agents, acetoxy-functionalized polyethylene models were successfully synthesized using cis-1,4-diacetoxybut-2-ene as the chain transfer agent. These models exhibit molecular weights ranging from 2.7 to 10.8 kg/mol, as presented in **Table 2.1**. The polymer structure was verified using $^{1}$H NMR spectroscopy, which allowed for detailed assignment of proton environments. Specifically, the olefinic proton signals were observed at 5.33–5.43 ppm (denoted as “d” in **Figure 2.6**), while methylene protons appeared between 1.26–1.37 ppm (designated “a” in **Figure 2.6**). Additional resonance signals included protons adjacent to the olefinic and terminal functionalities, detected at 1.93–2.03 ppm (labeled “b” in **Figure 2.6**), and those near the oxygen atom of the acetoxy moiety, located at 4.48–4.51 ppm (labeled “c” in **Figure 2.6**). Moreover, distinct peaks at 5.51–5.52 ppm were attributed to isomeric protons associated with the olefinic region, labeled as “e” and “f” in **Figure 2.6**. This comprehensive spectral assignment confirms the successful integration of acetoxy functionalities into the polyethylene backbone.

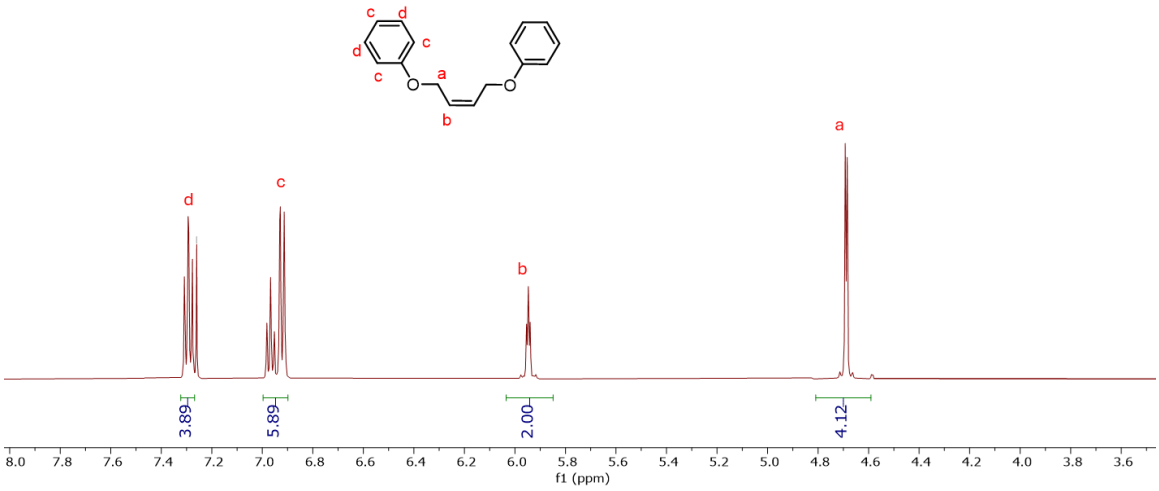


Figure 2.4 $^{1}$H NMR spectra of cis-1,4-diphenoxybut-2-ene

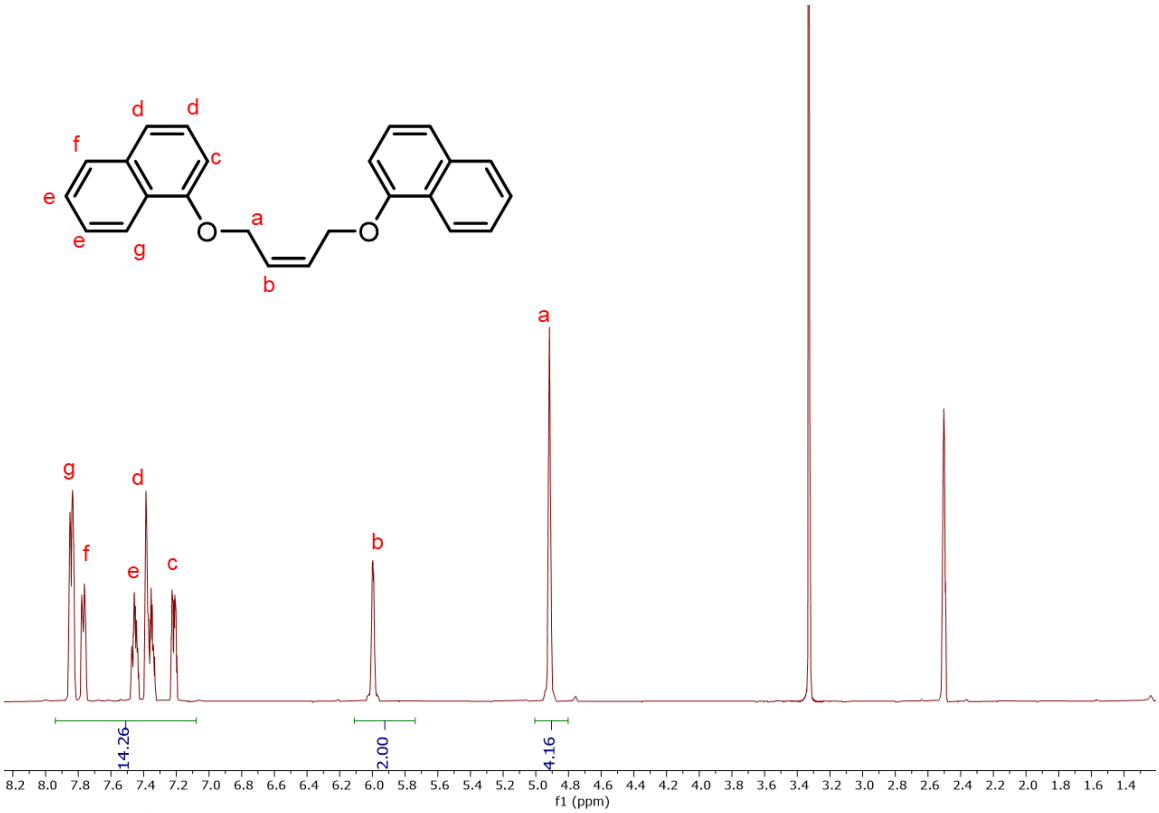


Figure 2.5 $^{1}$H NMR spectra of cis-1,4-dinaphthyloxybut-2-ene

**Table 2.1** Polymers with cis-1,4-diacetoxybut-2-ene before hydrogenation

| entry | ratio M:CTA:CAT | time (h) | % yield | $M_n^{theo}$ (kg/mol) | $M_n^{a}$ (kg/mol) | $Đ^{a}$ |
|---|---|---|---|---|---|---|
| 1 | 2000:450:1 | 24 | 91 | 0.6 | 2.7 | 1.3 |
| 2 | 2000:250:1 | 24 | 87 | 1.2 | 3.5 | 2.1 |
| 3 | 2000:150:1 | 24 | 93 | 2.3 | 4.4 | 2.7 |
| 4 | 2000:50:1 | 24 | 96 | 3.0 | 6.9 | 3.0 |
| 5 | 2000:30:1 | 24 | 89 | 4.5 | 10.8 | 3.1 |

Polymerization conditions: Grubbs Catalyst 2nd Gen (4.5 μmol), 14 mL of chlorobenzene, 30 °C, $t_{rxn}$ = 24 h, [a]Determined using EcoSEC GPC in tetrahydrofuran at room temperature

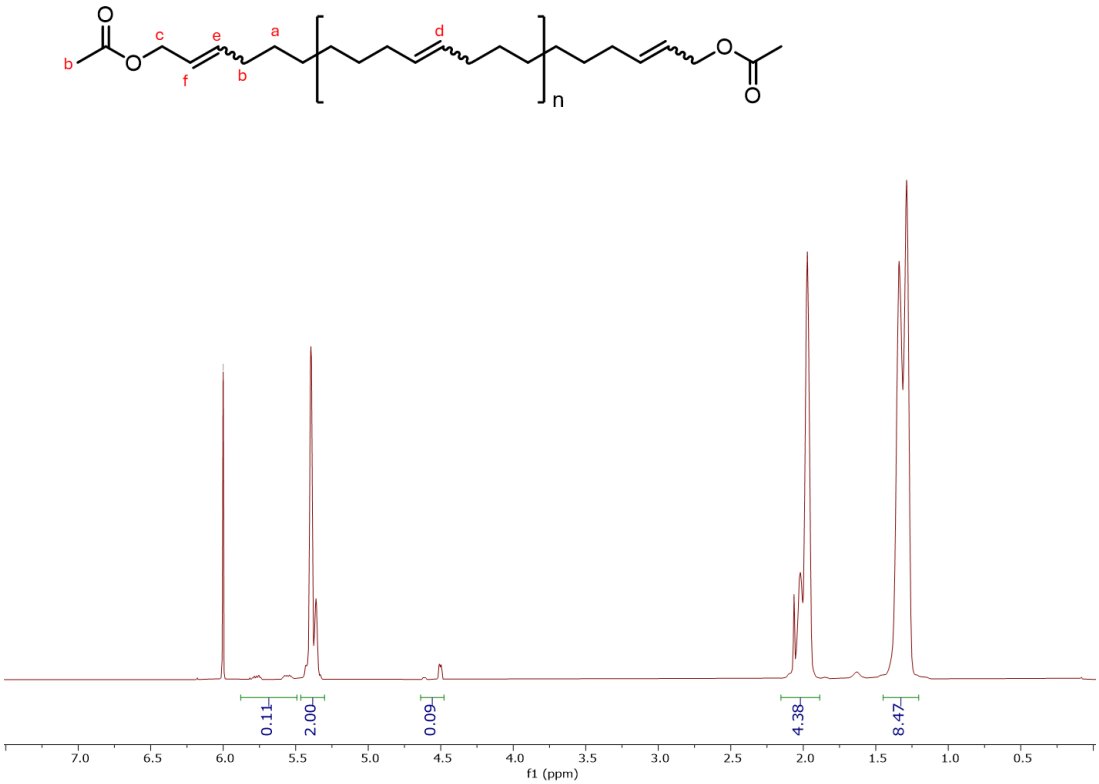


**Figure 2.6** General $^{1}$H NMR spectra of acetoxy end-capped PE taken in 1,1,2,2-tetrachloroethane

As discussed earlier in the document, access to various molecular weight regimes of polyethylene as well as telechelic polyethylene models will provide important insights for the selective cracking of polymer molecules over the catalyst surface. After successfully synthesizing acetoxy end-functionalized PE samples, I expanded the scope to produce PE models using trans-3-hexene as chain transfer agent to get the true polyethylene models after hydrogenation. Herein, polyethylene models of various molecular weight regimes were synthesized using the schemes mentioned above.
I synthesized samples ranging from 0.9 to 10.2 kg/mol for polyethylene. The complete set of data can be seen in **Table 2.2**. I was able to synthesize low to high molecular weight using trans-3-hexene as a chain transfer agent at the desired compositions. However, it was observed that with a decreasing monomer-to-chain transfer agent ratio molecular weight increased with dispersity stayed in the range of 1.9 to 2.2.

Following the successful synthesis of acetoxy end-capped PE and polyethylene, I proceeded to synthesize polyethylene models capped with phenoxy end groups using cis-1,4-diphenoxybut-2-ene as the chain transfer agent. The molecular weight of the resulting polymers ranged from 2.5 kg/mol to 6.6 kg/mol, as listed in **Table 2.3**. The confirmation of successful synthesis was achieved via $^{1}$H NMR spectroscopy. The NMR spectrum displayed integrated peak areas corresponding to the olefinic protons (5.32-5.41 ppm, labeled "d"), methylene protons (1.25-1.38 ppm, labeled "a"), protons adjacent to olefinic (1.91-2.04 ppm, labeled "b"), protons adjacent to the oxygen of the phenoxy group (4.50-4.53 ppm, labeled "c"), and aromatic protons (at 6.89-7.31 ppm; labeled “g” and “f”). Peaks at 5.50-5.53 ppm, labeled "e" and "f," in **Figure 2.8** were assigned to isomeric protons to the olefinic.

**Table 2.2** Polymers with trans-3-hexene CTA's before hydrogenation

| Entry | ratio M:CTA:CAT | time (h) | % yield | $M_n^{theo}$ (kg/mol) | $M_n^a$ (kg/mol) | $Đ^a$ |
|---|---|---|---|---|---|---|
| 1 | 2000:400:1 | 15 | 88 | 0.6 | 0.9 | 2.4 |
| 2 | 2000:100:1 | 15 | 97 | 2.3 | 4.9 | 1.9 |
| 3 | 2000:50:1 | 15 | 98 | 4.5 | 10.2 | 2.2 |

Polymerization conditions: Grubbs Catalyst 2nd Gen (4.5 μmol), 14 mL of chlorobenzene, 20 °C, $t^{rxn}$ = 15 h, [a] Determined using EcoSEC GPC in tetrahydrofuran at room temperature

$^1$H NMR was used to determine the success of synthesis. Synthesis of polycyclooctene before hydrogenation confirmed from integrated peak areas corresponding to olefinic protons (at 5.37-5.91 ppm; labeled "d" in " in the upper part of stacked spectra in **Figure 2.7**), methylene protons (at 1.23-1.37 ppm; labeled "a" in the upper part of stacked spectra in **Figure 2.7**), protons adjacent to olefinic protons (at 1.94-1.98 ppm; " in the upper part of stacked spectra in **Figure 2.7**) and terminal methylene protons (at 0.95-0.98 ppm; " in the upper part of stacked spectra in **Figure 2.7**). The unsaturated bonds along the polycyclooctene backbones were then reduced by diimide reduction and the resultant polymers were characterized by $^1$H NMR spectroscopy to confirm the removal of unsaturation along the polymer backbone. Disappearance of olefinic protons (at 5.37-5.91 ppm; labeled "d" in the upper part of stacked spectra in **Figure 2.7**) and protons adjacent to olefinic protons (at 1.94-1.98 ppm; labeled "b" in the upper part of stacked spectra in **Figure 2.7**) confirmed the reduction. Size exclusion chromatography (SEC) was used to measure the molecular weight and dispersity of each sample which can be found in **Table 2.2**.

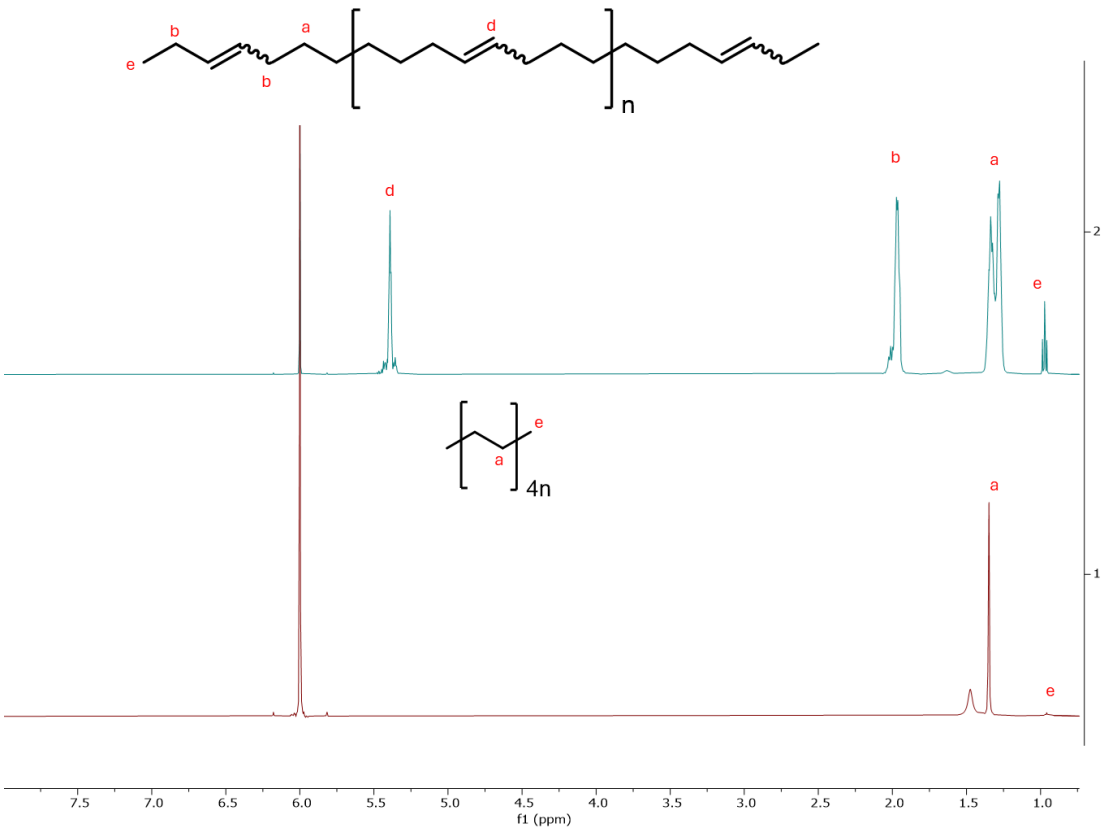


**Figure 2.7** Stacked $^{1}$H NMR spectra of polyethylene arranged such that the top is before hydrogenation and the bottom is after hydrogenation taken in 1,1,2,2-tetrachloroethane.

**Table 2.3** Polymers with cis-1,4-diphenyloxybut-2-ene CTA before hydrogenation

| Entry | Ratio M:CTA:CAT | time (h) | % yield | $M_n^{theo}$ (kg/mol) | $M_n^{a}$ (kg/mol) | $Đ^{a}$ |
|---|---|---|---|---|---|---|
| 1 | 2000:400:1 | 15 | 98 | 0.6 | 2.5 | 1.4 |
| 2 | 2000:300:1 | 15 | 99 | 0.9 | 2.9 | 1.5 |
| 3 | 2000:200:1 | 15 | 99 | 1.2 | 3.4 | 1.7 |
| 4 | 2000:150:1 | 15 | 99 | 1.6 | 4.6 | 1.7 |
| 5 | 2000:100:1 | 15 | 99 | 2.3 | 6.0 | 2.0 |
| 6 | 2000:50:1 | 15 | 98 | 4.5 | 6.6 | 2.7 |

Polymerization conditions: Grubbs Catalyst 2$^{nd}$ Gen (4.5 μmol), 14 mL of chlorobenzene, 30 °C, $t_{rxn}$ = 15 h, $^{a}$Determined using EcoSEC GPC in tetrahydrofuran at room temperature

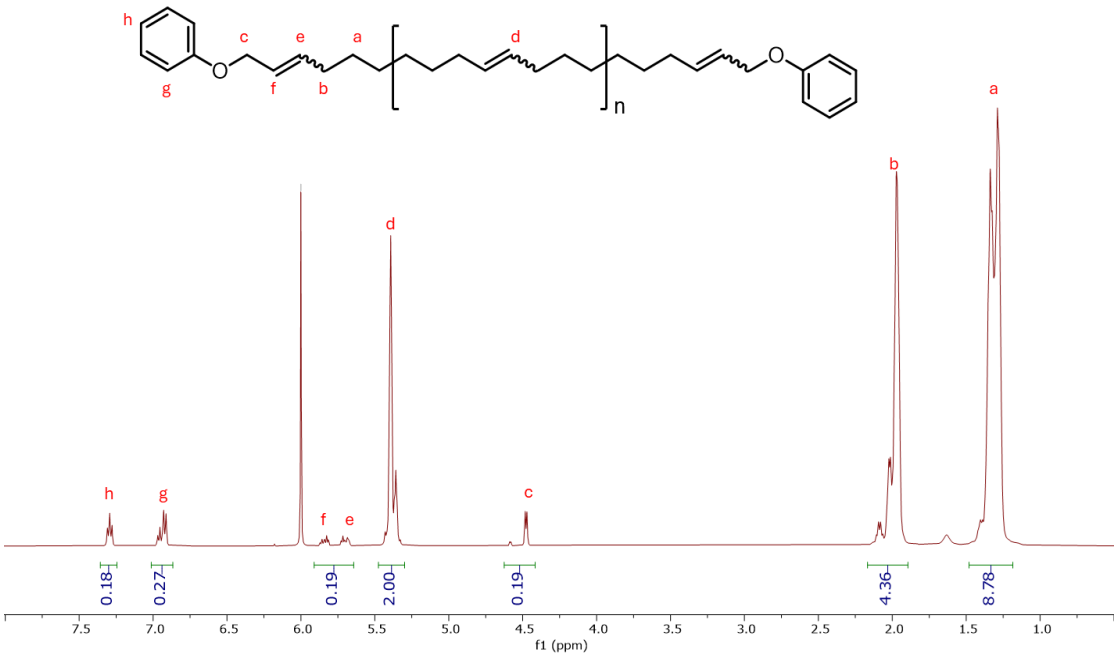


**Figure 2.8** General $^{1}$H NMR spectra of phenoxy end-capped PE taken in 1,1,2,2-tetrachloroethane

Following the successful synthesis of acetoxy end-capped polyethylene, I advanced to the synthesis of polyethylene models with naphthoxy end groups, using cis-1,4-dinaphthoxybut-2-ene as the chain transfer agent. The molecular weights of the synthesized polymers ranged from 2.8 kg/mol to 10.3 kg/mol, as detailed in **Table 2.4**. The synthesis was confirmed via $^{1}$H NMR spectroscopy, with peak integration revealing characteristic signals. The olefinic protons were observed at 5.34-5.43 ppm (labeled "d"), methylene protons appeared between 1.26-1.37 ppm (labeled "a"), and protons adjacent to the the olefinic were seen at 1.92-2.06 ppm (labeled "b") in **Figure 2.9**. Additionally, the protons next to oxygen of the naphthoxy groups resonated at 4.58-4.62 ppm (labeled "c"), while the aromatic protons of the naphthyl rings appeared between 7.12-7.80 ppm (labeled "g", “h”, “I”, and "j" in **Figure 2.9**). Peaks at 5.72-5.95 ppm labeled “e” and “f” were attributed to isomeric protons relative to the olefinic groups.

**Summary**

The synthesis of various polyethylene (PE) models with controlled molecular weights and end-functionalized chains was successfully achieved using ring-opening metathesis polymerization (ROMP) with chain transfer agents (CTAs). The results demonstrated that precise control over polymer properties, such as molecular weight and dispersity, can be achieved through systematic manipulation of the monomer-to-CTA ratio. The synthesized PE models were confirmed via $^{1}$H NMR spectroscopy and size exclusion chromatography (SEC), verifying their molecular weight and end-group functionality.

**Table 2.4** Polymers with cis-1,4-dinaphthyloxybut-2-ene CTA before hydrogenation

| Entry | Ratio M:CTA:CAT | time (h) | % yield | $M_n^{theo}$ (kg/mol) | $M_n^{a}$ (kg/mol) | $Đ^{a}$ |
|---|---|---|---|---|---|---|
| 1 | 2000:400:1 | 15 | 98 | 0.6 | 2.8 | 1.5 |
| 2 | 2000:300:1 | 15 | 99 | 0.9 | 5.7 | 1.9 |
| 3 | 2000:200:1 | 15 | 97 | 1.2 | 6.0 | 1.7 |
| 4 | 2000:150:1 | 15 | 94 | 1.6 | 3.4 | 1.6 |
| 5 | 2000:100:1 | 15 | 98 | 2.3 | 10.3 | 2.3 |

Polymerization conditions: Grubbs Catalyst 2nd Gen (4.5 μmol), 14 mL of chlorobenzene, 30 °C, $t_{rxn}$ = 15 h, [a]Determined using EcoSEC GPC in tetrahydrofuran at room temperature

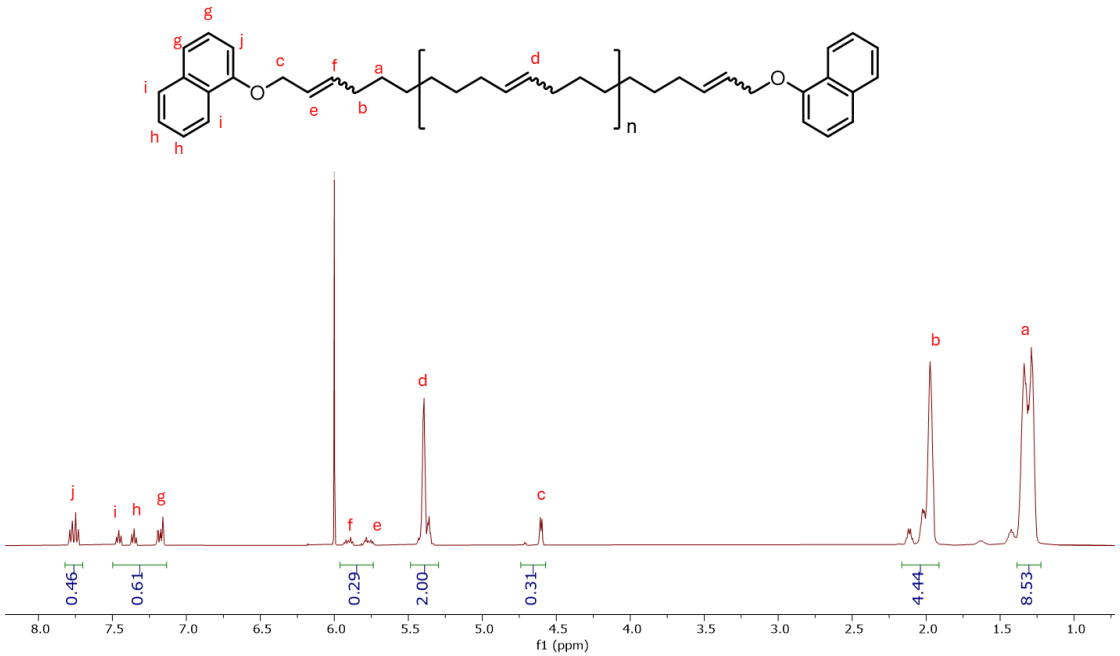


**Figure 2.9** General $^{1}$H NMR spectra for the naphthyloxy end-capped PE taken in 1,1,2,2-tetrachloroethane

Additionally, the introduction of functional end-groups, such as acetoxy and naphthyl groups, provides valuable tools for investigating selective polymer interactions with catalyst surfaces. These end-functionalized PE models serve as a foundation for further studies on the adsorption of polymer chains onto catalysts, which is crucial for optimizing polymer cracking processes. This chapter sets the stage for future research aimed at enhancing chemical recycling techniques by utilizing these well-defined polymers to improve catalyst design, thereby enabling more efficient and selective polymer degradation. The successful synthesis of these PE models marks a significant advancement in the understanding of polyolefin behavior during recycling and their potential conversion into valuable chemical products, paving the way for more sustainable plastic waste management solutions.

# CHAPTER THREE

# HIGH TEMPERATURE EXCLUSION CHROMATOGRAPHY FOR ADVANCED RECYCLING: SYSTEMATIC ERRORS IN ANALYSIS OF POLYETHYLENE-ALKANE MIXTURES

**Abstract**

Polyolefins, which dominate the plastic marketplace, require high-temperature size exclusion chromatography (HT-SEC) to characterize their molar masses and molar mass distribution. Chemical recycling methods designed to break down plastic waste into smaller molecules (i.e. depolymerization methods) similarly rely on size exclusion chromatography (SEC) to characterize the resulting product, but the reduction in molecular size achieved through depolymerization often yields a complex mixture of components. Some of these components are below the typical reported separation range of common HT-SEC columns. Herein, we report on our investigation of the accuracy and limitations of using triple detection HT-SEC to analyze chemical recycling products. We examined the chromatographic separation and quantification of individual components and mixtures of short polyethylene ($M_n$ = 1900 and 4400 g/mol), hexatriacontane ($C_{36}H_{74}$, $M$ = 507 g/mol), dotriacontane ($C_{32}H_{66}$, $M$ = 451 g/mol), octadecane ($C_{18}H_{38}$, $M$ = 254 g/mol). Despite hexatriacontane and the shorter alkanes exhibiting molar masses below the cut-off reported for the columns used, their mixtures could be distinguished when using a refractive index (RI) detector with two distinct peaks resolved for hexatriacontane-octadecane mixtures. However, the molar masses and the composition of these alkane mixtures determined from analysis of the SEC data did not agree with the known molar masses of intentionally prepared mixtures. Similarly, SEC analysis of mixtures containing discrete alkanes with low molar mass PE models revealed that their components in the mixture are not quantifiable by HT-SEC. The RI intensity measured suggests a lower concentration of the alkane than in the known mixture, leading to inaccurate molar masses and molar mass distributions. These inaccuracies are attributed

to the changing contrast (*dn*/*dc*) for the alkanes and solvation of the polyethylene by the alkanes in the solution. This later effect is hypothesized to cause the alkanes to elute at shorter retention times in mixtures with polyethylene relative to the single component retention times. These results illustrate the need for particular care when interpreting product identity and distributions for complex mixtures, particularly those resulting from chemical recycling and depolymerization of plastic waste.

**Introduction**

Mismanaged plastic waste in the environment[58] combined with poor recycling rates for most plastics[6] has initiated significant research efforts to develop alternative routes to improve the circularity of carbon contained within commodity plastic waste streams. The final disposition for plastics products is primarily landfilling,[59] but similar amounts of plastic waste are also commonly incinerated for energy or mismanaged and leaked into the environment as plastic waste from recycling streams.[60] The overall recycling rate for plastics is less than 9%;[6] this is dominated by mechanical recycling of a select few plastic.[61] However, mechanically recycled plastics are limited by (1) chain scission that occur during processing and re-extrusion[62] and (2) sorting of the plastic to avoid contamination and secondary phases.[63]

The convergence of plastic waste remediation issues with environmental, social, and governance (ESG) demands of stakeholders and governmental initiatives[64] has revitalized interests in chemical recycling of plastic waste.[65] In these processes, the plastic is ideally converted back to its original monomers to provide a route for all carbons within plastics to remain in circulation indefinitely, thus providing circularity to the plastics economy.[66] For condensation polymers like poly(ethylene terephthalate)

(PET), the functional groups contained within the polyester backbone provide obvious handles for depolymerization,[67] which has recently been scaled up for commercialization.[68] However, most plastics are produced by chain growth polymerizations of vinyl- or olefin-containing monomers. These polymers tend to undergo undesirable side reactions (e.g. decomposition) at temperatures at or below their ceiling temperature, making chemical depolymerization back to monomer difficult.[66]

Due to this challenge in depolymerization, catalytic upcycling of polyolefins to high value small molecules has gained significant momentum.[69-73] These strategies tend to rely on a cascade of reactions to break high molar mass polyolefins into smaller molecules.[74,75] Upcycling of polyolefin waste[76] to value-added products, including lubricants,[69] long-chain alkylaromatics,[77] and fuels,[78] has been demonstrated at the laboratory scale. However, the high molar mass of commercial grade polyolefins tends to make these reactions mass transfer limited. This leads to long reaction times and wide product distributions that often include small polymers mixed with a variety of liquid and solid alkanes. The reaction cascade during depolymerization can involve chain scission along with bond reformation, generating branched molecules.[79] Understanding the prevalence of these diverse components requires examination of the full distribution of molecular masses, not just average characteristics (moments) of the distribution.[79]

High-temperature SEC (HT-SEC), which was originally developed for the characterization of commercial polyolefins, is commonly employed to characterize these products **(Figure 3.1)**. However, the detection of molecules by SEC is limited by the characteristics of the columns and detectors used. Polymer detection typically involves monitoring changes in the refractive index (RI), viscosity, absorption in the UV, and/or

light scattering. Light scattering detectors are particularly useful because the combination of these techniques allows practitioners to determine the absolute molar mass, which corresponds to elution time, without the need to generate calibration curves from external standards. For an accurate determination of the distribution, the polymer needs to not interact with the column so that the separation is driven by the accessibility of the polymers to different sizes of pores in the column; this results in longer retention times for the smaller molecules. Thus, the range of molar masses that can be accurately determined depends on the column(s) used in the SEC. The polymer molecular mass distribution is generally determined from the change in RI as a function of elution time where the absolute change in RI is proportional to the concentration and the molar mass at this elution time is determined from light scattering or calibration standards. However, the options of size range for high-temperature columns are quite limited, especially with respect to low molar mass species that would be appropriate for the products from the catalytic conversions of polyolefins to lower molar mass species.

There is a significant disparity between the reported molar mass range for columns typically used with commercial high-temperature SEC systems and the resulting product distributions found from polyolefin upcycling efforts. This disconnect raises questions about the accuracy of these chromatographic systems for evaluating polyolefin upcycling reactions. For example, if separation is poor, molecules smaller than the column's lower separation size limit may elute at the same time. This could explain the emergence of narrow product distributions reported for catalytic polyolefin depolymerization reactions.[73, 80] but the elution time for the peak in SEC has been

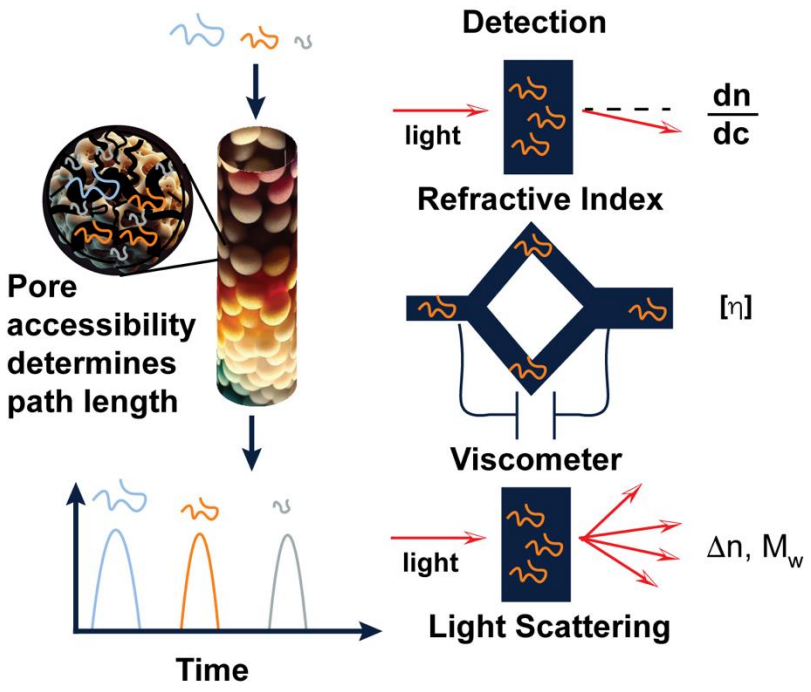


**Figure 3.1** Illustration showing the mechanisms for separation and detection of polymers using SEC. The elution time is inversely proportional to the hydrodynamic radius of the polymer in solution for polymers with molecular masses within the separation range of the column.

reported to be dependent on the reaction conditions, which indicates some separation and has been taken as evidence of the SEC providing a quantitative measure of the depolymerization products, including oligomers, from polyolefins.[81]

Although SEC data for compounds smaller than the established manufacturer molecular mass limits is commonly reported,[73, 79, 81] rigorous analysis validating the quantitative assessment of oligomeric polyolefins is lacking. Herein, we seek to understand and highlight the consequences of separating mixtures comprised of both short polyethylenes and well-defined alkanes using high-temperature SEC. With growing polyolefin depolymerization and chemical recycling efforts,[82] understanding the limits of HT-SEC for these compounds will be critical to prevent inaccurate conclusions about the quantitative distribution of depolymerization products. The findings described below emphasize the need for researchers to critically assess the interpretation of HT-SEC data and consider the impact of smaller molecules in their product mixtures when evaluating HT-SEC data.

**Materials and methods**

All manipulations were carried out under an atmosphere of nitrogen using standard Schlenk technique or in an inert atmosphere using an MBraun glovebox filled with nitrogen gas, unless otherwise noted. Cyclooctene (COE) and trans-3-hexene were purchased from Thermo Scientific Chemicals and purified via vacuum distillation from $CaH_2$, degassed using iterative freeze-pump-thaw cycles (3´), and stored in the glovebox prior to use. The catalyst [1,3-bis-(2,4,6-trimethylphenyl)-2-imidazolidinylidene] dichloro(phenylmethylene)(tricyclohexylphosphino) ruthenium (Grubbs 2$^{nd}$ Gen (**G2**)) was purchased from Millipore Sigma, stored in a glovebox, and used as received.

Dichloromethane ($CH_2Cl_2$) was purchased from Fischer Scientific, dried via passage through an Innovative Technologies PurSolv solvent purification system, and degassed via iterative freeze-pump-thaw cycles (3´) prior to use. Chlorobenzene was purchased from Fischer Scientific, dried over 4 Å molecular sieves, and degassed via iterative freeze-pump-thaw cycles (3´) prior to use. Tetrahydrofuran (THF), methanol, xylenes, and 1,1,2,2-tetrachloroethane-$d_2$ ($C_2D_2Cl_4$) were purchased from Fischer Scientific and used as received. Hexatriacontane ($C_{36}H_{74}$, 98%), dotriacontane ($C_{32}H_{66}$, 97%), and octadecane ($C_{18}H_{38}$, 99%) were purchased from Millipore Sigma and used as received. $^1$H NMR spectra of all monomers and polymers were obtained in 1,1,2,2-tetrachloroethane-$d_2$ ($C_2D_2Cl_4$) using a Bruker 500 MHz spectrometer and referenced to the residual $C_2D_2Cl_4$ peak.

All components were analyzed by size exclusion chromatography (SEC) using 1,2,4-trichlorobenezene (TCB), which is stabilized by butylated hydroxytoluene (BHT) (100 ppm), as the eluent using a Malvern Viscotek 350B High-Temperature SEC equipped with one TSKgel $H_{HR}$ (S) HT2 guard column and two TSKgel $GMH_{HR}$-H (S) HT2 SEC columns that are heated at 150 °C and at a flow rate of 1.0 mL/min. The injection volume was 200 µL. Molar mass ($M_n$) and dispersity ($Đ = M_w/M_n$) data are reported using triple detection: refractive index, viscometer, and light scattering detectors. $M_n$ and $M_w/M_n$ values were obtained using the OMNISEC software, and the triple detection system was calibrated using a narrow dispersity polystyrene ($M_n$ = 105 kg/mol) standard.

The non-polymeric alkanes were also analyzed with gas chromatography (Agilent 6890 N GC) using a methyl silicone capillary column (Agilent HP-1; 50 m ´ 0.32 mm ´

1.05 μm) and flame ionization detection (FID). The FID was calibrated using a series of n-alkanes from decane to hexatriacontane with an internal standard of dodecane to determine the size dependent retention factor (**Figure B1**).

**Synthesis of polyethylene model 1 (PE1).**

In a nitrogen filled glovebox, cyclooctene (1.5 g, 13.6 mmol) and chlorobenzene (12.7 mL) were added to a vial equipped with a magnetic stir bar. A solution of **G2** (5.8 mg, 0.0068 mmol), trans-3-hexene (0.057 g, 0.68 mmol), and chlorobenzene (0.93 mL) was prepared in a separate vial, and added in a single portion to the vial containing the monomer. The reaction mixture was sealed and stirred at 25 °C for 15 h before being quenched by injection of ethylvinyl ether and the resultant polymer precipitated by dropwise addition to excess stirring methanol. The precipitate was filtered and dried under vacuum at room temperature overnight to yield polycyclooctene (1.466 g, 97 % yield). The alkenes along the polycyclooctene backbone were then reduced by diimide reduction using the following procedure. Polycyclooctene (1 g, 9.1 mmol) and toluenesulfonylhydrazide (5.1 g, 27.3 mmol) were added to a flask containing xylenes (40 mL) and a magnetic stir bar, which was then heated at 140 °C for 24 h before being cooled to room temperature and the polymeric product precipitated into excess stirring methanol. The precipitate was filtered and dried under vacuum at room temperature overnight to yield low molar mass, narrower dispersity, linear polyethylene model **PE1** (0.789 g, 77% yield). HT-SEC (TCB, 150 °C): $M_n$ =4.4 kg/mol, $Đ$ = 1.34; $^1$H NMR ($C_2D_2Cl_4$) d: 1.33-1.37 (m, $CH_2$), 0.94-0.98 (t, $CH_3$). **Figure B2** illustrates the $^1$H NMR trace for **PE2**.

**Synthesis of polyethylene model 2 (PE2).**

In a nitrogen filled glovebox, cyclooctene (0.75 g, 6.8 mmol), trans-3-hexene (0.057 g, 0.68 mmol), and DCM (7 mL) were added to a vial equipped with a magnetic stir bar. A solution of **G2** (0.2 g, 0.24 mmol) in DCM (4.0 mL) was then prepared in a separate vial. A portion of the **G2** solution (115 μL) was added to the vial containing the monomer and chain transfer agent. The reaction mixture was sealed and stirred at 30 °C for 24 h before being quenched by injection of ethylvinyl ether and the resultant polymer precipitated by dropwise addition to excess stirring methanol. The precipitate was filtered and dried under vacuum at room temperature overnight to yield polycyclooctene (0.5251 g, 70 % yield). The alkenes along the polycyclooctene backbone were then reduced by diimide reduction using the following procedure. Polycyclooctene (0.400 g, 3.6 mmol) and toluenesulfonylhydrazide (2.03 g, 10.9 mmol) were added to a flask containing xylenes (20 mL) and a magnetic stir bar, which was then heated at 140 °C for 24 h before being cooled to room temperature and the polymeric product precipitated into excess stirring methanol. The precipitate was filtered and dried under vacuum at room temperature overnight to yield low molar mass, broader dispersity, linear polyethylene model **PE2** (0.306 g, 76.5% yield). HT-SEC (TCB, 150 °C): $M_n$ =1.9 kg/mol, $Đ$ = 2.28; $^1$H NMR ($C_2D_2Cl_4$) d: 1.33-1.37 (m, $CH_2$), 0.94-0.98 (t, $CH_3$). **Figure B3** illustrates the $^1$H NMR trace for **PE2**.

**Results and discussion**

We investigated the limits of SEC detection using a set of general-purpose SEC columns (TSKgel $GMH_{HR}$-H (S) HT2) to analyze a series of model compounds comprised of short polyethylene and alkanes; all were either commercially available in

pure form or readily synthesized. Commercially available models include linear alkanes: hexatriacontane ($C_{36}H_{74}$, $M_n$ = 507 g/mol) (**C36**), dotriacontane ($C_{32}H_{66}$, $M_n$ = 451 g/mol) (**C32**), and octadecane ($C_{18}H_{38}$, $M_n$ = 254 g/mol) (**C18**). These short alkanes are representative compounds commonly found in product distributions from polyolefin hydrogenolysis and hydrocracking reactions.[69, 70, 73, 82, 83] More importantly, these alkanes are readily available at low cost to enable us to probe SEC separations using well-defined mixtures of linear alkanes and/or polyolefins.

Short polymeric polyethylene models were synthesized as illustrated in **Scheme 3.1**. First, we employed cyclooctene ring-opening metathesis polymerization (ROMP) using Grubb's second-generation catalyst (**G2**) in the presence of trans-3-hexene. Trans-3-hexene acts as a chain-transfer agent to regulate the molar mass of the resultant polyethylene, restricting the products to short oligomer/polymer chains. The residual unsaturated bonds from the ROMP polymerization were then reduced via diimide reduction using toluenesulfonylhydrazide at 140 °C in xylenes for 24 h, yielding the linear polyethylene models **PE1** and **PE2**. The synthesized polymers were characterized with $^1$H NMR spectroscopy to confirm alkene removal **(Figures B2** and **B3),** and HT-SEC to determine the molar mass and dispersity. The synthesized polyethylene models are characterized as a narrow dispersity sample (**PE1**: $M_n$ = 4.4 kg/mol and $Đ$ = 1.34) and a lower molar mass broad dispersity sample (**PE2**: $M_n$ = 1.9 kg/mol and $Đ$ = 2.28).

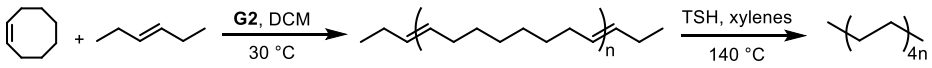


**Scheme 3.1** Synthesis of low molar mass, linear PE models **PE1** and **PE2** using ROMP in the presence of a chain-transfer agent followed by diimide reduction.

Purity of the commercially obtained **C36** ($C_{36}H_{74}$, $M_n$ = 507 g/mol), **C32** ($C_{32}H_{66}$, $M_n$ = 451 g/mol), and **C18** ($C_{18}H_{38}$, $M_n$ = 254 g/mol) samples was confirmed with GC **(Figure 3.2a** and **Figure B4)**, which revealed single sharp peaks in the gas chromatograms. **Figure 3.2b** shows single component HT-SEC analyses of the individual hydrocarbons, using sample concentrations of ≈10 mg/mL and injection volumes of 200 μL. HT-SEC was able to distinguish **C18** from **C32** and **C36**, but **C32** and **C36** had nearly identical retention times. The peaks from HT-SEC are significantly broadened due to band broadening in comparison to the GC peaks for the same molecules.

We routinely found the hydrocarbon molar masses determined by HT-SEC using light scattering were significantly lower than the true molar mass values. For example, HT-SEC determined the molar masses of **C36** and **C32** to be approximately 1/3 of their true molar masses (**Table 3.1**); the molar mass for **C18** was determined from light scattering to be only 56 g/mol – roughly the equivalent molecular weight of butane. Molar mass determination from light scattering arises from the application of a virial expression with fluctuation theory to describe the angular and concentration dependence of scattered light.[84] This results in a simple expression for the molecular weight (M):

$$\frac{1}{M} = \lim_{c \to 0} \frac{Kc}{R_\theta} \quad (1)$$

with $K \propto \left(\frac{dn}{dc}\right)^2$, $n$ is the refractive index, $R_\theta$ is the Raleigh ratio, and $c$ is the concentration. While any concentration unit can be used, a mass concentration (e.g. mg/mL) conveniently accounts for differences in molar mass between components and simplifies the analysis.

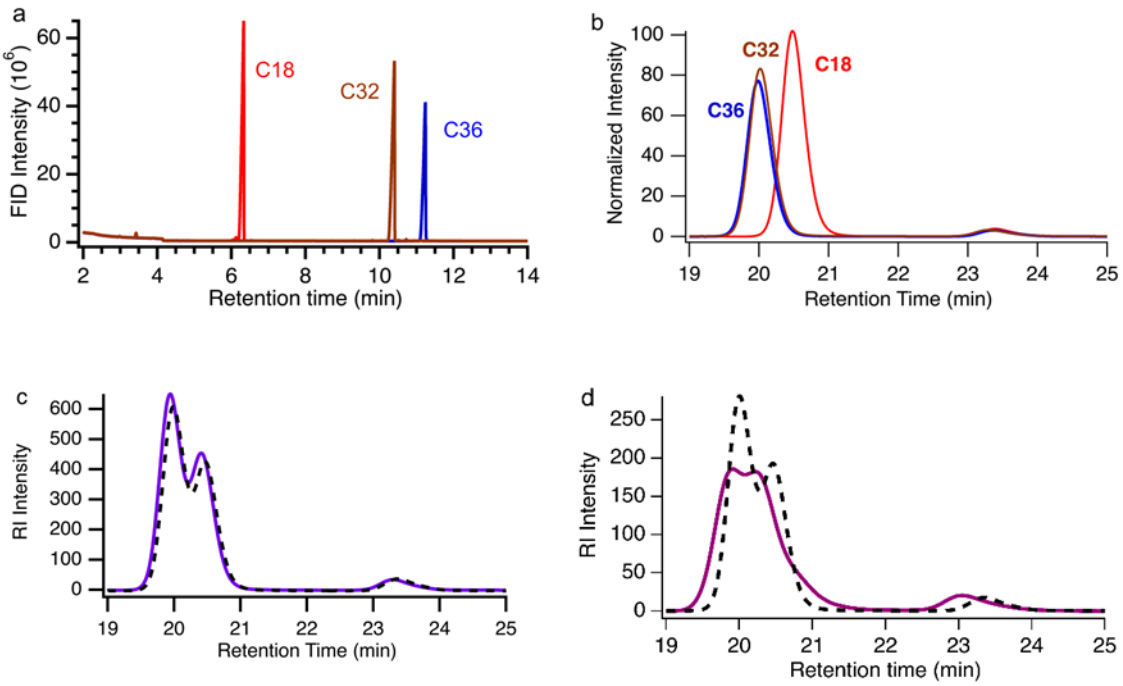


**Figure 3.2** (a) Overlaid gas chromatograms using toluene as carrier solvent and (b) overlaid HT-SEC traces for **C18**, **C32** and **C36** in 1,2,4-trichlorobenzene at 150 °C. The RI intensity in the HT-SEC traces is normalized by alkane concentration in mg/mL. HT-SEC traces for blends of (c) 1:1 mol:mol **C18**:**C36** and (d) 1:1:1 mol:mol:mol **C18**:**C32**:**C36**. The measured traces (solid lines) are compared to predicted profiles using concentration weighted averages (black dashed lines) of individual component HT-SEC traces (as shown in b).

**Table 3.1** Molar mass determined for alkanes and polymers from HT-SEC using light scattering for absolute molecular weight.

| Sample | Exact $M_n$ (g/mol) | HT-SEC[a] $M_n$ (g/mol) | $Đ$[a] |
|---|---|---|---|
| **C18** | 254.5 | 56 | 1.13 |
| **C32** | 450.9 | 134 | 1.09 |
| **C36** | 507.0 | 165 | 1.15 |
| **PE1** | --- | 4400 | 1.34 |
| **PE2** | --- | 1900 | 2.28 |

[a]Determined using triple detection HT-GPC at 150 °C in 1,2,4-trichlorobenzene.

The intensity, *I*, from the RI detector used to generate the traces shown in **Figure 3.2b** is defined as:

$$I = K_{RI} \cdot \left(\frac{dn}{dc}\right) \cdot c \qquad (2)$$

where $K_{RI}$ relates to the sensitivity of the RI detector and is distinct from *K* in equation 1. The refractive index increment, *dn/dc*, is a key property required to calculate the molar mass and the molecular weight distribution from the intensity, as one generally assumes $I \propto c$.[85] The RI intensity data presented in Figure 2b is normalized by the concentration of the alkane (mg/mL) in the solution injected into the HT-SEC column. Thus, if *dn/dc* is constant, the mass normalized peak area should be the same for the three molecules. However, the peak area for **C18** is nearly 30% greater than that for **C36**, indicating *dn/dc* is size dependent for these alkanes. As the molar mass of polymers becomes small, the *dn/dc* is known to become dependent on $M_n$.[85] We note that specific *dn/dc* are not commonly reported with **SEC** data in polyolefin upcycling.

SEC characterization quality, a series of well-defined mixtures of the three molecular compounds were examined. **Figure 3.2c** illustrates the HT-SEC trace for a 1:1 (mol:mol) mixture of **C18** and **C36** prepared at a total concentration of 11.8 mg/mL. The resulting chromatogram displays a broad bimodal trace. The predicted curves (dashed lines in **Figure 3.2c**) are determined simply by multiplying the normalized traces of the individual components **(Figure 3.2b)** by their absolute concentration in the injection mixture and summing these for all components. This weighting of the individual components leads to good agreement with the measured traces for this mixture (solid

lines in **Figure 3.2c**). Similar results were found for a 1:1 (mol:mol) **C32**:**C36** mixture, as shown in **Figure B6**.

This agreement illustrates that, at least for the column and detection system we employed, the HT-SEC can reproducibly separate equimolar binary alkane mixtures. However, when the concentration of the two components was varied, agreement between the measured HT-SEC trace and the predicted chromatogram based on the chromatograms measured for the individual components decreases tremendously, as shown in **Figure B7**.

**Figure 3.2d** shows the HT-SEC trace for a 1:1:1 (mol:mol:mol) mixture of **C18**, **C32**, and **C36** at a concentration of 12.2 mg/mL. The shape of the curve is qualitatively different than the expected curve from the weighted average of the traces based on the individual components. A similar disagreement is found for a ternary mixture prepared at a 1:1:1 (wt:wt:wt) ratio as shown in **Figure B8**. These results again suggest a composition dependence to the RI response in the HT-SEC for these model alkanes that depends on the relative fraction of small and long alkanes. This is not a total concentration effect, as varying the concentration for an alkane blend from 2.8 to 11.8 mg/mL leads to the same trace when normalized by concentration **(Figure B9)**.

These complications are dramatically exacerbated for the alkane blends. **Table 3.2** and **Table B1** compare the known mixture $M_n$ and $Đ$ values to values determined from HT-SEC. Substantial determinate errors in the measured single component molar mass values (systematic under-measurement of $M_n$) carry through to the mixtures. The measured dispersity values of known mixtures are substantially larger than the true values. In the context of a polyolefin upcycling experiment, the measured values show a

**Table 3.2** Molecular mass for equimolar mixtures from theoretical calculation based on pure alkanes, calculated from SEC of individual components, and measured with HT-SEC using light scattering for absolute molecular weight.

| Sample[a] | Exact $M_n$[b] (g/mol) | Exact $Đ$[b] | Calculated $M_n$[c] (g/mol) | HT-SEC $M_n$[d] (g/mol) | HT-SEC $Đ$[d] |
|---|---|---|---|---|---|
| **C18:C32** | 352.6 | 1.08 | 95.0 | 72 | 1.16 |
| **C18:C36** | 380.7 | 1.11 | 110.5 | 105 | 1.25 |
| **C32:C36** | 478.9 | 1.00 | 149.5 | 151 | 1.22 |
| **C18:C32:C36** | 403.2 | 1.07 | 118.3 | 109 | 1.35 |

[a]All samples are either 1:1 or 1:1:1 molar ratio (equimolar) mixtures. [b]Exact $M_n$ of the equimolar mixture was calculated based on the exact known masses of the pure components (reported in Table 1). [c]$M_n$ of the equimolar mixture determined from the HT-SEC measured masses (reported in Table 1). [d]HT-SEC $M_n$ values were measured using triple detection HT-GPC at 150 °C in 1,2,4-trichlorobenzene.

wider distribution of substantially shorter alkanes than are truly present in the analyte. It appears this can be accounted for by calibrating with the poor $M_n$ determinations using single components; however, given the complexity of the analytes examined in polyolefin upcycling, it will remain difficult to distinguish between a broadly eluting pure component and a mixture of components. Uncorrected HT-SEC data could therefore lead to significant systematic errors in evaluating the low end of polymer upcycling catalysis product distributions.

HT-SEC is more commonly used to characterize polyolefins, which have much larger average hydrodynamic radii than the model alkanes examined in **Figure 3.2**. Polymers tend to exhibit properties that are constant at sufficiently high molar mass.[85] Examples include glass transition temperature ($T_g$), crystallization temperature ($T_m$), and, generally, *dn*/*dc*. This enables the RI signal from SEC to be directly correlated with the concentration of polymers at a specific elution time.[85] **Figures 3.3a** and **3.3b** show representative HT-SEC traces for **PE1** ($M_n$ = 4.4 kg/mol and $Đ$ = 1.34) and **PE2**, which has a lower molar mass but a much broader distribution ($M_n$ = 1.9 kg/mol, $Đ$ = 2.28). The traces were normalized by their solution concentration (2.67 and 3.17 mg/mL, respectively). In the context of polyolefin upcycling measurements, these are low molar mass polymers that might be found at the tail of an HT-SEC analysis of polyethylenes; elution times for these small polymers approach the elution time for **C36**.

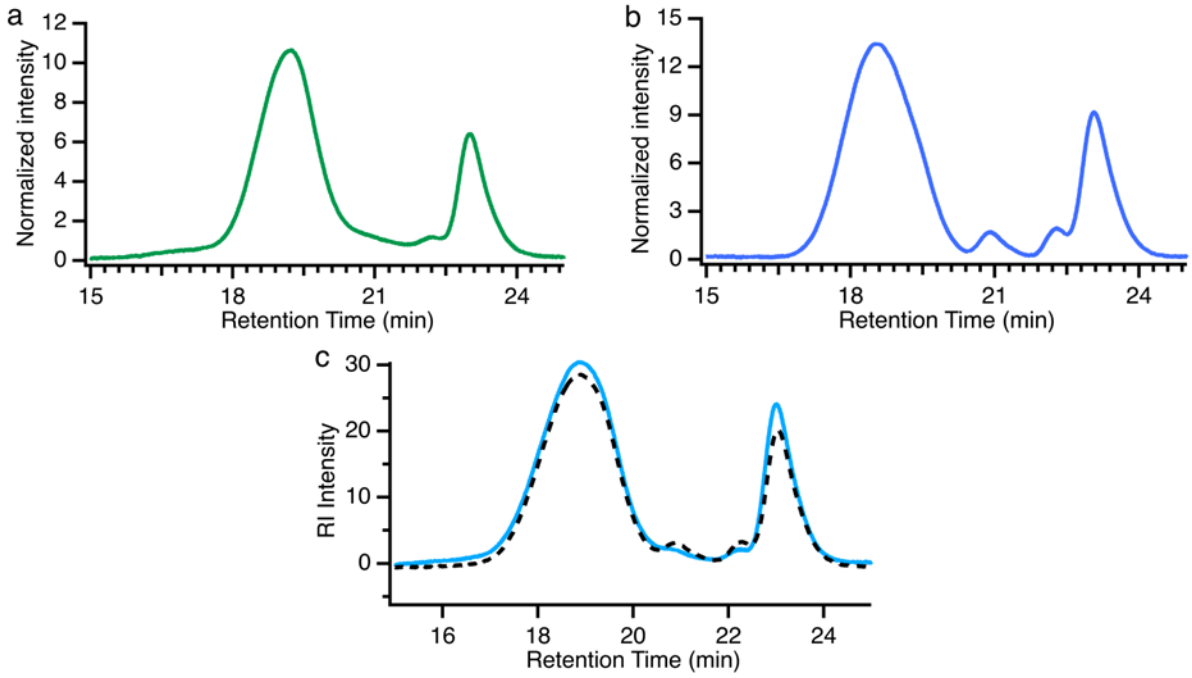


**Figure 3.3** HT-SEC traces of (a) **PE1**, (b) **PE2**, and (c) a 50 wt % blend of **PE1** and **PE2** in 1,2,4-trichlorobenzene at 150 °C. The measured traces are shown by solid lines and the dashed black line in c) is the predicted RI response for the blend based on concentration weighted combination of the HT-SEC traces of the individual components.

An equal mass blend of **PE2** and **PE1** was measured using HT-SEC as shown in **Figure 3c**. Measurements with blends including polymers are reported on a mass basis due to the finite dispersity of the samples for ease of calculations. The trace for the blend is effectively an average of the traces of the individual components that is weighted by their concentrations in mg/mL that was injected into the HT-SEC. This direct relationship between concentration and the RI signal is used to calculate the molecular weight distributions of the polymer from HT-SEC.[85] The RI elugram (HT-SEC trace) can be used to directly calculate the moments of the distributions of mass to determine $M_n$, $M_w$, $M_z$ for the polyolefin characterized. Similarly, the HT-SEC trace for two of the model alkane blends **(Figure 3.2c** and **Figure B4)** could be predicted from individual component traces, albeit with significant inaccuracies relative to the true values. This suggests the assumptions associated with equation (2) and an effectively invariant *dn/dc* may apply to simple alkane mixtures. However, as mixtures become more complicated (e.g. the ternary mixture in **Figure 3.2d**), the prediction based on the individual component traces fails to accurately represent the measured HT-SEC trace for the mixture. This suggests a combination of the separation being dependent on the composition and breakdown in the assumption that $I \propto c$ for the SEC in these mixtures.

For the chemical recycling of polyolefins, a broad distribution of products is commonly found, which makes our understanding of how HT-SEC separates and measures mixtures of polyolefins and large alkanes key to the interpretation of the complex products from chemical recycling processes. To examine this, we analyzed model mixtures (all equal mass ratios) composed of polyethylene and alkanes using HT-

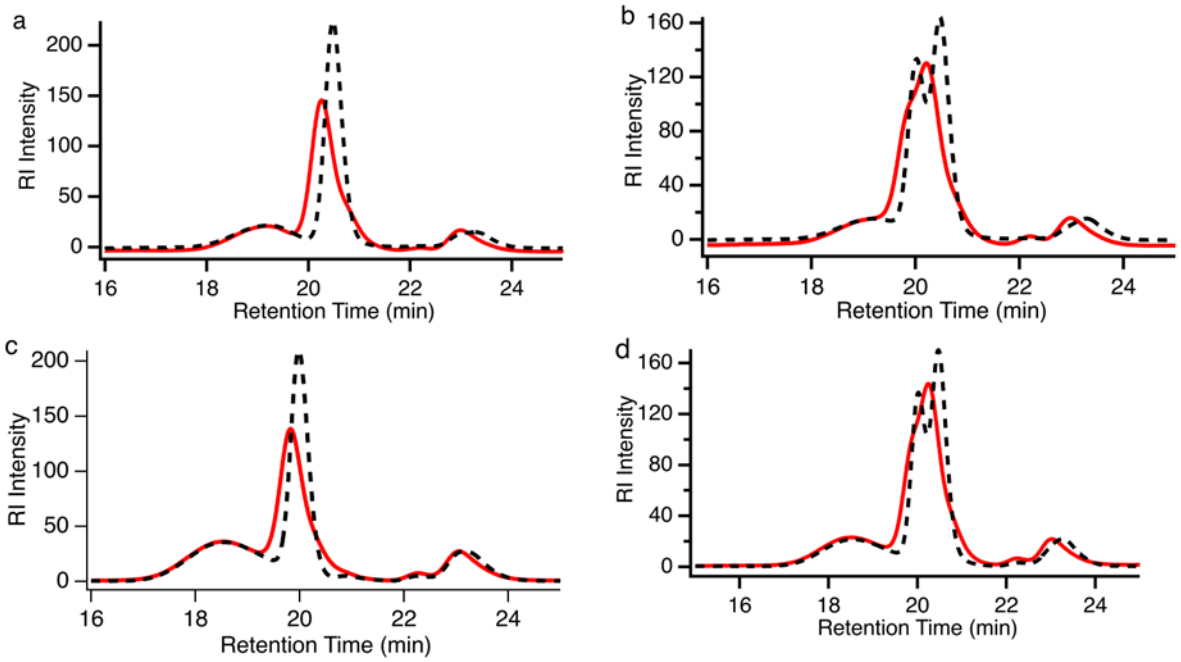


**Figure 3.4** HT-SEC traces of blends in trichlorobenzene at 150 °C for (a) 1:1 (w:w) **PE2** : **C18**, (b) 1:1:1 (w:w:w) **PE2** : **C36** : **C18**, (c) 1:1 (w:w) **PE1** : **C36** and (d) 1:1:1 (w:w:w) **PE1** : **C36**: **C18**. The red lines are the HT-SEC measured traces for the blends and the black dashed lines are predictions based on the concentrations and the measured HT-SEC traces for the individual components.

SEC as shown in **Figure 3.4** mixtures of **PE2** with **C18** and **C36** + **C18** are shown in **Figures 3.4a** and **3.4b**.

We also analyzed how the relative polymer/alkane composition impacts HT-SEC traces. **Figure 3.5** shows HT-SEC RI signals for a series of **PE1-C36** mixtures, where the relative fraction of the two components was varied from 25-75 wt.%. At the low **PE1** concentration, the **C36** elution time is approximately as expected based on the single component analyses but continues to yield a lower-than-expected **C36** peak area. As the **PE1** concentration increases, the **C36** peak shifts to shorter retention times; the lower-than-expected **C36** peak area remains consistent throughout the series. We offer a potential explanation for the shift in alkane retention times. The results are consistent with solvation of the polymer by the alkane. Alkanes solvating polymers or possibly intercalated into the polymer volume would elute with the polymer likely be indistinguishable from the polymer molecular weight.

Examination of mixtures of polymers with small amounts of well-defined larger alkanes with HT-SEC provides a method for evaluating the accuracy and precision of HT-SEC for polyolefin upcycling analyses. In the case of **C36** and smaller alkanes, consistent mismatches between the expected and measured chromatograms of known mixtures demonstrates failure of HT-SEC to accurately determine the molecular weight distribution, even when the column clearly can separate the components. Moreover, not observing components at longer elution times does not mean that the smaller species are not present in appreciable quantities in the mixture. These results indicate extreme care should be taken in interpreting product distributions from HT-SEC data alone, particularly data that include low molecular weight tails.

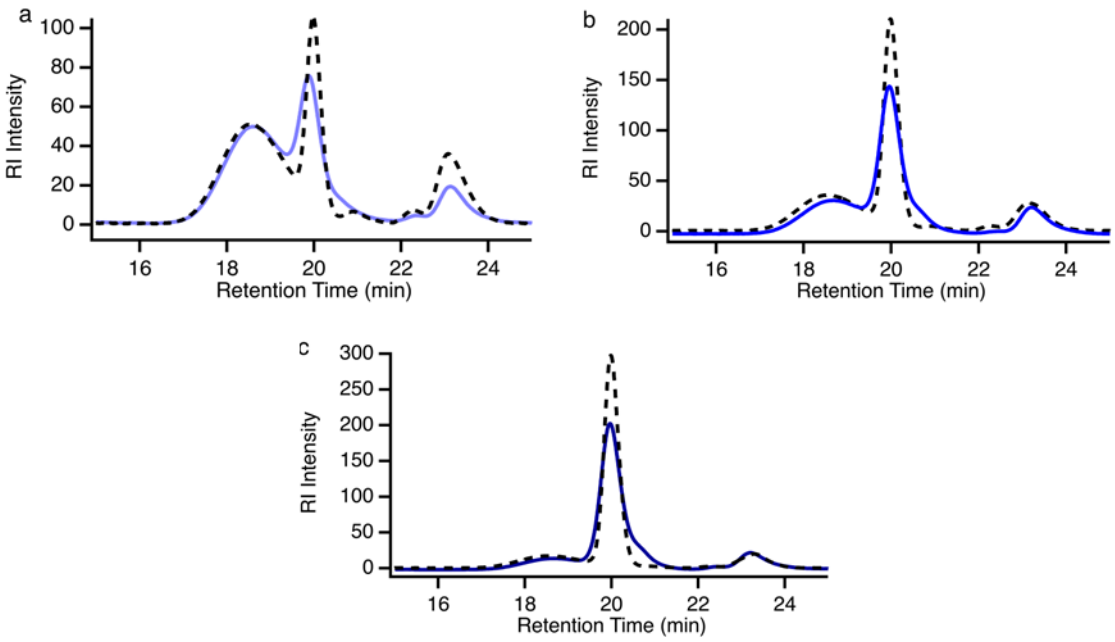


**Figure 3.5** HT-SEC traces for blends of **PE1** and **C36** at mass ratios of (a) 1:3 **PE1**:**C36**, (b) 1:1 **PE1**:**C36** and (c) 3:1 **PE1**:**C36**. The total concentration used was approximately 5 mg/mL in all cases. The black dashed lines are predictions based on the concentrations and the measured HT-SEC traces for the individual components.

## Conclusion

Quantitative characterization of products from chemical recycling processes involving polyolefins is important to advance these methods from the laboratory to commercialization. Here we examined the measurement limits of high-temperature size exclusion chromatography (HT-SEC) to quantify molecular weight distributions of polyethylene that contains alkanes. Surprisingly, a standard commercial column commonly used for characterizing polyolefins was able to observe and quantify alkanes as small as octadecane (**C18**) when analyzed as an individual compound via HT-SEC. However, standard molecular weight determination by light scattering led to significant underprediction of the molar masses of model alkanes examined from **C18** to hexatriacontane (**C36**). Two model low molar mass polyethylenes with narrow and broad dispersity were then used to evaluate HT-SEC performance in quantifying alkane concentrations. Known mixtures containing both short polymers and alkanes demonstrated a second chromatographic peak at longer elution times attributable to the alkane; however, quantitative analysis of the trace demonstrated a consistent and substantial underprediction of the alkane content and shift in the observed elution time/volume. These results demonstrate that reporting molar mass distributions obtained from HT-SEC for molecules smaller than rated by the column likely results in a significant misrepresentation of this low molar mass content. Quantification of the HT-SEC performance using known mixtures that include smaller molecules of known molar mass distributions provides a calibration route to examine the sensitivity of the column to some of the species produced in chemical recycling. Quantitative evaluation of the alkanes with HT-SEC is extremely challenging. This suggests extraction of smaller

components for characterization with alternative chromatographic techniques is likely necessary to increase the confidence of product distribution analyses of chemical recycling product mixtures.

# CHAPTER FOUR

# CONCLUSION AND FUTURE OUTLOOK

The research presented in this thesis provides a comprehensive investigation into the synthesis of well-defined polyethylene (PE) models with controlled molecular weights and end-functionalized groups to understand the complex interactions involved in polymer degradation and catalytic conversion into fuel-range hydrocarbons. These PE models will serve as important tools in assessing polymer adsorption, catalyst efficiency, and cracking selectivity in chemical recycling processes. The primary challenge identified in this work involves the limitations of mechanical recycling, such as inefficient sorting, contamination, and degradation of polymers during processing. Technologies such as FT-NIR sorting systems have been instrumental, but still face significant hurdles when dealing with multilayer plastics, labels, and dark-colored plastics, requiring manual intervention and leading to higher costs and time delays. Contamination remains a critical issue, reducing the quality and usability of recycled materials. Furthermore, the degradation of polymer chains due to thermal and mechanical stresses during reprocessing limits the lifespan of recycled plastics and their ability to be used in high-value applications.

In terms of chemical recycling, this thesis demonstrated that the hydrocracking of polyolefins using advanced catalytic systems, including bifunctional catalysts supported on zeolites and alumina, significantly improves conversion efficiency and product selectivity. However, catalyst deactivation due to char remains a concern, limiting long-term use. The use of solvents in the hydrocracking process facilitated better mass transfer and enhanced hydrogenation, but solvent recovery systems need further refinement to

improve economic viability and reduce environmental impact. The synthesis of end-functionalized PE models will allow for a detailed investigation of polymer-catalyst interactions, providing insights into how polymer chain length and end groups influence adsorption and cracking efficiency. These models offer a valuable framework for designing catalysts that will be more selective for fuel production and for optimizing the hydrocracking process to minimize by-products and improve overall conversion efficiency.

Future studies should focus on developing catalysts that can resist deactivation, particularly due to char. Enhancing the stability and reusability of catalysts in hydrocracking processes will be essential for scaling up these methods for industrial applications. A hybrid approach combining mechanical and chemical recycling methods could offer a more comprehensive solution for managing polyolefin waste. Such systems could leverage the strengths of both methods, using mechanical recycling to process simpler plastic streams and chemical recycling to handle more complex or degraded materials.

Further research into designing polymers that are easier to recycle through both mechanical and chemical processes is crucial. This includes the development of polymers that are less prone to degradation during reprocessing and those that can be more easily converted into valuable products through hydrocracking. Improving solvent recovery systems in chemical recycling will be key to reducing the environmental footprint of the hydrocracking process. Future research should explore more sustainable solvent systems and more efficient recovery techniques. By addressing these challenges, the field of polyolefin recycling can make significant strides toward achieving a circular economy for

plastics. This research not only contributes to the development of more effective recycling technologies but also highlights the potential for converting plastic waste into valuable fuel products, helping to mitigate the environmental impact of plastic pollution while providing a sustainable source of energy.

## LIST OF REFERENCES


1. Williams, A. T.; Rangel-Buitrago, N., The past, present, and future of plastic pollution. *Marine Pollution Bulletin* **2022,** *176*, 113429.

2. Williams, A.; Rangel-Buitrago, N., Marine litter: Solutions for a major environmental problem. *Journal of coastal research* **2019,** *35* (3), 648-663.

3. Kedzierski, M.; Frère, D.; Le Maguer, G.; Bruzaud, S., Why is there plastic packaging in the natural environment? Understanding the roots of our individual plastic waste management behaviours. *Science of The Total Environment* **2020,** *740*, 139985.

4. Jiang, J.; Shi, K.; Zhang, X.; Yu, K.; Zhang, H.; He, J.; Ju, Y.; Liu, J., From plastic waste to wealth using chemical recycling: A review. *Journal of Environmental Chemical Engineering* **2022,** *10* (1), 106867.

5. Parker, L., The world's plastic pollution crisis explained. *National Geographic* **2019,** *7* (06).

6. Geyer, R.; Jambeck, J. R.; Law, K. L., Production, use, and fate of all plastics ever made. *Science Advances* **2017,** *3* (7), e1700782.

7. Uhrin, A. V.; Schellinger, J., Marine debris impacts to a tidal fringing-marsh in North Carolina. *Marine Pollution Bulletin* **2011,** *62* (12), 2605-2610.

8. Browne, M. A.; Dissanayake, A.; Galloway, T. S.; Lowe, D. M.; Thompson, R. C., Ingested Microscopic Plastic Translocates to the Circulatory System of the Mussel, Mytilus edulis (L.). *Environmental Science & Technology* **2008,** *42* (13), 5026-5031.

9. Ragaert, K.; Delva, L.; Van Geem, K., Mechanical and chemical recycling of solid plastic waste. *Waste Management* **2017,** *69*, 24-58.

10. Shen, M.; Huang, W.; Chen, M.; Song, B.; Zeng, G.; Zhang, Y., (Micro) plastic crisis: un-ignorable contribution to global greenhouse gas emissions and climate change. *Journal of Cleaner Production* **2020,** *254*, 120138.

11. Mark, L. O.; Cendejas, M. C.; Hermans, I., The Use of Heterogeneous Catalysis in the Chemical Valorization of Plastic Waste. *ChemSusChem* **2020,** *13* (22), 5808-5836.

12. Chen, X.; Wang, Y.; Zhang, L., Recent Progress in the Chemical Upcycling of Plastic Wastes. *ChemSusChem* **2021,** *14* (19), 4137-4151.

13. Ellis, L. D.; Rorrer, N. A.; Sullivan, K. P.; Otto, M.; McGeehan, J. E.; Román-Leshkov, Y.; Wierckx, N.; Beckham, G. T., Chemical and biological catalysis for plastics recycling and upcycling. *Nature Catalysis* **2021,** *4* (7), 539-556.

14. Serrano, D. P.; Aguado, J.; Escola, J. M., Developing Advanced Catalysts for the Conversion of Polyolefinic Waste Plastics into Fuels and Chemicals. *ACS Catalysis* **2012,** *2* (9), 1924-1941.

15. Anuar Sharuddin, S. D.; Abnisa, F.; Wan Daud, W. M. A.; Aroua, M. K., A review on pyrolysis of plastic wastes. *Energy Conversion and Management* **2016,** *115*, 308-326.

16. Kunwar, B.; Cheng, H. N.; Chandrashekaran, S. R.; Sharma, B. K., Plastics to fuel: a review. *Renewable and Sustainable Energy Reviews* **2016,** *54*, 421-428.

17. Dogu, O.; Pelucchi, M.; Van de Vijver, R.; Van Steenberge, P. H. M.; D'Hooge, D. R.; Cuoci, A.; Mehl, M.; Frassoldati, A.; Faravelli, T.; Van Geem, K. M., The chemistry of chemical recycling of solid plastic waste via pyrolysis and gasification: State-of-the-art, challenges, and future directions. *Progress in Energy and Combustion Science* **2021,** *84*, 100901.

18. Dufaud, V.; Basset, J.-M., Catalytic Hydrogenolysis at Low Temperature and Pressure of Polyethylene and Polypropylene to Diesels or Lower Alkanes by a Zirconium Hydride Supported on Silica-Alumina: A Step Toward Polyolefin Degradation by the Microscopic Reverse of Ziegler–Natta Polymerization. *Angewandte Chemie International Edition* **1998,** *37* (6), 806-810.

19. Rorrer, J. E.; Beckham, G. T.; Román-Leshkov, Y., Conversion of Polyolefin Waste to Liquid Alkanes with Ru-Based Catalysts under Mild Conditions. *JACS Au* **2021,** *1* (1), 8-12.

20. Ellis, L. D.; Orski, S. V.; Kenlaw, G. A.; Norman, A. G.; Beers, K. L.; Román-Leshkov, Y.; Beckham, G. T., Tandem Heterogeneous Catalysis for Polyethylene Depolymerization via an Olefin-Intermediate Process. *ACS Sustainable Chemistry & Engineering* **2021,** *9* (2), 623-628.

21. Rorrer, J. E.; Troyano-Valls, C.; Beckham, G. T.; Román-Leshkov, Y., Hydrogenolysis of Polypropylene and Mixed Polyolefin Plastic Waste over Ru/C to Produce Liquid Alkanes. *ACS Sustainable Chemistry & Engineering* **2021,** *9* (35), 11661-11666.

22. Du, B.; Chen, X.; Ling, Y.; Niu, T.; Guan, W.; Meng, J.; Hu, H.; Tsang, C.-W.; Liang, C., Hydrogenolysis-Isomerization of Waste Polyolefin Plastics to Multibranched Liquid Alkanes. *ChemSusChem* **2023,** *16* (3), e202202035.

23. Zhang, Z.; Hirose, T.; Nishio, S.; Morioka, Y.; Azuma, N.; Ueno, A.; Ohkita, H.; Okada, M., Chemical Recycling of Waste Polystyrene into Styrene over Solid Acids and Bases. *Industrial & Engineering Chemistry Research* **1995,** *34* (12), 4514-4519.

24. Uemichi, Y.; Makino, Y.; Kanazuka, T., Degradation of polyethylene to aromatic hydrocarbons over metal-supported activated carbon catalysts. *Journal of Analytical and Applied Pyrolysis* **1989,** *14* (4), 331-344.

25. Vasile, C.; Onu, P.; Bărboiu, V.; Sabliovschi, M.; Moroi, G.; Gânju, D.; Florea, M., Catalytic decomposition of polyolefins. III. Decomposition over the ZSM-5 catalyst. *Acta Polymerica* **1988,** *39* (6), 306-310.

26. Ohkita, H.; Nishiyama, R.; Tochihara, Y.; Mizushima, T.; Kakuta, N.; Morioka, Y.; Ueno, A.; Namiki, Y.; Tanifuji, S., Acid properties of silica-alumina catalysts and catalytic degradation of polyethylene. *Industrial & Engineering Chemistry Research* **1993,** *32* (12), 3112-3116.

27. Songip, A. R.; Masuda, T.; Kuwahara, H.; Hashimoto, K., Test to screen catalysts for reforming heavy oil from waste plastics. *Applied Catalysis B: Environmental* **1993,** *2* (2), 153-164.

28. Galadima, A.; Masudi, A.; Muraza, O., Towards low-temperature catalysts for sustainable fuel from plastic: A review. *Journal of Environmental Chemical Engineering* **2021,** *9* (6), 106655.

29. Iqbal, F.; Shafeeq, A.; Aslam, R.; Rauf, A., Comparative Analysis of Catalytic Cracking and Hydrocracking of Waste Plastic. *Chemical Engineering & Technology* **2023,** *46* (4), 723-730.

30. Tarach, K. A.; Akouche, M.; Pyra, K.; Valtchev, V.; Jajko, G.; Gilson, J.-P.; Góra-Marek, K., Polypropylene cracking on embryonic and ZSM-5 catalysts – An operando study. *Applied Catalysis B: Environmental* **2023,** *334*, 122871.

31. Aguado, J.; Serrano, D. P.; Miguel, G. S.; Escola, J. M.; Rodríguez, J. M., Catalytic activity of zeolitic and mesostructured catalysts in the cracking of pure and waste polyolefins. *Journal of Analytical and Applied Pyrolysis* **2007,** *78* (1), 153-161.

32. Aguado, J.; Serrano, D. P.; Vicente, G.; Sánchez, N., Enhanced Production of α-Olefins by Thermal Degradation of High-Density Polyethylene (HDPE) in Decalin Solvent: Effect of the Reaction Time and Temperature. *Industrial & Engineering Chemistry Research* **2007,** *46* (11), 3497-3504.

33. Abbas-Abadi, M. S.; Haghighi, M. N.; Yeganeh, H., The effect of temperature, catalyst, different carrier gases and stirrer on the produced transportation hydrocarbons of LLDPE degradation in a stirred reactor. *Journal of Analytical and Applied Pyrolysis* **2012,** *95*, 198-204.

34. National Academies of Sciences, E.; Medicine, *Reckoning with the US role in global ocean plastic waste*. 2021.

35. Forman, G. S.; Divita, V. B.; Han, J.; Cai, H.; Elgowainy, A.; Wang, M., U.S. Refinery Efficiency: Impacts Analysis and Implications for Fuel Carbon Policy Implementation. *Environmental Science & Technology* **2014,** *48* (13), 7625-7633.

36. Seymour, R. B.; Carraher, C. E., Properties of Polyolefins. In *Structure—Property Relationships in Polymers*, Seymour, R. B.; Carraher, C. E., Eds. Springer US: Boston, MA, 1984; pp 133-145.

37. Zhang, F.; Zeng, M.; Yappert, R. D.; Sun, J.; Lee, Y.-H.; LaPointe, A. M.; Peters, B.; Abu-Omar, M. M.; Scott, S. L., Polyethylene upcycling to long-chain alkylaromatics by tandem hydrogenolysis/aromatization. *Science* **2020,** *370* (6515), 437-441.

38. Rorrer, N. A.; Nicholson, S.; Carpenter, A.; Biddy, M. J.; Grundl, N. J.; Beckham, G. T., Combining Reclaimed PET with Bio-based Monomers Enables Plastics Upcycling. *Joule* **2019,** *3* (4), 1006-1027.

39. Pandey, S.; Karakoti, M.; Surana, K.; Dhapola, P. S.; SanthiBhushan, B.; Ganguly, S.; Singh, P. K.; Abbas, A.; Srivastava, A.; Sahoo, N. G., Graphene nanosheets derived from plastic waste for the application of DSSCs and supercapacitors. *Scientific Reports* **2021,** *11* (1), 3916.

40. Algozeeb, W. A.; Savas, P. E.; Luong, D. X.; Chen, W.; Kittrell, C.; Bhat, M.; Shahsavari, R.; Tour, J. M., Flash Graphene from Plastic Waste. *ACS Nano* **2020,** *14* (11), 15595-15604.

41. Chaudhary, S.; Kumari, M.; Chauhan, P.; Ram Chaudhary, G., Upcycling of plastic waste into fluorescent carbon dots: An environmentally viable transformation to biocompatible C-dots with potential prospective in analytical applications. *Waste Management* **2021,** *120*, 675-686.

42. Saito, K.; Jehanno, C.; Meabe, L.; Olmedo-Martínez, J. L.; Mecerreyes, D.; Fukushima, K.; Sardon, H., From plastic waste to polymer electrolytes for batteries through chemical upcycling of polycarbonate. *Journal of Materials Chemistry A* **2020,** *8* (28), 13921-13926.

43. Calderon, N., Ring-Opening Polymerization of Cycloolefins. *Journal of Macromolecular Science, Part C* **1972,** *7* (1), 105-159.

44. Bielawski, C. W.; Grubbs, R. H., Living ring-opening metathesis polymerization. *Progress in Polymer Science* **2007,** *32* (1), 1-29.

45. Grubbs, R. H.; Tumas, W., Polymer Synthesis and Organotransition Metal Chemistry. *Science* **1989,** *243* (4893), 907-915.

46. Lummiss, J. A. M.; Higman, C. S.; Fyson, D. L.; McDonald, R.; Fogg, D. E., The divergent effects of strong NHC donation in catalysis. *Chemical Science* **2015,** *6* (12), 6739-6746.

47. Schrock, R. R., Multiple Metal–Carbon Bonds for Catalytic Metathesis Reactions (Nobel Lecture). *Angewandte Chemie International Edition* **2006,** *45* (23), 3748-3759.

48. Slugovc, C., The Ring Opening Metathesis Polymerisation Toolbox. *Macromolecular Rapid Communications* **2004,** *25* (14), 1283-1297.

49. Hilf, S.; Kilbinger, A. F. M., Functional end groups for polymers prepared using ring-opening metathesis polymerization. *Nature Chemistry* **2009,** *1* (7), 537-546.

50. Crowe, W.; Mitchell, J.; Gibson, V.; Schrock, R., Chain-transfer agents for living ROMP [Ring-Opening Metathesis Polymerization] reactions of norbornene. *Macromolecules* **1990,** *23* (14), 3534-3536.

51. Hillmyer, M. A.; Nguyen, S. T.; Grubbs, R. H., Utility of a Ruthenium Metathesis Catalyst for the Preparation of End-Functionalized Polybutadiene. *Macromolecules* **1997,** *30* (4), 718-721.

52. Morita, T.; Maughon, B. R.; Bielawski, C. W.; Grubbs, R. H., A Ring-Opening Metathesis Polymerization (ROMP) Approach to Carboxyl- and Amino-Terminated Telechelic Poly(butadiene)s. *Macromolecules* **2000,** *33* (17), 6621-6623.

53. Ji, S.; Hoye, T. R.; Macosko, C. W., Controlled Synthesis of High Molecular Weight Telechelic Polybutadienes by Ring-Opening Metathesis Polymerization. *Macromolecules* **2004,** *37* (15), 5485-5489.

54. Maughon, B. R.; Morita, T.; Bielawski, C. W.; Grubbs, R. H., Synthesis of Cross-Linkable Telechelic Poly(butenylene)s Derived from Ring-Opening Metathesis Polymerization. *Macromolecules* **2000,** *33* (6), 1929-1935.

55. Scherman, O. A.; Rutenberg, I. M.; Grubbs, R. H., Direct Synthesis of Soluble, End-Functionalized Polyenes and Polyacetylene Block Copolymers. *Journal of the American Chemical Society* **2003,** *125* (28), 8515-8522.

56. Fraser, C.; Hillmyer, M. A.; Gutierrez, E.; Grubbs, R. H., Degradable cyclooctadiene/acetal copolymers: versatile precursors to 1, 4-hydroxytelechelic polybutadiene and hydroxytelechelic polyethylene. *Macromolecules* **1995,** *28* (21), 7256-7261.

57. Matt, C.; Kölblin, F.; Streuff, J., Reductive C–O, C–N, and C–S Cleavage by a Zirconium Catalyzed Hydrometalation/β-Elimination Approach. *Organic Letters* **2019,** *21* (17), 6983-6988.

58. MacLeod, M.; Arp, H. P. H.; Tekman, M. B.; Jahnke, A., The global threat from plastic pollution. *Science* **2021,** *373* (6550), 61-65.

59. Chen, Y.; Awasthi, A. K.; Wei, F.; Tan, Q. Y.; Li, J. H., Single-use plastics: Production, usage, disposal, and adverse impacts. *Science of the Total Environment* **2021,** *752*, 141772.

60. Vogt, B. D.; Stokes, K. K.; Kumar, S. K., Why is Recycling of Postconsumer Plastics so Challenging? *Acs Applied Polymer Materials* **2021,** *3* (9), 4325-4346.

61. Bernat, K., Post-Consumer Plastic Waste Management: From Collection and Sortation to Mechanical Recycling. *Energies* **2023,** *16* (8).

62. Schyns, Z. O. G.; Shaver, M. P., Mechanical Recycling of Packaging Plastics: A Review. *Macromolecular Rapid Communications* **2021,** *42,* 2000415.

63. Maris, J.; Bourdon, S.; Brossard, J. M.; Cauret, L.; Fontaine, L.; Montembault, V., Mechanical recycling: Compatibilization of mixed thermoplastic wastes. *Polymer Degradation and Stability* **2018,** *147*, 245-266.

64. Tullo, A., POLYMERS Europe is implementing a tax on plastic. *Chemical & Engineering News* **2021,** *99* (2), 34-34.

65. Chen, H.; Wan, K.; Zhang, Y. Y.; Wang, Y. Q., Waste to Wealth: Chemical Recycling and Chemical Upcycling of Waste Plastics for a Great Future. *Chemsuschem* **2021,** *14* (19), 4123-4136.

66. Coates, G. W.; Getzler, Y., Chemical recycling to monomer for an ideal, circular polymer economy. *Nature Reviews Materials* **2020,** *5* (7), 501-516.

67. Geyer, B.; Lorenz, G.; Kandelbauer, A., Recycling of poly(ethylene terephthalate) - A review focusing on chemical methods. *Express Polymer Letters* **2016,** *10* (7), 559-586.

68. Eastman and Governor Lee Announce World-Scale Plastic-to-Plastic Molecular Recycling Facility to be Built in Kingsport, Tenn. Eastman Chemical: Kingsport, TN, 2021.

69. Tennakoon, A.; Wu, X.; Paterson, A. L.; Patnaik, S.; Pei, Y. C.; LaPointe, A. M.; Ammal, S. C.; Hackler, R. A.; Heyden, A.; Slowing, II; Coates, G. W.; Delferro, M.; Peters, B.; Huang, W. Y.; Sadow, A. D.; Perras, F. A., Catalytic upcycling of high-density polyethylene via a processive mechanism. *Nature Catalysis* **2020,** *3* (11), 893-901.

70. Liu, S. B.; Kots, P. A.; Vance, B. C.; Danielson, A.; Vlachos, D. G., Plastic waste to fuels by hydrocracking at mild conditions. *Science Advances* **2021,** *7* (17), eabf8283.

71. Thiounn, T.; Smith, R. C., Advances and approaches for chemical recycling of plastic waste. *Journal of Polymer Science* **2020,** *58* (10), 1347-1364.

72. Vollmer, I.; Jenks, M. J. F.; Roelands, M. C. P.; White, R. J.; van Harmelen, T.; de Wild, P.; van der Laan, G. P.; Meirer, F.; Keurentjes, J. T. F.; Weckhuysen, B. M., Beyond Mechanical Recycling: Giving New Life to Plastic Waste. *Angewandte Chemie-International Edition* **2020,** *59* (36), 15402-15423.

73. Celik, G.; Kennedy, R. M.; Hackler, R. A.; Ferrandon, M.; Tennakoon, A.; Patnaik, S.; LaPointe, A. M.; Ammal, S. C.; Heyden, A.; Perras, F. A.; Pruski, M.; Scott, S. L.; Poeppelmeier, K. R.; Sadow, A. D.; Delferro, M., Upcycling Single-Use Polyethylene into High-Quality Liquid Products. *Acs Central Science* **2019,** *5* (11), 1795-1803.

74. Kosloski-Oh, S. C.; Wood, Z. A.; Manjarrez, Y.; de los Rios, J. P.; Fieser, M. E., Catalytic methods for chemical recycling or upcycling of commercial polymers. *Materials Horizons* **2021,** *8* (4), 1084-1129.

75. Chu, M. Y.; Tu, W. L.; Yang, S. Q.; Zhang, C. Y.; Li, Q. Y.; Zhang, Q.; Chen, J. X., Sustainable chemical upcycling of waste polyolefins by heterogeneous catalysis. *Susmat* **2022,** *2* (2), 161-185.

76. Korley, L. T. J.; Epps, T. H.; Helms, B. A.; Ryan, A. J., Toward polymer upcycling - adding value and tackling circularity. *Science* **2021,** *373* (6550), 66-69.

77. Zhang, F.; Zeng, M. H.; Yappert, R. D.; Sun, J. K.; Lee, Y. H.; LaPointe, A. M.; Peters, B.; Abu-Omar, M. M.; Scott, S. L., Polyethylene upcycling to long-chain alkylaromatics by tandem hydrogenolysis/aromatization. *Science* **2020,** *370* (6515), 437-441.

78. Aguado, J.; Serrano, D. P.; Escola, J. M.; Garagorri, E.; Fernandez, J. A., Catalytic conversion of polyolefins into fuels over zeolite beta. *Polymer Degradation and Stability* **2000,** *69* (1), 11-16.

79. Balzer, A.; Hinton, Z.; Vance, B.; Vlachos, D.; Korley, L.; Epps, T. I., Tracking Chain Populations and Branching Structure during Polyethylene Deconstruction Processes. *ACS CENTRAL SCIENCE* **2024,** *10*, 1755-1764.

80. Hackler, R.; Lamb, J.; Peczak, I.; Kennedy, R.; Kanbur, U.; LaPointe, A.; Poeppelmeier, K.; Sadow, A.; Delferro, M., Effect of Macro- and Microstructures on Catalytic Hydrogenolysis of Polyolefins. *MACROMOLECULES* **2022,** *55*, 6801-6810.

81. Lamb, J.; Lee, Y.; Sun, J.; Byron, C.; Uppuluri, R.; Kennedy, R.; Meng, C.; Behera, R.; Wang, Y.; Qi, L.; Sadow, A.; Huang, W.; Ferrandon, M.; Scott, S.; Poeppelmeier, K.; Abu-Omar, M.; Delferro, M., Supported Platinum Nanoparticles Catalyzed Carbon-Carbon Bond Cleavage of Polyolefins: Role of the Oxide Support Acidity. *ACS APPLIED MATERIALS & INTERFACES* **2024,** *16*, 11361-11376.

82. Sun, J.; Dong, J.; Gao, L.; Zhao, Y.; Moon, H.; Scott, S., Catalytic Upcycling of Polyolefins. *CHEMICAL REVIEWS* **2024,** *124*, 9457-9579.

83. Kots, P. A.; Vance, B. C.; Vlachos, D. G., Polyolefin plastic waste hydroconversion to fuels, lubricants, and waxes: a comparative study. *Reaction Chemistry & Engineering* **2021,** *7* (1), 41-54.

84. Huglin, M. B., Determination of molecular weights by light scattering. In *Inorganic and Physical Chemistry. Topics in Current Chemistry*, Springer: Berlin, 1978; Vol. 77, p https://doi.org/10.1007/BFb0048039.

85. Hiemenz, P.; Lodge, T., *Polymer Chemistry*. 2nd ed.; CRC Press: Boca Raton, FL, 2007.

# APPENDICES

**APPENDIX A**
**SUPPORTING INFORMATION -CHAPTER 2**

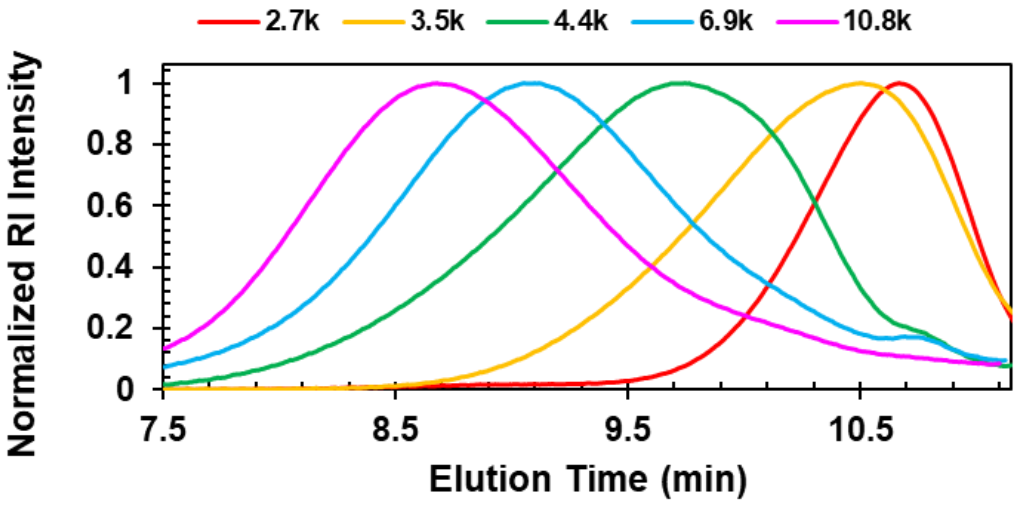


**Figure A.1** GPC traces of acetoxy end-capped PE models before hydrogenation

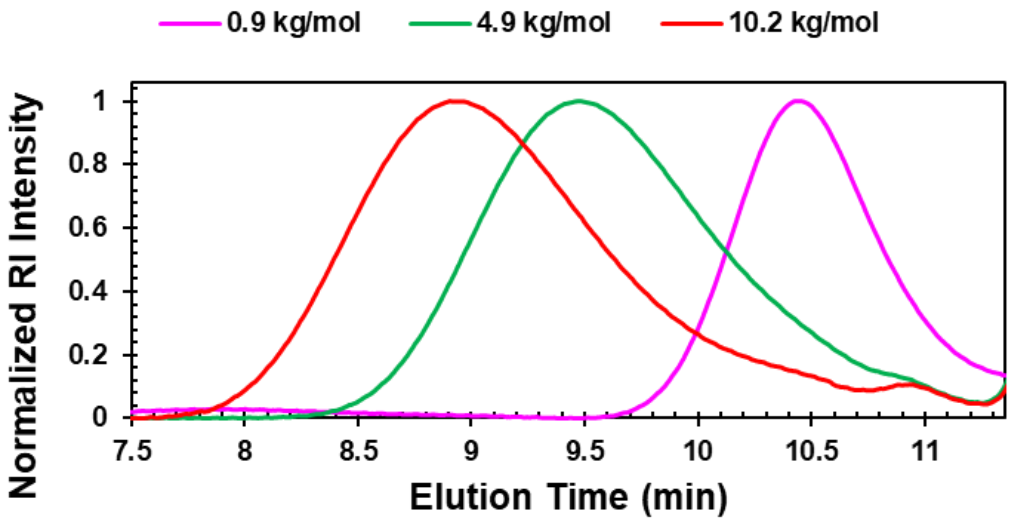


**Figure A.2** GPC traces of PE models before hydrogenation

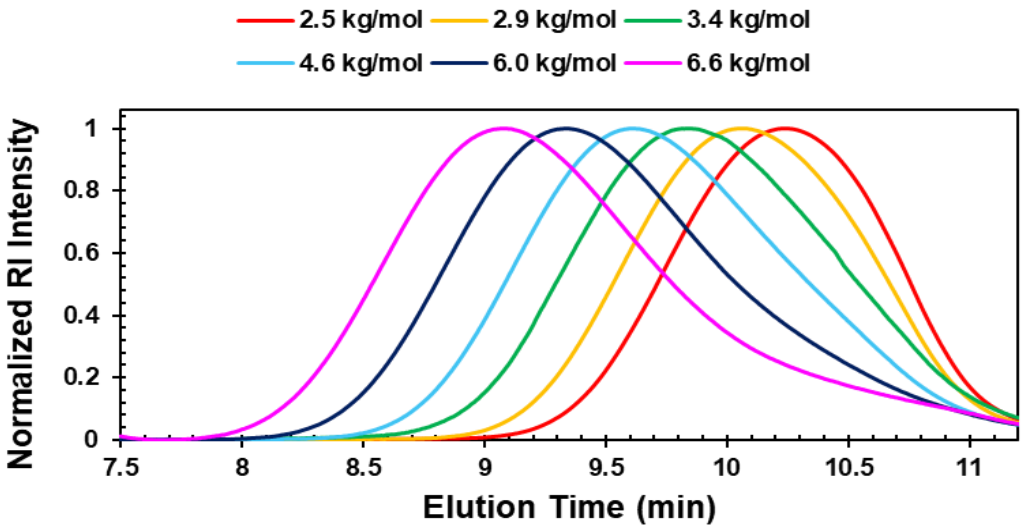


**Figure A.3** GPC traces of phenoxy end-capped PE models before hydrogenation

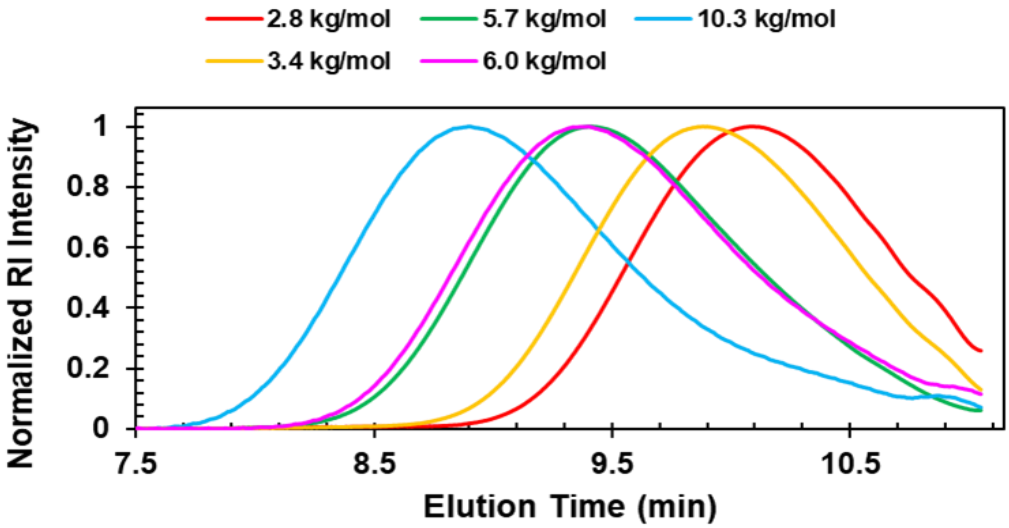


**Figure A.4** GPC traces of naphthyloxy end-capped PE models before hydrogenation

**Appendix B**
**SUPPORTING INFORMATION - CHAPTER 3**

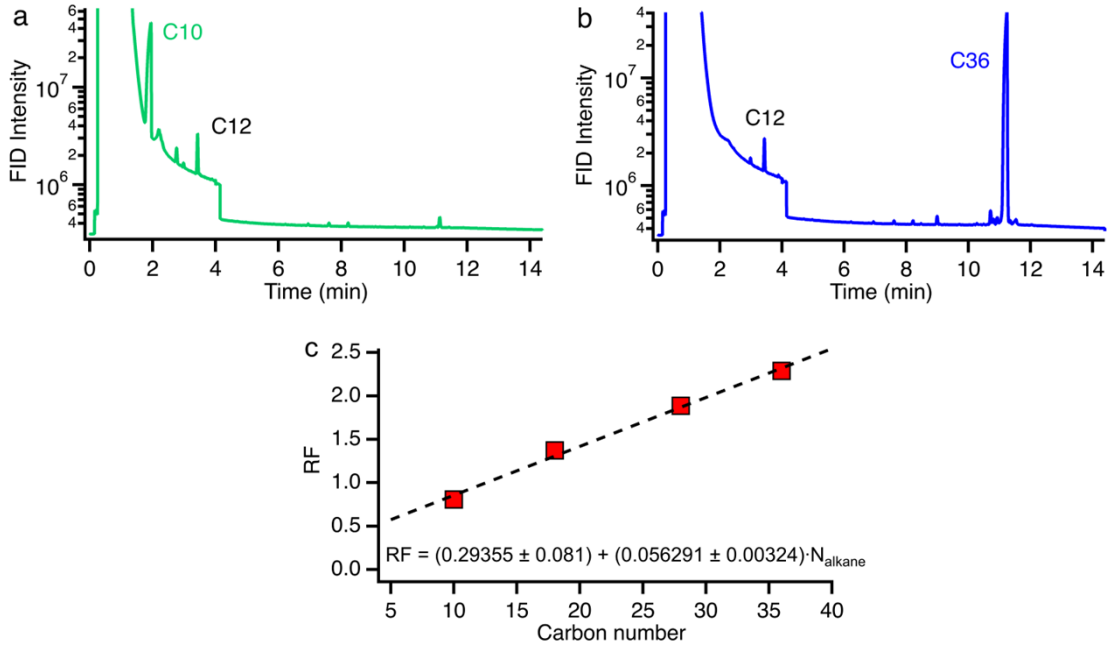


**Figure B.1** GC calibration for (a) **C10** and (b) **C36** using **C12** as an internal standard and toluene as the carrier solvent. (c) Retention factors for GC for a series of n-alkanes determined using **C12** as internal standard.

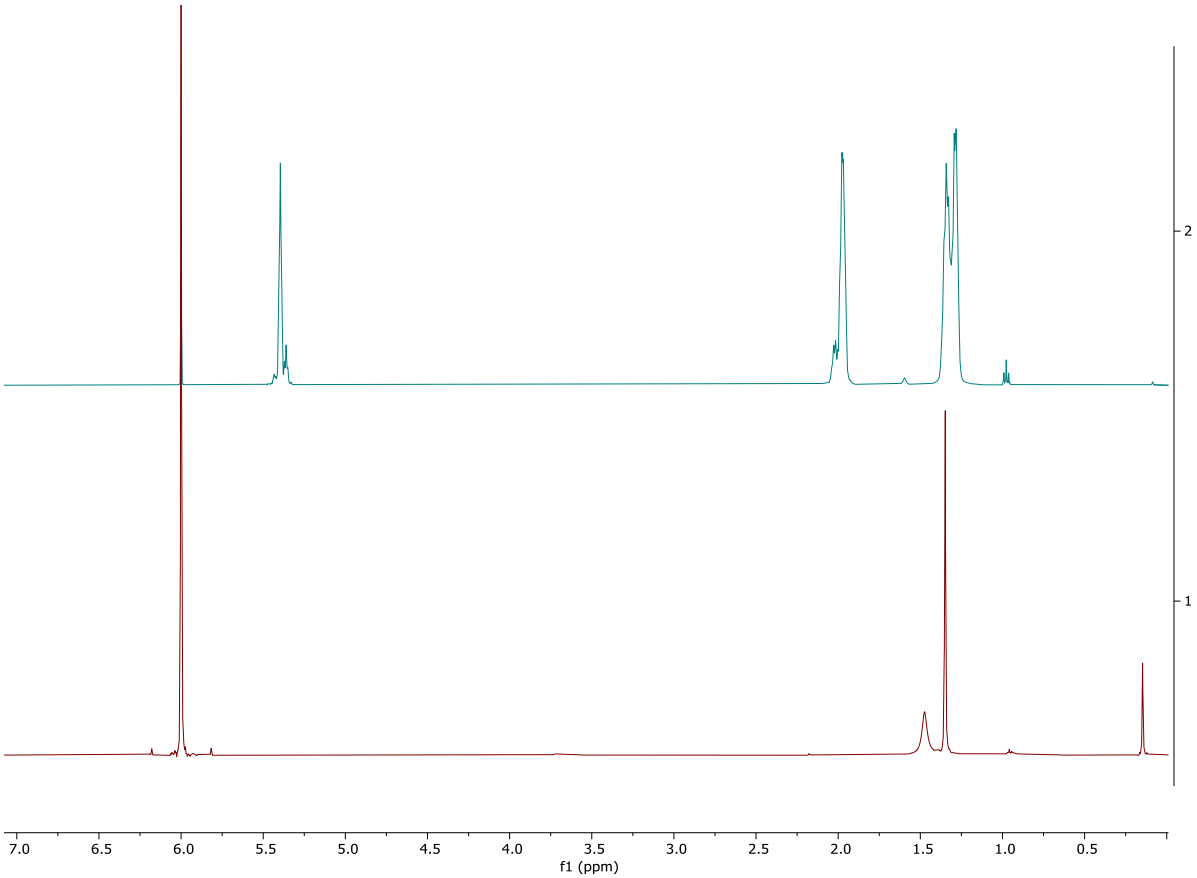


**Figure B.2** $^{1}$H NMR spectra of **PE1** before (top) and after (bottom) reduction/hydrogenation of the double bonds. Spectra taken in 1,1,2,2-tetrachloroethane-$d_2$ (residual solvent peak at 6 ppm).

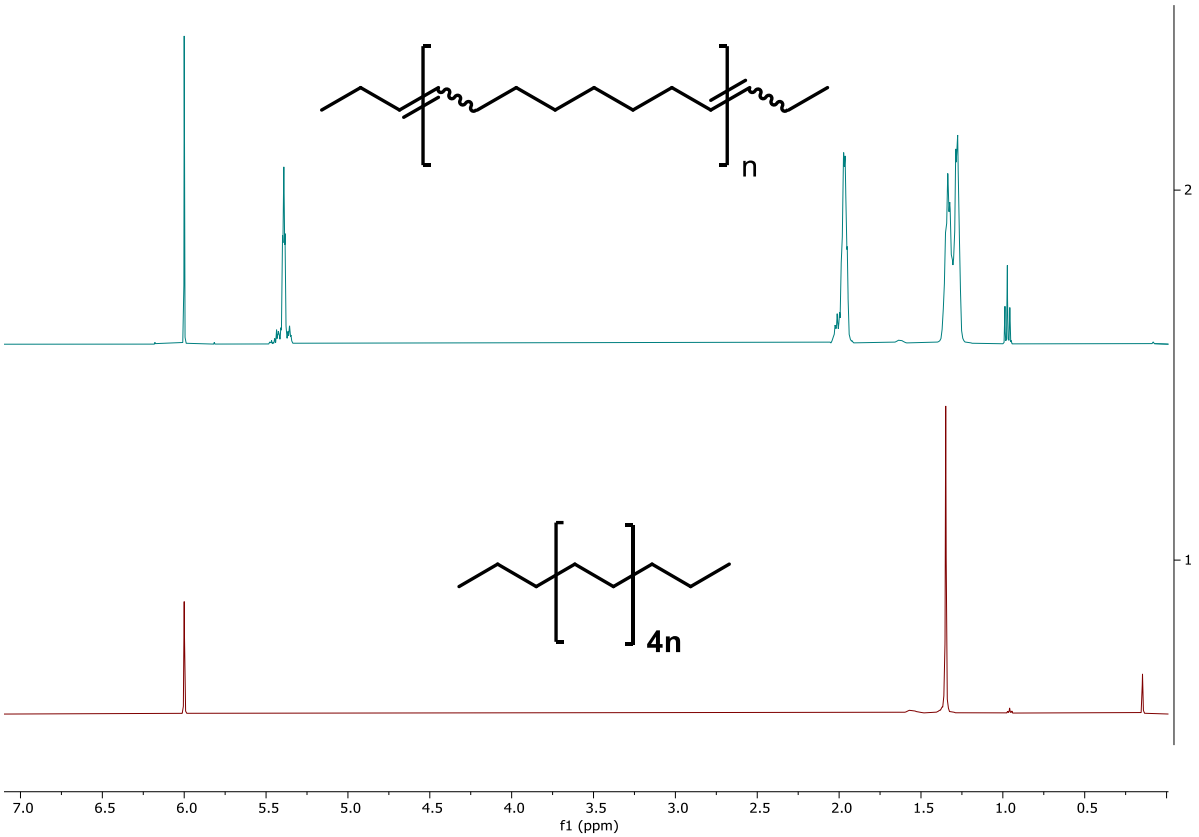


**Figure B.3** $^{1}$H NMR spectra of **PE2** before (top) and after (bottom) reduction/hydrogenation of the double bonds. Spectra taken in 1,1,2,2-tetrachloroethane-$d_2$ (residual solvent peak at 6 ppm).

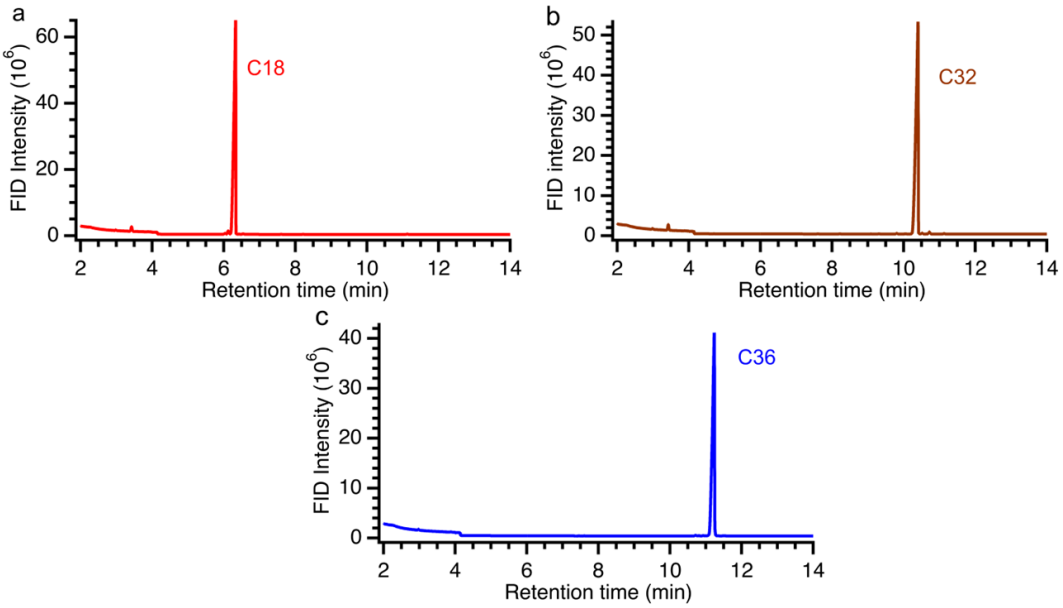


**Figure B.4** GC traces for the model alkanes, (a) **C18**, (b) **C32** and (c) **C36**, in toluene.

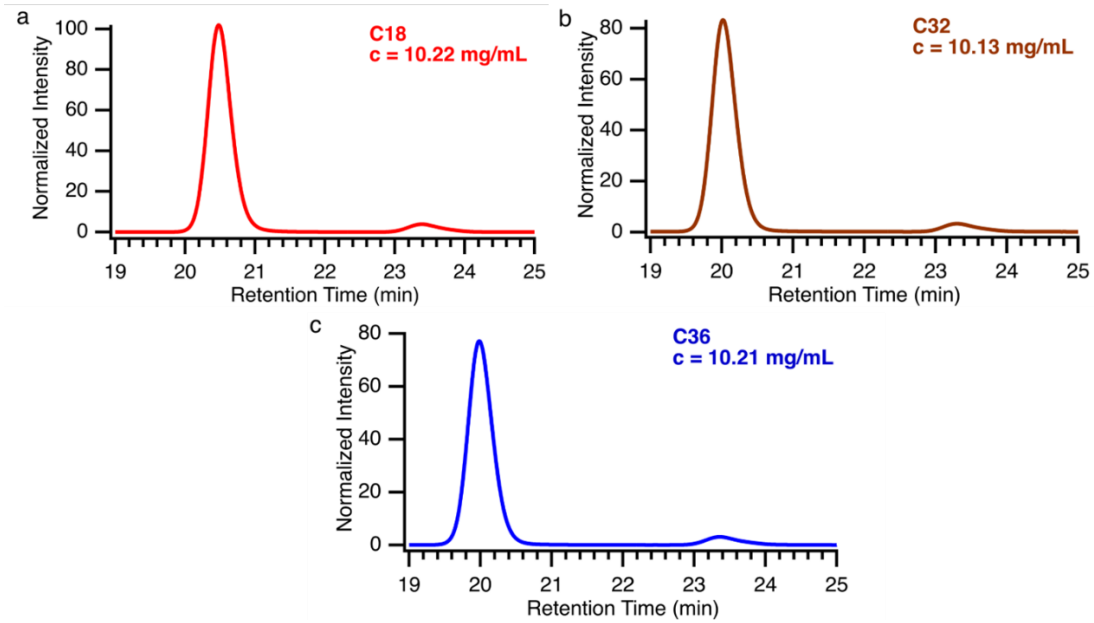


**Figure B.5** HT-SEC traces for (a) **C18**, (b) **C32** and (c) **C36** in 1,2,4-trichlorobenzene at 150 °C. The RI intensity is normalized by the concentration noted in each panel. The peak at 23-24 min is the injection void volume and is not associated with components in the solution.

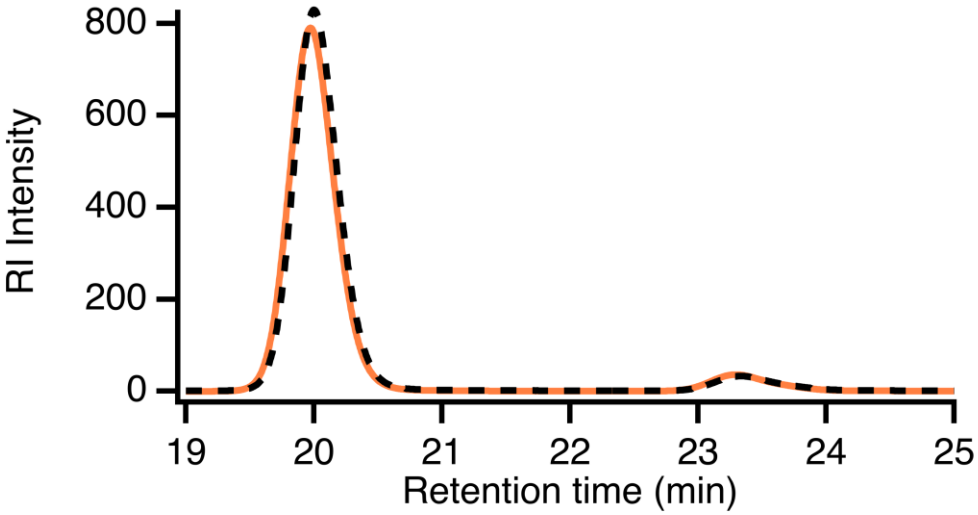


**Figure B.6** HT-SEC traces for blend of 1:1 mol:mol **C32**:**C36**. The measured traces (solid lines) are compared to predicted profiles using concentration-weighted averages (black dashed) of individual component HT-SEC traces. The total concentration used for HT-SEC was 10.42 mg/mL. The peak at 23-24 min is the injection void volume and is not associated with components in the solution.

**Table B.1** Molecular mass for equimolar mixtures from theoretical calculation based on pure alkanes and measured with HT-SEC using light scattering for absolute molecular weight.

[a]All samples are either 1:1 or 1:1:1 molar ratio (equimolar) mixtures. [b]Exact $M_n$ of the equimolar mixture was calculated based on the exact known masses of the pure components (reported in Table 1). [c]HT-SEC $M_n$ values were measured using triple detection HT-GPC at 150 °C in 1,2,4-trichlorobenzene.

| Sample[a] | Exact $M_n$[b] (g/mol) | Exact $Đ$[c] | HT-SEC $M_n$[c] (g/mol) | HT-SEC $Đ$[d] |
|---|---|---|---|---|
| **C18:C32** | 325.34 | 1.08 | 72 | 1.16 |
| **C18:C36** | 338.87 | 1.12 | 105 | 1.25 |
| **C32:C36** | 477.25 | 1.003 | 151 | 1.22 |
| **C18:C32:C36** | 369.46 | 1.09 | 109 | 1.35 |

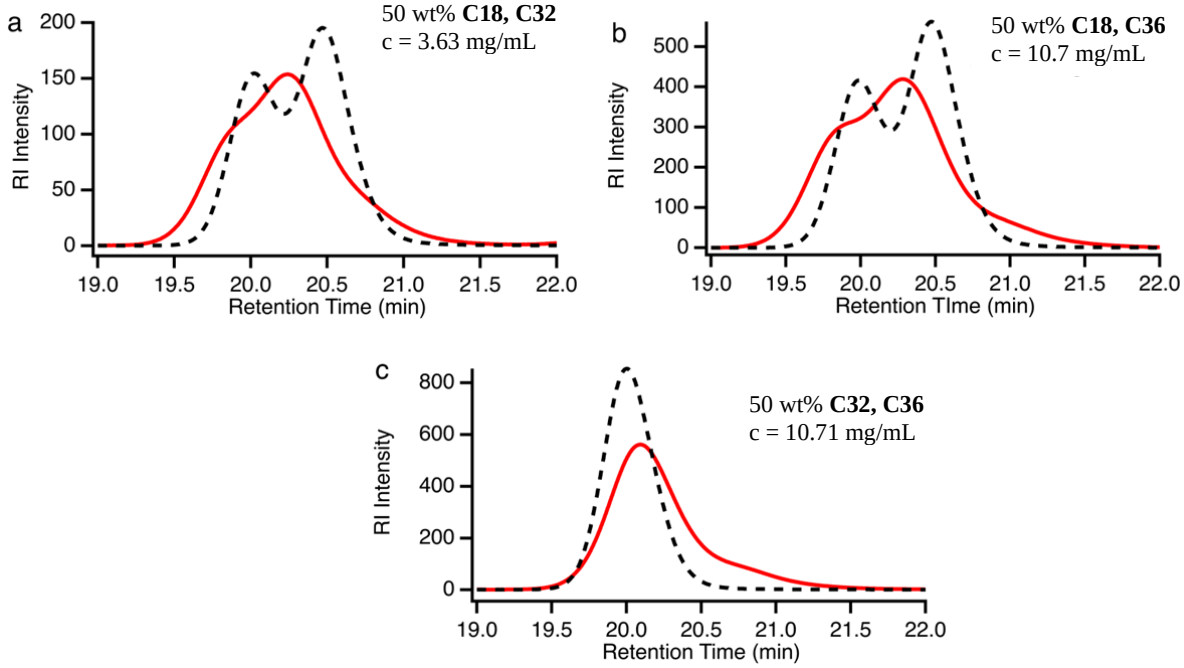


**Figure B.7** HT-SEC trace of 1:1 (wt:wt) blends of (a) **C18:C32**, (b) **C18:C36**, and (c) **C32:C36** in 1,2,4-trichlorobenzene at 150 °C.

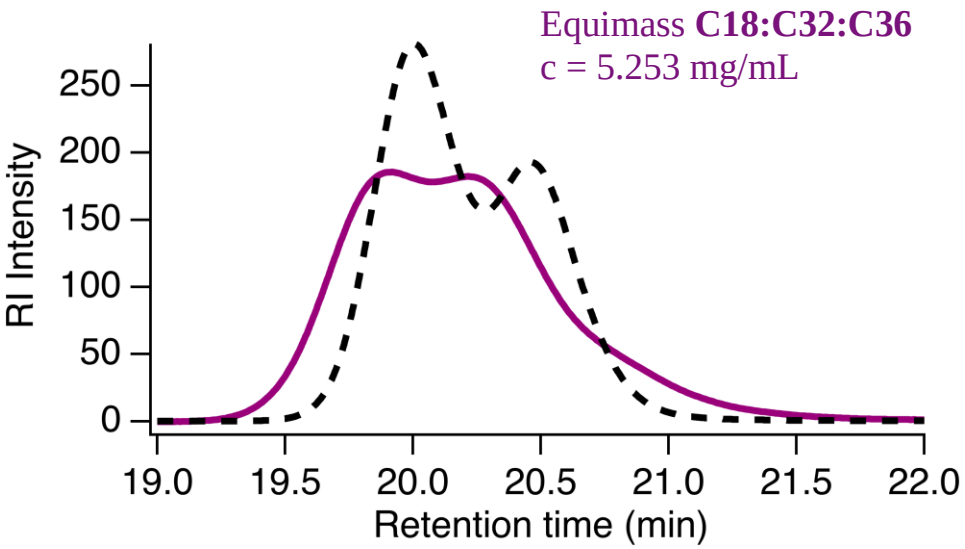


**Figure B.8** HT-SEC trace of 1:1:1 (wt:wt:wt) blend of **C18:C32:C36** in 1,2,4-trichlorobenzene at 150 °C.

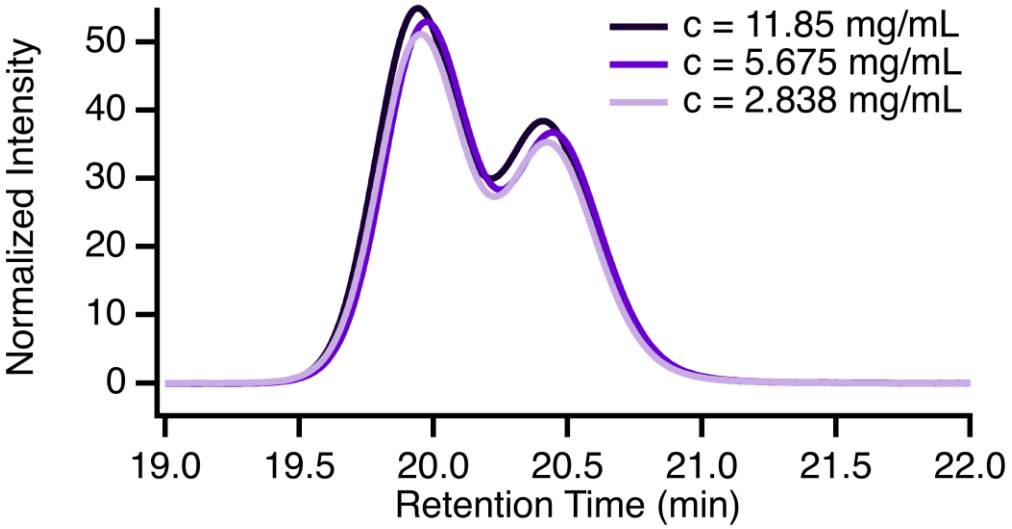


**Figure B.9** HT-SEC traces for 1:1 blend of **C18** and **C36** at different dilutions in 1,2,4-trichlorobenzene at 150 °C. The traces are normalized by the concentration as noted in the panel.

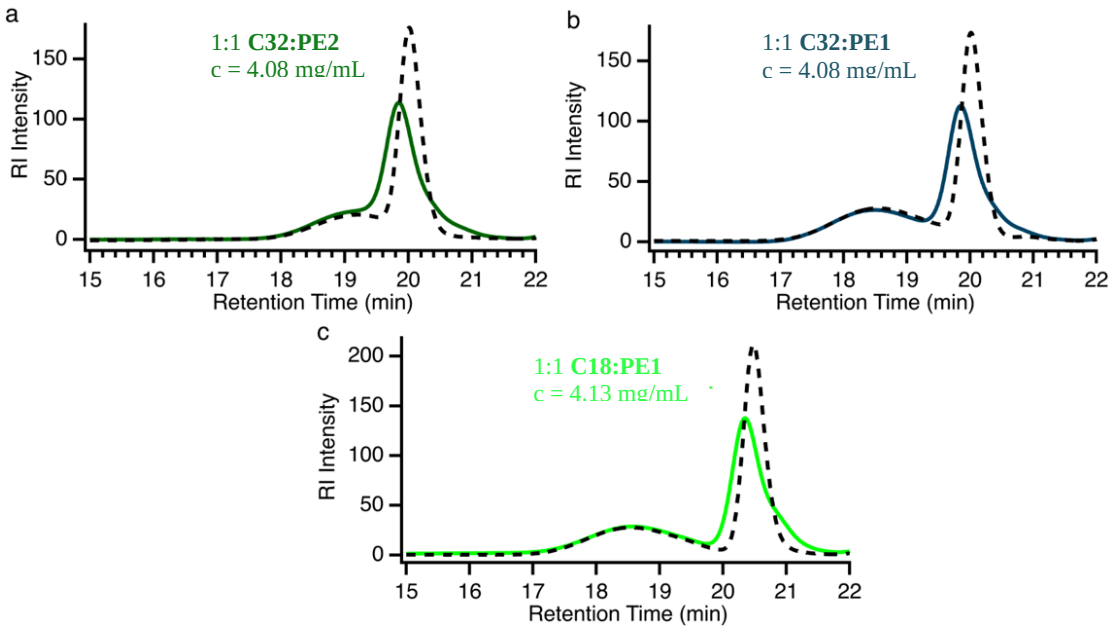


**Figure B.10** HT-SEC traces of binary blends in 1,2,4-trichlorobenzene at 150 °C for (a) 1:1 (w:w) **PE2** – **C32**, (b) 1:1 (w:w) **PE1** – **C32**, (c) 1:1 (w:w) **PE1** – **C18**. The solid lines are the measured traces for the blends and the black dashed lines are predictions based on the concentrations and the measured HT-SEC traces for the individual components.

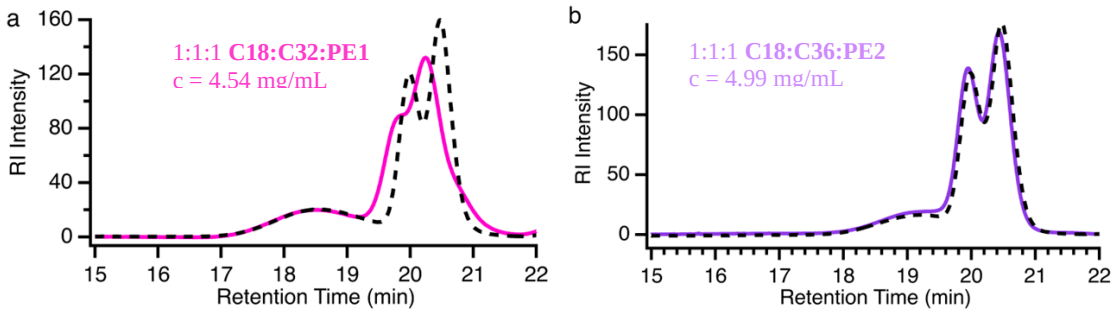


**Figure B.11** HT-SEC traces of ternary blends in 1,2,4-trichlorobenzene at 150 °C for (a) 1:1:1 (w:w:w) **PE1 – C36 – C18** and (b) 1:1:1 (w:w:w) **PE2 – C36 – C18**. The solid lines are the measured traces for the blends and the black dashed lines are predictions based on the concentrations and the measured HT-SEC traces for the individual components. The peak at 23-24 min is the injection void volume and is not associated with components in the solution.

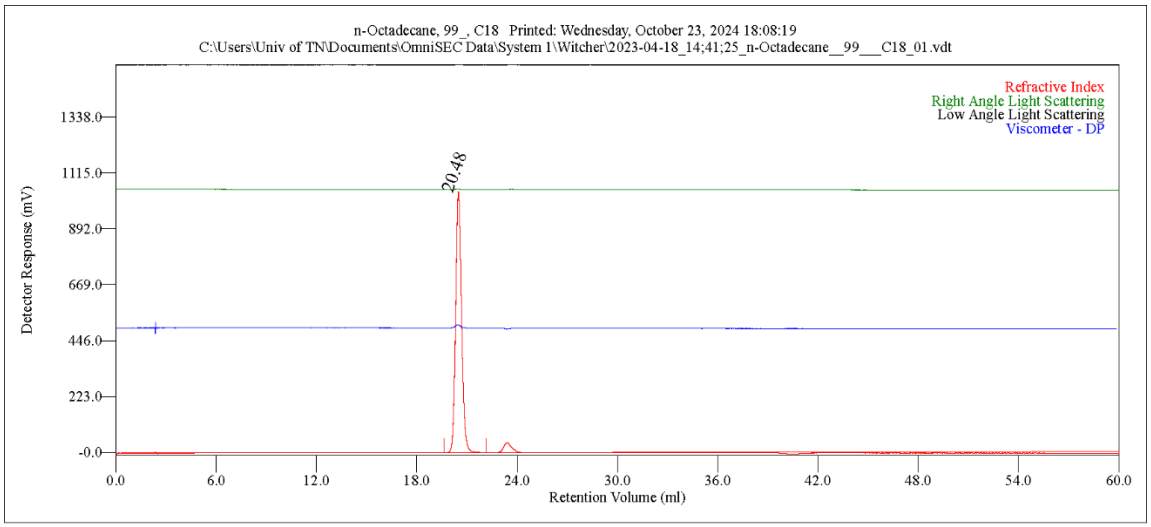


Multi-Detectors - Homopolymers : Results

| | |
|---|---|
| Peak RV - (ml) | 20.480 |
| Mn - (Daltons) | 56 |
| Mw - (Daltons) | 63 |
| Mz - (Daltons) | 71 |
| Mp - (Daltons) | 59 |
| Mw / Mn | 1.126 |
| Percent Above Mw: 0 | 100.000 |
| Percent Below Mw: 0 | 0.000 |
| IV - (dl/g) | 0.0040 |
| Rh(w) - (nm) | 0.157 |
| Rg(w) - (nm) | No Calc |
| Wt Fr (Peak) | 1.000 |
| Mark-Houwink a | 0.881 |
| Mark-Houwink logK | -3.985 |
| Branches | 0.000 |
| Branch Freq. | 0.000 |
| RI Area - (mvml) | 431.42 |
| UV Area - (mvml) | 0.00 |
| RALS Area - (mvml) | 0.57 |
| LALS Area - (mvml) | 0.88 |
| IVDP Area - (mvml) | 5.16 |

| Sample Parameters | Input | Calculated |
|---|---|---|
| Sample Conc - (mg/ml) | 10.220 | 0.000 |
| Sample Recovery (%) | 0.000 | 0.000 |
| dn/dc - (ml/g) | 0.0000 | 0.1670 |
| dA/dc - (ml/g) | 0.0000 | 0.0000 |

| Annotation | |
|---|---|
| Method File | Long group calibration 04-18-2023-0011.vcm |
| Limits File | |
| Date Acquired | Apr 18, 2023 - 14:41:25 |
| Solvent | TCB |
| Acquisition Operator | admin : Administrator |
| Calculation Operator | admin : Administrator |
| Column Set | CLM6210 - HT X 3 |
| System | System 1 |
| Flow Rate - (ml/min) | 1.000 |
| Inj Volume - (ul) | 200.0 |
| Volume Increment - (ml) | 0.00333 |
| Detector Temp. - (deg C) | 150.0 |
| Column Temp. - (deg C) | 150.0 |
| OmniSEC Build Number | 406 |

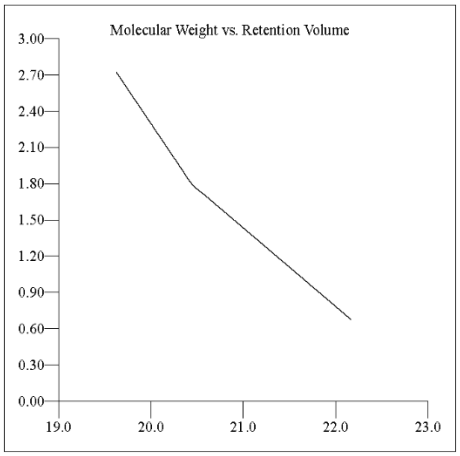


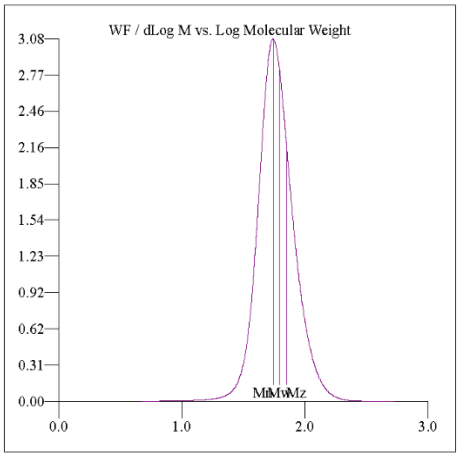


**Figure B.12** HT-SEC trace of **C18** (octadecane) in 1,2,4-trichlorobenzene at 150 °C.

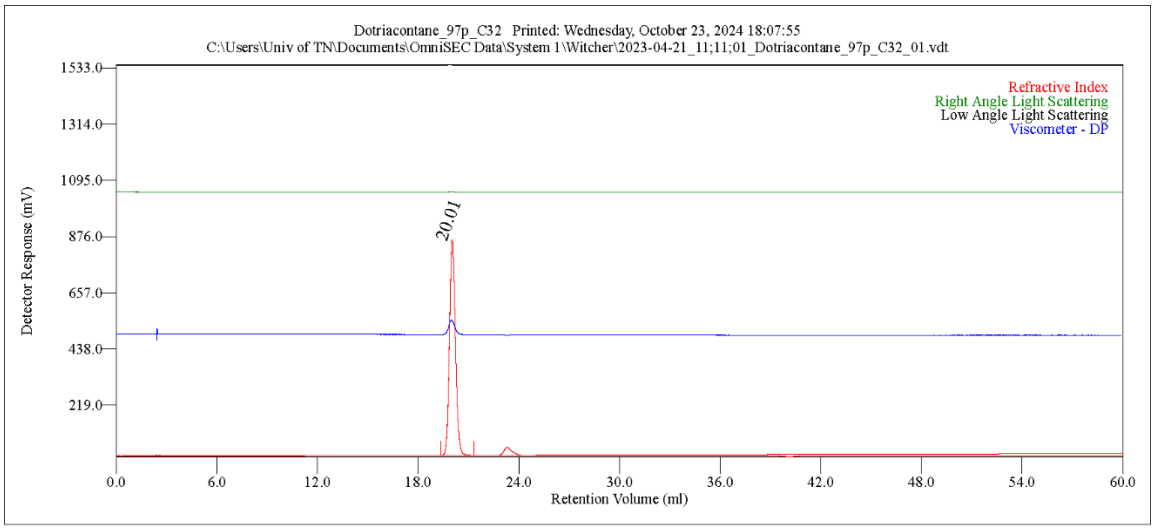


Multi-Detectors - Homopolymers : Results

| | |
|---|---|
| Peak RV - (ml) | 20.013 |
| Mn - (Daltons) | 134 |
| Mw - (Daltons) | 146 |
| Mz - (Daltons) | 158 |
| Mp - (Daltons) | 141 |
| Mw / Mn | 1.085 |
| Percent Above Mw: 0 | 100.000 |
| Percent Below Mw: 0 | 0.000 |
| IV - (dl/g) | 0.0190 |
| Rh(w) - (nm) | 0.349 |
| Rg(w) - (nm) | No Calc |
| Wt Fr (Peak) | 1.000 |
| Mark-Houwink a | 0.695 |
| Mark-Houwink logK | -3.221 |
| Branches | 0.000 |
| Branch Freq. | 0.000 |
| RI Area - (mvml) | 347.48 |
| UV Area - (mvml) | 0.00 |
| RALS Area - (mvml) | 0.95 |
| LALS Area - (mvml) | 1.41 |
| IVDP Area - (mvml) | 24.16 |

| Sample Parameters | Input | Calculated |
|---|---|---|
| Sample Conc - (mg/ml) | 10.130 | 0.000 |
| Sample Recovery (%) | 0.000 | 0.000 |
| dn/dc - (ml/g) | 0.0000 | 0.1451 |
| dA/dc - (ml/g) | 0.0000 | 0.0000 |

| Annotation | |
|---|---|
| Method File | Long Group Calibration 5-18-2023-0016.vcm |
| Limits File | |
| Date Acquired | Apr 21, 2023 - 11:11:01 |
| Solvent | TCB |
| Acquisition Operator | admin : Administrator |
| Calculation Operator | admin : Administrator |
| Column Set | CLM6210 - HT X 3 |
| System | System 1 |
| Flow Rate - (ml/min) | 1.000 |
| Inj Volume - (ul) | 200.0 |
| Volume Increment - (ml) | 0.00333 |
| Detector Temp. - (deg C) | 150.0 |
| Column Temp. - (deg C) | 150.0 |
| OmniSEC Build Number | 406 |

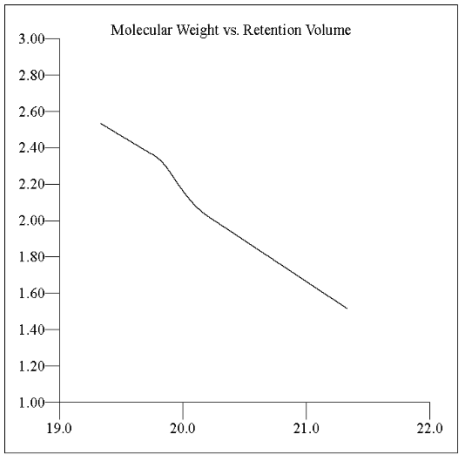


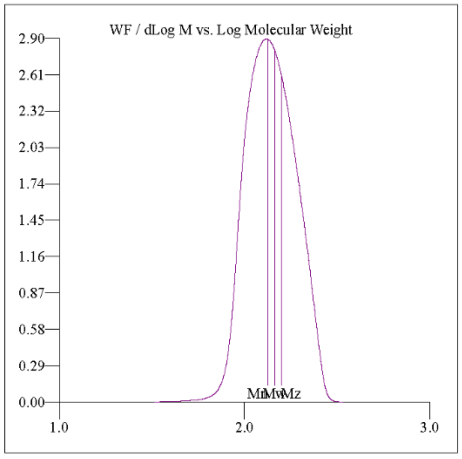


**Figure B.13** HT-SEC trace of **C32** (dotriacontane) in 1,2,4-trichlorobenzene at 150 °C.

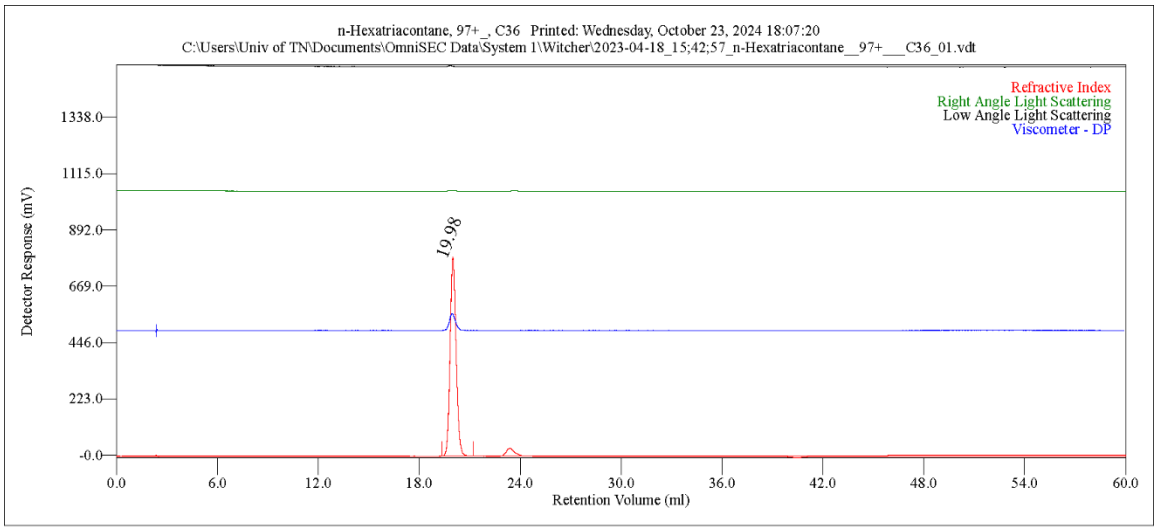


Multi-Detectors - Homopolymers : Results

| | |
|---|---|
| Peak RV - (ml) | 19.980 |
| Mn - (Daltons) | 165 |
| Mw - (Daltons) | 189 |
| Mz - (Daltons) | 210 |
| Mp - (Daltons) | 190 |
| Mw / Mn | 1.146 |
| Percent Above Mw: 0 | 100.000 |
| Percent Below Mw: 0 | 0.000 |
| IV - (dl/g) | 0.0219 |
| Rh(w) - (nm) | 0.399 |
| Rg(w) - (nm) | No Calc |
| Wt Fr (Peak) | 1.000 |
| Mark-Houwink a | 0.742 |
| Mark-Houwink logK | -3.353 |
| Branches | 0.000 |
| Branch Freq. | 0.000 |
| RI Area - (mvml) | 328.20 |
| UV Area - (mvml) | 0.00 |
| RALS Area - (mvml) | 1.12 |
| LALS Area - (mvml) | 1.62 |
| IVDP Area - (mvml) | 27.98 |

| Sample Parameters | Input | Calculated |
|---|---|---|
| Sample Conc - (mg/ml) | 10.210 | 0.000 |
| Sample Recovery (%) | 0.000 | 0.000 |
| dn/dc - (ml/g) | 0.0000 | 0.1360 |
| dA/dc - (ml/g) | 0.0000 | 0.0000 |

| Annotation | |
|---|---|
| Method File | Long Group Calibration 5-18-2023-0016.vcm |
| Limits File | |
| Date Acquired | Apr 18, 2023 - 15:42:57 |
| Solvent | TCB |
| Acquisition Operator | admin : Administrator |
| Calculation Operator | admin : Administrator |
| Column Set | CLM6210 - HT X 3 |
| System | System 1 |
| Flow Rate - (ml/min) | 1.000 |
| Inj Volume - (ul) | 200.0 |
| Volume Increment - (ml) | 0.00333 |
| Detector Temp. - (deg C) | 150.0 |
| Column Temp. - (deg C) | 150.0 |
| OmniSEC Build Number | 406 |

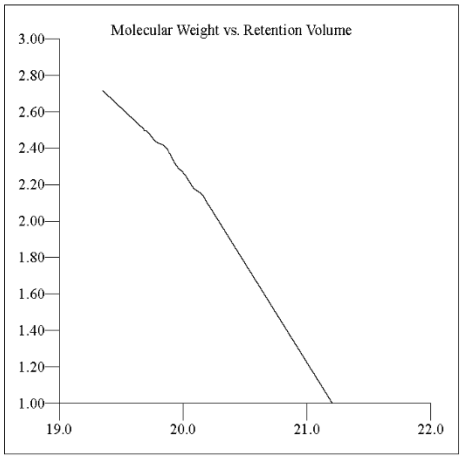


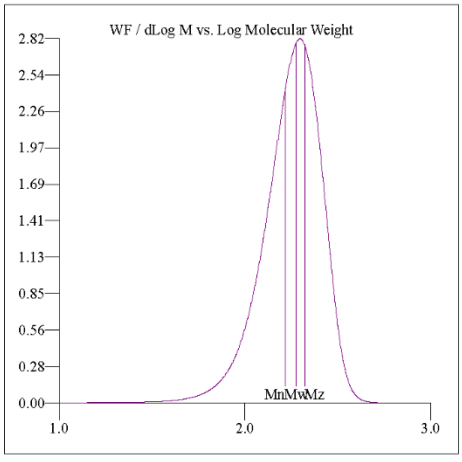


**Figure B.14** HT-SEC trace of **C36** (n-hexatriacontane) in 1,2,4-trichlorobenzene at 150 °C.

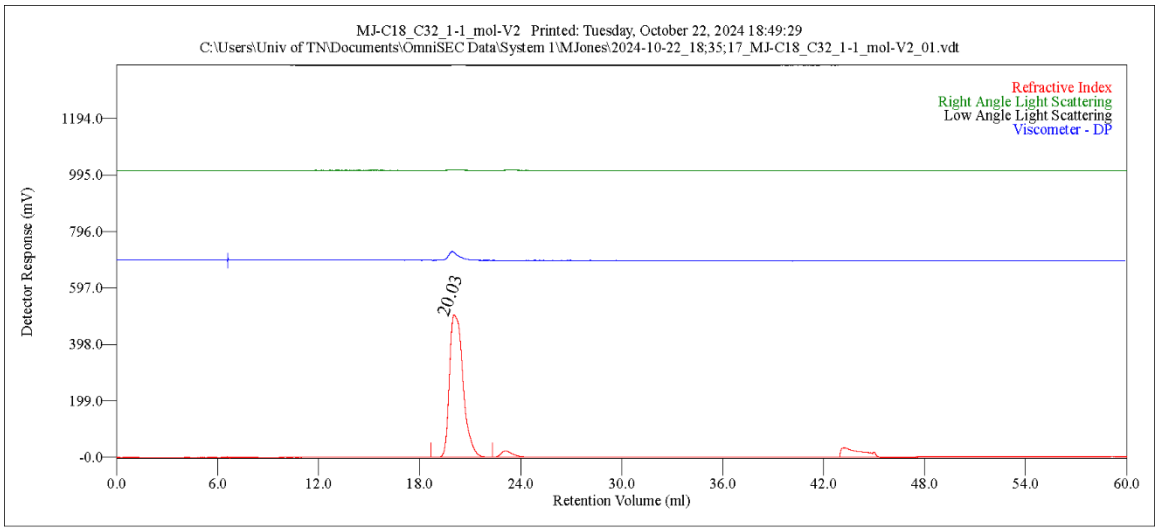


Multi-Detectors - Homopolymers : Results

| | |
|---|---|
| Peak RV - (ml) | 20.033 |
| Mn - (Daltons) | 72 |
| Mw - (Daltons) | 83 |
| Mz - (Daltons) | 96 |
| Mp - (Daltons) | 76 |
| Mw / Mn | 1.162 |
| Percent Above Mw: 0 | 100.000 |
| Percent Below Mw: 0 | 0.000 |
| IV - (dl/g) | 0.0124 |
| Rh(w) - (nm) | 0.243 |
| Rg(w) - (nm) | No Calc |
| Wt Fr (Peak) | 1.000 |
| Mark-Houwink a | 1.982 |
| Mark-Houwink logK | -5.709 |
| Branches | 0.000 |
| Branch Freq. | 0.000 |
| RI Area - (mvml) | 469.98 |
| UV Area - (mvml) | 0.00 |
| RALS Area - (mvml) | 0.93 |
| LALS Area - (mvml) | 2.15 |
| IVDP Area - (mvml) | 22.10 |

| Sample Parameters | Input | Calculated |
|---|---|---|
| Sample Conc - (mg/ml) | 12.690 | 0.000 |
| Sample Recovery (%) | 0.000 | 0.000 |
| dn/dc - (ml/g) | 0.0000 | 0.1639 |
| dA/dc - (ml/g) | 0.0000 | 0.0000 |

| Annotation | |
|---|---|
| Method File | Long group calibration 10-08-2024-new-0004.vcm |
| Limits File | |
| Date Acquired | Oct 22, 2024 - 18:35:17 |
| Solvent | TCB |
| Acquisition Operator | admin : Administrator |
| Calculation Operator | admin : Administrator |
| Column Set | CLM6210 - HT X 2 |
| System | System 1 |
| Flow Rate - (ml/min) | 1.000 |
| Inj Volume - (ul) | 200.0 |
| Volume Increment - (ml) | 0.00333 |
| Detector Temp. - (deg C) | 150.0 |
| Column Temp. - (deg C) | 150.0 |
| OmniSEC Build Number | 406 |

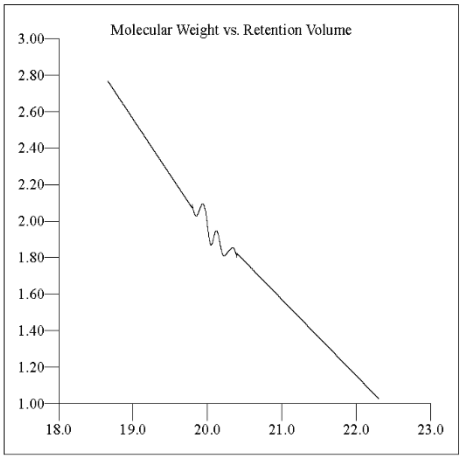


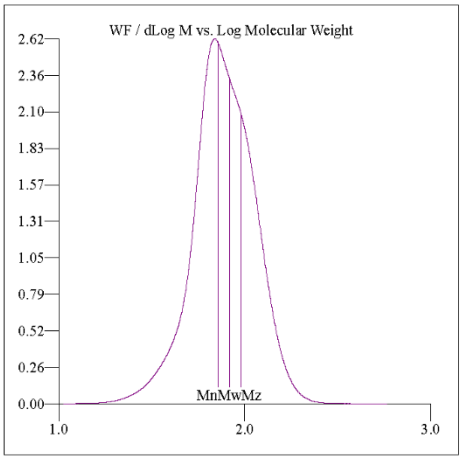


**Figure B.15** HT-SEC trace of **C18:C32** (1:1 mol:mol) blend in 1,2,4-trichlorobenzene at 150 °C.

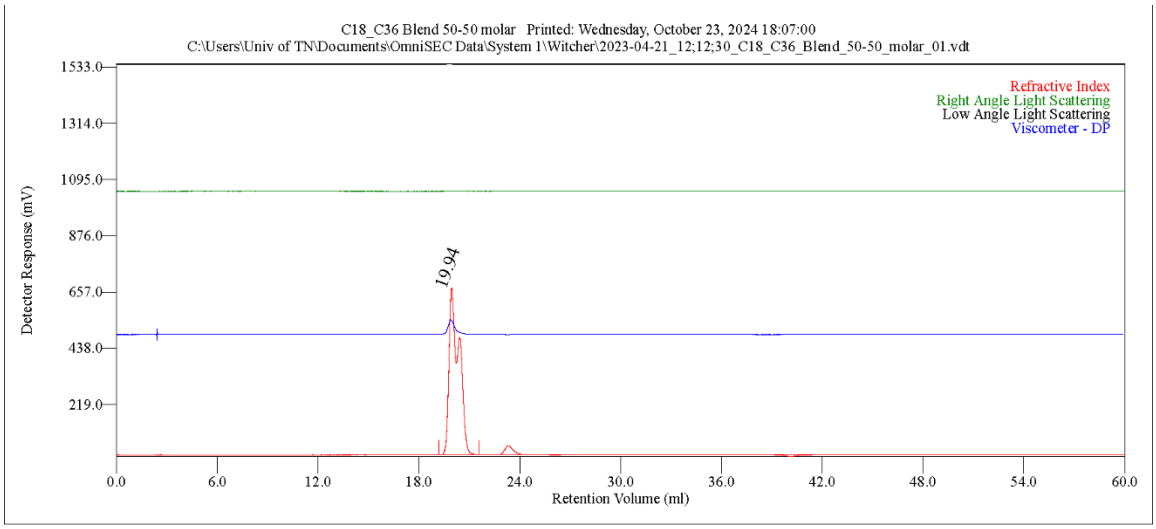


Multi-Detectors - Homopolymers : Results

| | |
|---|---|
| Peak RV - (ml) | 19.937 |
| Mn - (Daltons) | 105 |
| Mw - (Daltons) | 131 |
| Mz - (Daltons) | 161 |
| Mp - (Daltons) | 166 |
| Mw / Mn | 1.246 |
| Percent Above Mw: 0 | 100.000 |
| Percent Below Mw: 0 | 0.000 |
| IV - (dl/g) | 0.0171 |
| Rh(w) - (nm) | 0.311 |
| Rg(w) - (nm) | No Calc |
| Wt Fr (Peak) | 1.000 |
| Mark-Houwink a | 1.565 |
| Mark-Houwink logK | -5.073 |
| Branches | 0.000 |
| Branch Freq. | 0.000 |
| RI Area - (mvml) | 450.77 |
| UV Area - (mvml) | 0.00 |
| RALS Area - (mvml) | 1.29 |
| LALS Area - (mvml) | 1.92 |
| IVDP Area - (mvml) | 25.39 |

| Sample Parameters | Input | Calculated |
|---|---|---|
| Sample Conc - (mg/ml) | 11.850 | 0.000 |
| Sample Recovery (%) | 0.000 | 0.000 |
| dn/dc - (ml/g) | 0.0000 | 0.1609 |
| dA/dc - (ml/g) | 0.0000 | 0.0000 |

| Annotation | |
|---|---|
| Method File | Long Group Calibration 5-18-2023-0016.vcm |
| Limits File | |
| Date Acquired | Apr 21, 2023 - 12:12:30 |
| Solvent | TCB |
| Acquisition Operator | admin : Administrator |
| Calculation Operator | admin : Administrator |
| Column Set | CLM6210 - HT X 3 |
| System | System 1 |
| Flow Rate - (ml/min) | 1.000 |
| Inj Volume - (ul) | 200.0 |
| Volume Increment - (ml) | 0.00333 |
| Detector Temp. - (deg C) | 150.0 |
| Column Temp. - (deg C) | 150.0 |
| OmniSEC Build Number | 406 |

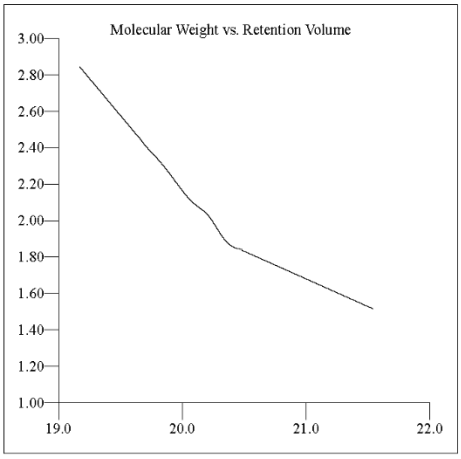


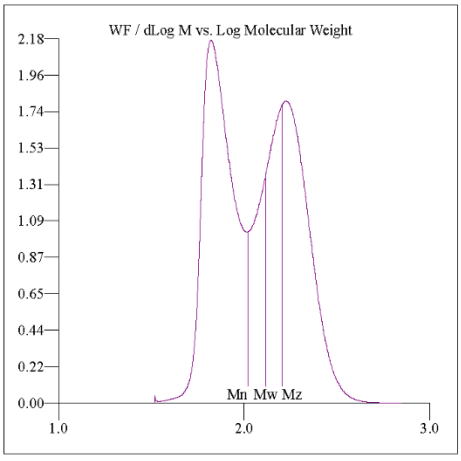


**Figure B.16** HT-SEC trace of **C18:C36** (1:1 mol:mol) blend in 1,2,4-trichlorobenzene at 150 °C.

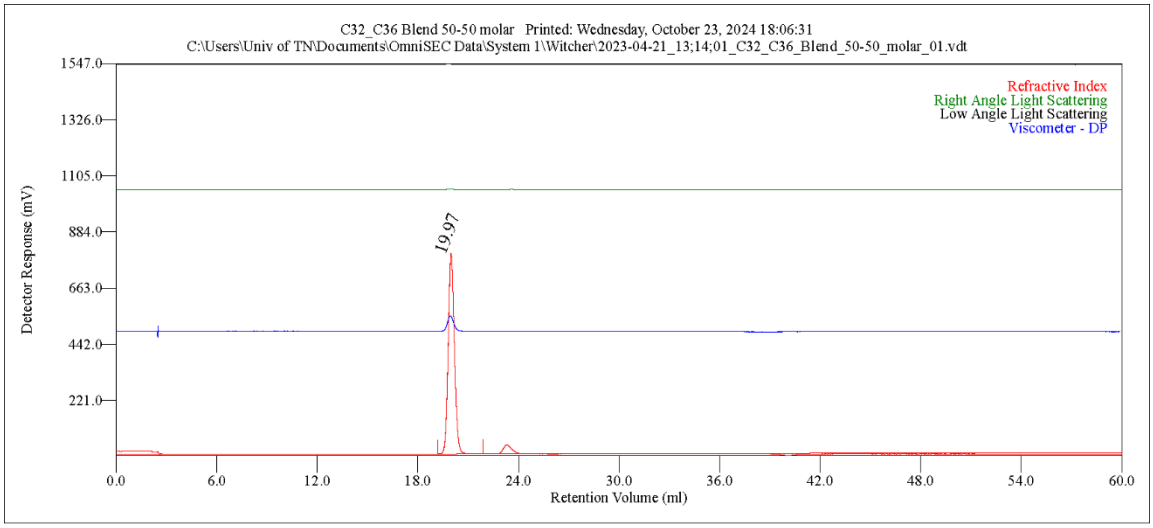


Multi-Detectors - Homopolymers : Results

| | |
|---|---|
| Peak RV - (ml) | 19.973 |
| Mn - (Daltons) | 151 |
| Mw - (Daltons) | 183 |
| Mz - (Daltons) | 203 |
| Mp - (Daltons) | 179 |
| Mw / Mn | 1.215 |
| Percent Above Mw: 0 | 100.000 |
| Percent Below Mw: 0 | 0.000 |
| IV - (dl/g) | 0.0206 |
| Rh(w) - (nm) | 0.384 |
| Rg(w) - (nm) | No Calc |
| Wt Fr (Peak) | 1.000 |
| Mark-Houwink a | 0.849 |
| Mark-Houwink logK | -3.621 |
| Branches | 0.000 |
| Branch Freq. | 0.000 |
| RI Area - (mvml) | 339.08 |
| UV Area - (mvml) | 0.00 |
| RALS Area - (mvml) | 1.16 |
| LALS Area - (mvml) | 1.61 |
| IVDP Area - (mvml) | 26.64 |

| Sample Parameters | Input | Calculated |
|---|---|---|
| Sample Conc - (mg/ml) | 10.420 | 0.000 |
| Sample Recovery (%) | 0.000 | 0.000 |
| dn/dc - (ml/g) | 0.0000 | 0.1377 |
| dA/dc - (ml/g) | 0.0000 | 0.0000 |

| Annotation | |
|---|---|
| Method File | Long Group Calibration 5-18-2023-0016.vcm |
| Limits File | |
| Date Acquired | Apr 21, 2023 - 13:14:01 |
| Solvent | TCB |
| Acquisition Operator | admin : Administrator |
| Calculation Operator | admin : Administrator |
| Column Set | CLM6210 - HT X 3 |
| System | System 1 |
| Flow Rate - (ml/min) | 1.000 |
| Inj Volume - (ul) | 200.0 |
| Volume Increment - (ml) | 0.00333 |
| Detector Temp. - (deg C) | 150.0 |
| Column Temp. - (deg C) | 150.0 |
| OmniSEC Build Number | 406 |

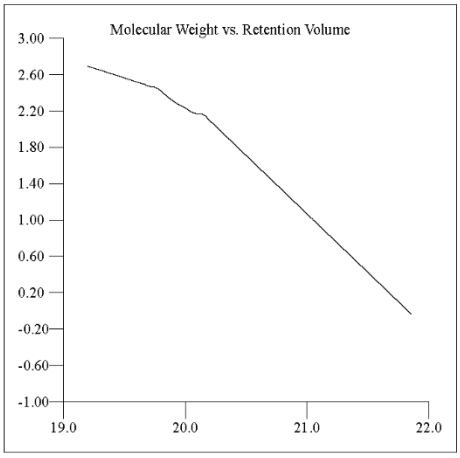


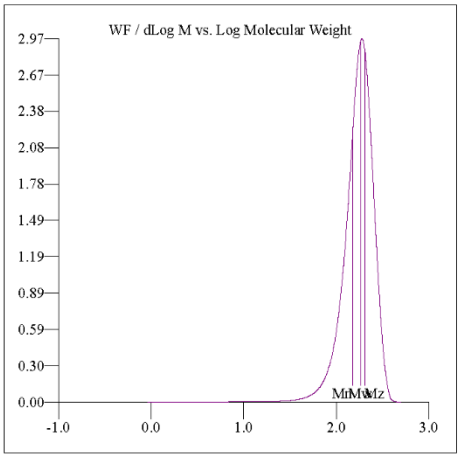


**Figure B.17** HT-SEC trace of **C32:C36** (1:1 mol:mol) blend in 1,2,4-trichlorobenzene at 150 °C.

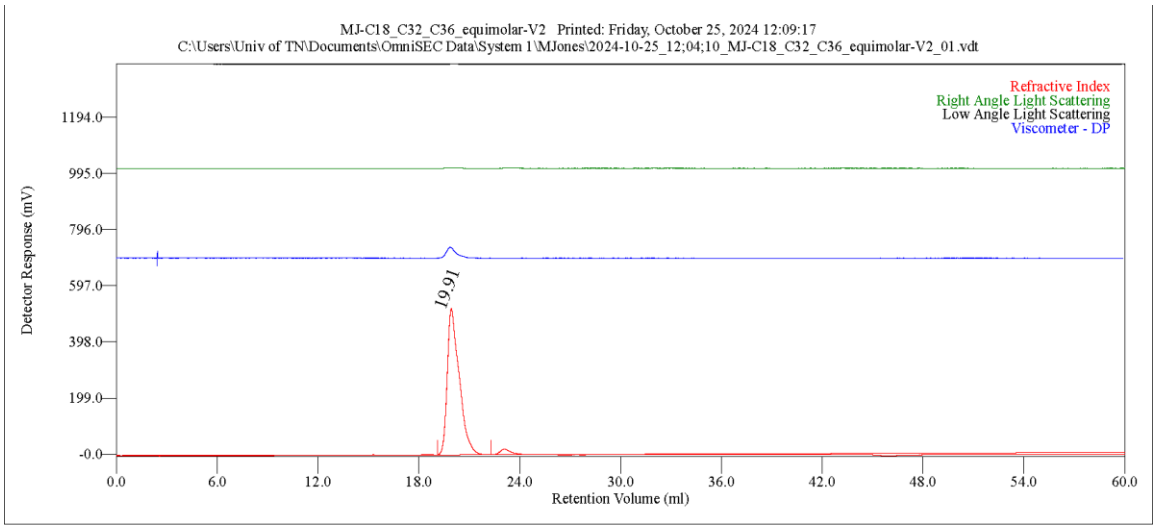


Multi-Detectors - Homopolymers : Results

| | |
|---|---|
| Peak RV - (ml) | 19.913 |
| Mn - (Daltons) | 109 |
| Mw - (Daltons) | 147 |
| Mz - (Daltons) | 186 |
| Mp - (Daltons) | 168 |
| Mw / Mn | 1.351 |
| Percent Above Mw: 0 | 100.000 |
| Percent Below Mw: 0 | 0.000 |
| IV - (dl/g) | 0.0157 |
| Rh(w) - (nm) | 0.314 |
| Rg(w) - (nm) | No Calc |
| Wt Fr (Peak) | 1.000 |
| Mark-Houwink a | 1.063 |
| Mark-Houwink logK | -4.112 |
| Branches | 0.000 |
| Branch Freq. | 0.000 |
| RI Area - (mvml) | 428.05 |
| UV Area - (mvml) | 0.00 |
| RALS Area - (mvml) | 0.89 |
| LALS Area - (mvml) | 1.23 |
| IVDP Area - (mvml) | 27.38 |

| Sample Parameters | Input | Calculated |
|---|---|---|
| Sample Conc - (mg/ml) | 12.170 | 0.000 |
| Sample Recovery (%) | 0.000 | 0.000 |
| dn/dc - (ml/g) | 0.0000 | 0.1316 |
| dA/dc - (ml/g) | 0.0000 | 0.0000 |

| Annotation | |
|---|---|
| Method File | Long group calibration 07-31-2024-0007.vcm |
| Limits File | |
| Date Acquired | Oct 25, 2024 - 12:04:10 |
| Solvent | TCB |
| Acquisition Operator | admin : Administrator |
| Calculation Operator | admin : Administrator |
| Column Set | CLM6210 - HT X 2 |
| System | System 1 |
| Flow Rate - (ml/min) | 1.000 |
| Inj Volume - (ul) | 200.0 |
| Volume Increment - (ml) | 0.00333 |
| Detector Temp. - (deg C) | 150.0 |
| Column Temp. - (deg C) | 150.0 |
| OmniSEC Build Number | 406 |

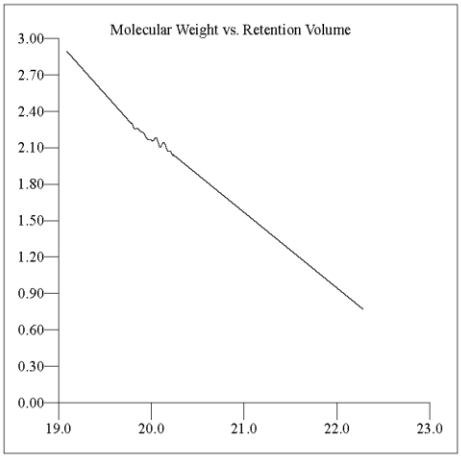


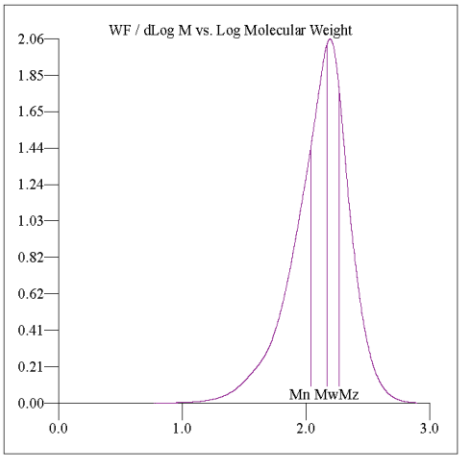


**Figure B.18** HT-SEC trace of **C18:C32:C36** (1:1:1 mol:mol:mol) blend in 1,2,4-trichlorobenzene at 150 °C.

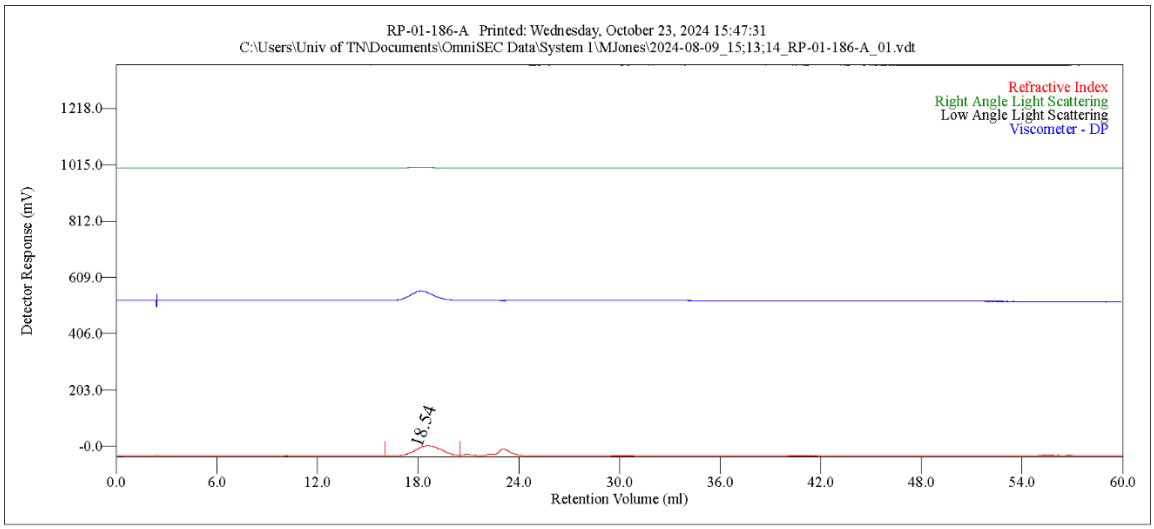


Multi-Detectors - Homopolymers : Results

| | |
|---|---|
| Peak RV - (ml) | 18.537 |
| Mn - (Daltons) | 4,432 |
| Mw - (Daltons) | 5,921 |
| Mz - (Daltons) | 8,205 |
| Mp - (Daltons) | 5,065 |
| Mw / Mn | 1.336 |
| Percent Above Mw: 0 | 100.000 |
| Percent Below Mw: 0 | 0.000 |
| IV - (dl/g) | 0.1390 |
| Rh(w) - (nm) | 2.269 |
| Rg(w) - (nm) | No Calc |
| Wt Fr (Peak) | 1.000 |
| Mark-Houwink a | 0.935 |
| Mark-Houwink logK | -4.361 |
| Branches | 0.000 |
| Branch Freq. | 0.000 |
| RI Area - (mvml) | 59.79 |
| UV Area - (mvml) | 0.00 |
| RALS Area - (mvml) | 3.84 |
| LALS Area - (mvml) | 2.18 |
| IVDP Area - (mvml) | 53.00 |

| Sample Parameters | Input | Calculated |
|---|---|---|
| Sample Conc - (mg/ml) | 2.670 | 0.000 |
| Sample Recovery (%) | 0.000 | 0.000 |
| dn/dc - (ml/g) | 0.0000 | 0.0838 |
| dA/dc - (ml/g) | 0.0000 | 0.0000 |

| Annotation | |
|---|---|
| Method File | Long group calibration 07-31-2024-0007.vcm |
| Limits File | |
| Date Acquired | Aug 09, 2024 - 15:13:14 |
| Solvent | TCB |
| Acquisition Operator | admin : Administrator |
| Calculation Operator | admin : Administrator |
| Column Set | CLM6210 - HT X 2 |
| System | System 1 |
| Flow Rate - (ml/min) | 1.000 |
| Inj Volume - (ul) | 200.0 |
| Volume Increment - (ml) | 0.00333 |
| Detector Temp. - (deg C) | 150.0 |
| Column Temp. - (deg C) | 150.0 |
| OmniSEC Build Number | 406 |

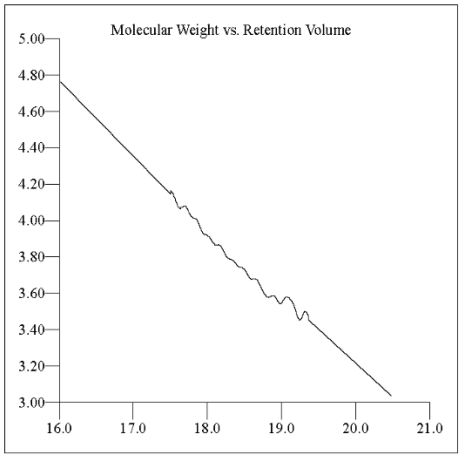


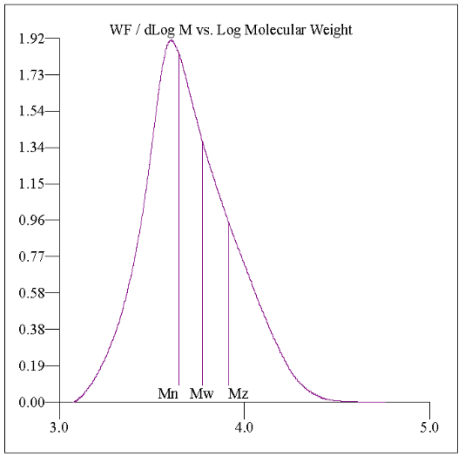


**Figure B.19** HT-SEC trace of **PE1** in 1,2,4-trichlorobenzene at 150 °C.

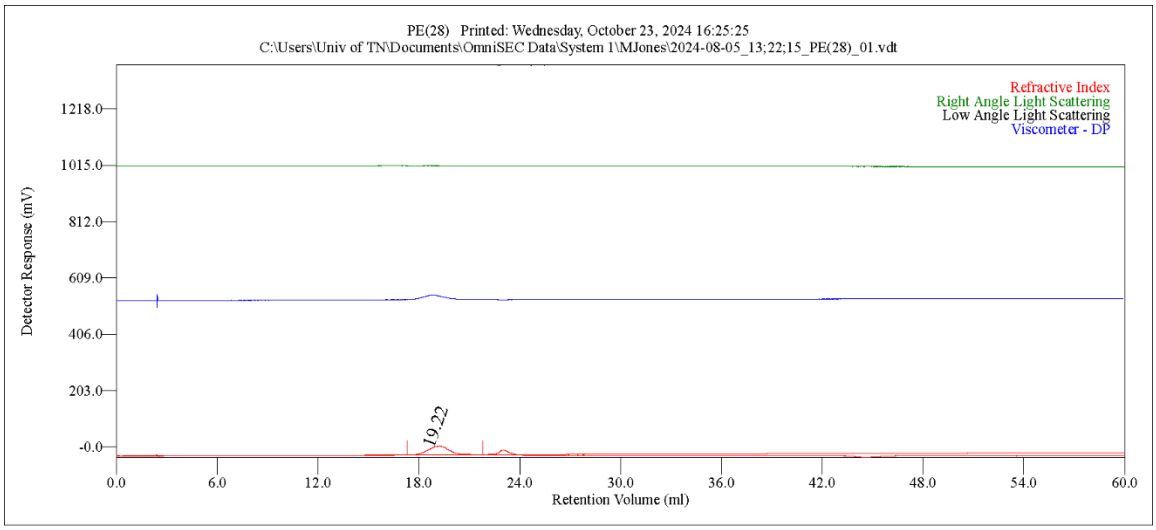


Multi-Detectors - Homopolymers : Results

| | |
|---|---|
| Peak RV - (ml) | 19.217 |
| Mn - (Daltons) | 1,863 |
| Mw - (Daltons) | 4,242 |
| Mz - (Daltons) | 5,480 |
| Mp - (Daltons) | 4,334 |
| Mw / Mn | 2.277 |
| Percent Above Mw: 0 | 100.000 |
| Percent Below Mw: 0 | 0.000 |
| IV - (dl/g) | 0.0554 |
| Rh(w) - (nm) | 1.433 |
| Rg(w) - (nm) | No Calc |
| Wt Fr (Peak) | 1.000 |
| Mark-Houwink a | 1.187 |
| Mark-Houwink logK | -5.676 |
| Branches | 0.000 |
| Branch Freq. | 0.000 |
| RI Area - (mvml) | 46.52 |
| UV Area - (mvml) | 0.00 |
| RALS Area - (mvml) | 2.15 |
| LALS Area - (mvml) | 0.86 |
| IVDP Area - (mvml) | 25.11 |

| Sample Parameters | Input | Calculated |
|---|---|---|
| Sample Conc - (mg/ml) | 3.170 | 3.170 |
| Sample Recovery (%) | 0.000 | 0.000 |
| dn/dc - (ml/g) | 0.0000 | 0.0549 |
| dA/dc - (ml/g) | 0.0000 | 0.0000 |

| | |
|---|---|
| Annotation | |
| Method File | Long group calibration 07-31-2024-0001.vcm |
| Limits File | |
| Date Acquired | Aug 05, 2024 - 13:22:15 |
| Solvent | TCB |
| Acquisition Operator | admin : Administrator |
| Calculation Operator | admin : Administrator |
| Column Set | CLM6210 - HT X 2 |
| System | System 1 |
| Flow Rate - (ml/min) | 1.000 |
| Inj Volume - (ul) | 200.0 |
| Volume Increment - (ml) | 0.00333 |
| Detector Temp. - (deg C) | 150.0 |
| Column Temp. - (deg C) | 150.0 |
| OmniSEC Build Number | 406 |

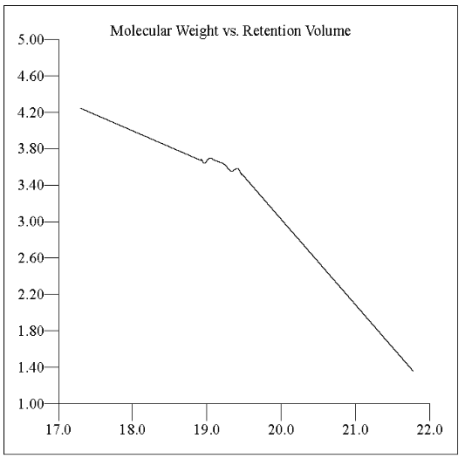


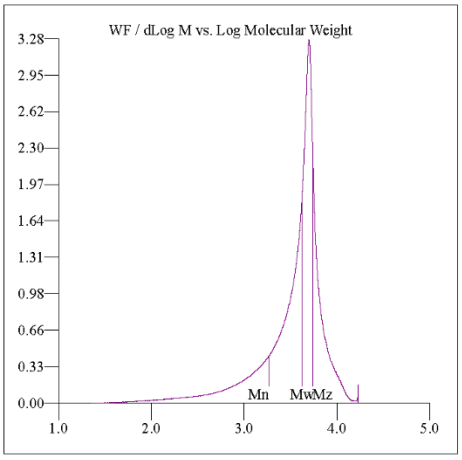


**Figure B.20** HT-SEC trace of **PE2** in 1,2,4-trichlorobenzene at 150 °C.

# VITA

Rakesh was born in the small village of Bithmara, located in the Hisar district of Haryana, India. He completed his early education in a nearby town before moving to the national capital, New Delhi, to pursue his undergraduate studies, majoring in chemistry. During his undergraduate studies, he developed a strong interest in organic chemistry and decided to pursue a Master of Science degree in the same field from Hemvati Nandan Bahuguna Garhwal University. He also earned a Bachelor of Education degree from Chaudhary Devi Lal University and taught for three years thereafter. In August 2022, Rakesh moved to the United States to pursue a Master of Science in Polymer Chemistry at the University of Tennessee, Knoxville. Upon graduation, he plans to join the industry as a professional chemist. Rakesh feels fortunate to have the support of his advisor, lab mates, and friends throughout graduate school, as well as the unwavering encouragement from his father, brother, wife, and son back home.